Iron and Cobalt "Lacunar" Complexes as Dioxygen Carriers

Daryle H. Busch*,† and Nathaniel W. Alcock‡

Department of Chemistry, University of Kansas, Lawrence, Kansas 66045, and Department of Chemistry & Molecular Sciences, University of Warwick, Coventry CV4 7AL, United Kingdom

Received September 17, 1993 (Revised Manuscript Received February 3, 1994)

Contents

I. Introduction

A. Scope and Definitions

This review summarizes the published work on the dioxygen chemistry of lacunar transition metal dioxygen carriers. The adjective lacunar[1] is used in the context often applied in anatomy and biology to indicate the presence of a space or cavity where there would ordinarily be none. In biology one might mean a void or cavity in or among cells, whereas here we mean a void or cavity among atoms of a molecular species rather than extended materials like zeolites. For transition metal complexes that are potential dioxygen carriers, the lacuna is a cavity or void that can be used to accommodate dioxygen or some other small ligand. A general view of the molecular structure of lacunar dioxygen carriers defines the portion of the ligand that binds the metal ion as the parent ligand or platform and the additional structural features that produce the lacuna as superstructure.[2] The most common platforms for lacunar complexes are macrocyclic or acyclic tetradentate and pentadentate ligands (Figure 1). This summary considers only lacunar complexes that are strictly of synthetic origin; the many superstructured porphyrins are specifically excluded.

The properties of importance to dioxygen transport and storage include dioxygen affinity, enthalpy of dioxygen binding, kinetics of dioxygen binding and dissociation, kinetics and mechanism of autoxidation of the dioxygen carrier, thermodynamics of the redox processes, and for some purposes the mobility of the dioxygen carrier (e.g., in extraction processes). Lacunar structures modify the dioxygen binding systems by interceding in reactions and by affecting the immediate environment of the bound dioxygen. Most obviously, a cavity may crowd the bound dioxygen and decrease the dioxygen affinity, or the hydrophobic environment within a cavity may contrast strongly with a surrounding protic solvent. Of great importance, two electron oxidations by dioxygen often involve simultaneous binding of O_2 to two metal ions; a lacuna can easily prevent this kind of interaction. Sections to follow treat the structures and synthesis of lacunar complexes, their

† University of Kansas.
‡ University of Warwick.

0009-2665/94/0794-0585$14.00/0

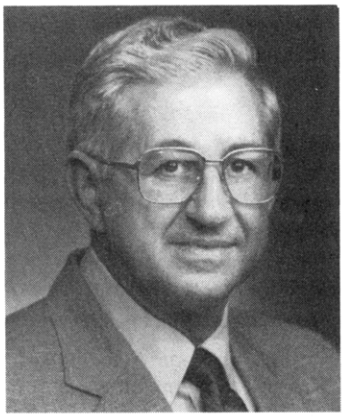

Daryle H. Busch received the B.A. from Southern Illinois University in 1951 and the M.S. (1952) and Ph.D. (1954) from the University of Illinois (Urbana) in Inorganic Chemistry. From 1988 until the present he has held the position Roy A. Roberts Distinguished Professor of Chemistry at the University of Kansas. From 1954 through 1988 he was a member of the chemistry faculty at The Ohio State University, his last title being Presidential Professor. Recognitions have included the Bailar Medal (University of Illinois), the Dwyer Medal (Chemical Society of New South Wales), and the American Chemical Society awards for research in Inorganic Chemistry and for Distinguished Service in the Advancement of Inorganic Chemistry. He has served as consultant to Dupont, 3M, Monsanto, Air Products, and others, and he has served the professional societies and journals in many ways. He chaired the IUPAC Commission on Inorganic Nomenclature while the 1990 recommendations were being brought to publication. He is author of over 314 publications and 6 patents. His research interests proceed from transition metal coordination chemistry, featuring original synthesis, to the control of chemical reactions by metal atoms including functional biomimics, such as oxygen carriers, catalysis, and the general subject of molecular organization and such subfields, as inclusion chemistry, template reactions, and design of extended structures.

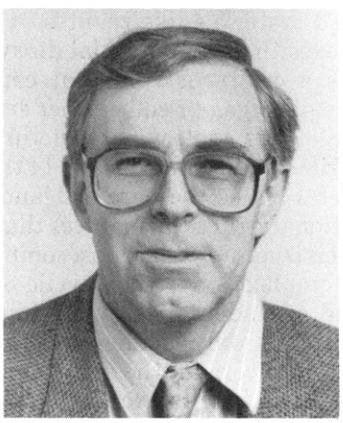

Nathaniel W. Alcock received his B.A. in 1960 and his Ph.D. in 1963 from Cambridge University (Trinity College). He has been in the Department of Chemistry, University of Warwick, Coventry, England, since 1966, successively as Lecturer, Senior Lecturer, and Reader (1983). He has served as a Co-Editor for *Acta Crystallographica* and as a member of the Commission on Journals of the International Union of Crystallography since 1984. He is the author of almost 310 papers and the text book *Structure and Bonding in Inorganic and Organic Chemistry*. His research interests lie in structural inorganic chemistry in the widest sense with a special emphasis on intermolecular interactions, on main group element coordination and on macrocycle conformations.

redox and spectroscopic properties, dioxygen affinities and thermodynamics of O_2 binding, and autoxidation kinetics. Because many excellent reviews provide much background,[3-11] most of the topics can be treated with relatively little preliminary discussion, but a more detailed presentation is offered for the autoxidation of dioxygen carriers because of the paucity of published reviews.[12]

B. Families of Lacunar Ligands

A substantial number of ligand systems have already been modified to incorporate intramolecular cavities or lacunae and some of these have been used in the study of transition metal dioxygen carriers. The potential for such superstructured complexes is very great. The full range of ligand families containing lacunar examples that is considered in this review is shown in Figure 1, along with the abbreviations used to identify the families. Of these, the cyclidene system has been by far the most extensively studied, with more than 300 compounds prepared and the dioxygen affinities measured for about 100 of them.[13-16] The various cyclidenes are labeled Cyc, Cyd, Dcy, Vcy, and Cyf in Figure 1. They are neutral tetraazamacrocycles having characteristic unsaturation patterns and superstructures linked to two additional nitrogen atoms. While the addition of superstructures to any parent ligand systems provides them with more or less well-protected cavities, the intrinsic cleft-like, or saddle, structure of the [16]cyclidenes makes them extraordinarily suited to form lacunae. Almost serendipitously, they are particularly efficacious because of the flexibility of their synthetic procedures and the range of available structural variables and substituents. The latter provide facile control of key electronic and steric properties. Other families give promise of similar advantages, but these have not yet been fully realized.

C. Nomenclature

To avoid both the obfuscation of using numbers to identify the numerous complexes discussed here, and the verbosity of full or even abbreviated names, a system of abbreviated formulas has been adopted which is intended to provide immediate recognition of the complex being considered and of its structural characteristics. The usual formula for a complex comprises: bracket, symbol for metal ion with superscripted oxidation number, ligand abbreviation in parentheses, close bracket, followed either by superscripted net charge or by the formulas for the counterions. The distinctive treatment in this manuscript is the ligand abbreviation. As is the general practice in the nomenclature of coordination compounds,[17] brackets are commonly left out when the formula of the complex does not include the counterions. The abbreviations are used both in text and in the tables. For a quick view of the nature of the abbreviations, look at Table 1.

(1) Ligand abbreviations build on the set of roots (usually 3 letters) given with the structural formulas in Figure 1, and all additional symbols precede that set of roots. Further, a simplistic assumption is made that the structures have either 2-fold or mirror symmetry.

(2) Directly preceding the root is an *enclosed* number, sometimes along with additional letters.

(a) If the ligand is a *macrocycle*, this number indicates the ring size and is enclosed in *brackets*; e.g., [16]. Unusual substituents, on the macrocycle, that are not otherwise treated in this system (see below) might also appear; e.g., [$Me_2$16Me_2] has been used to indicate the presence of *gem*-dimethyl groups as components of both saturated chelate rings in a [16]cyclidene. X-ring

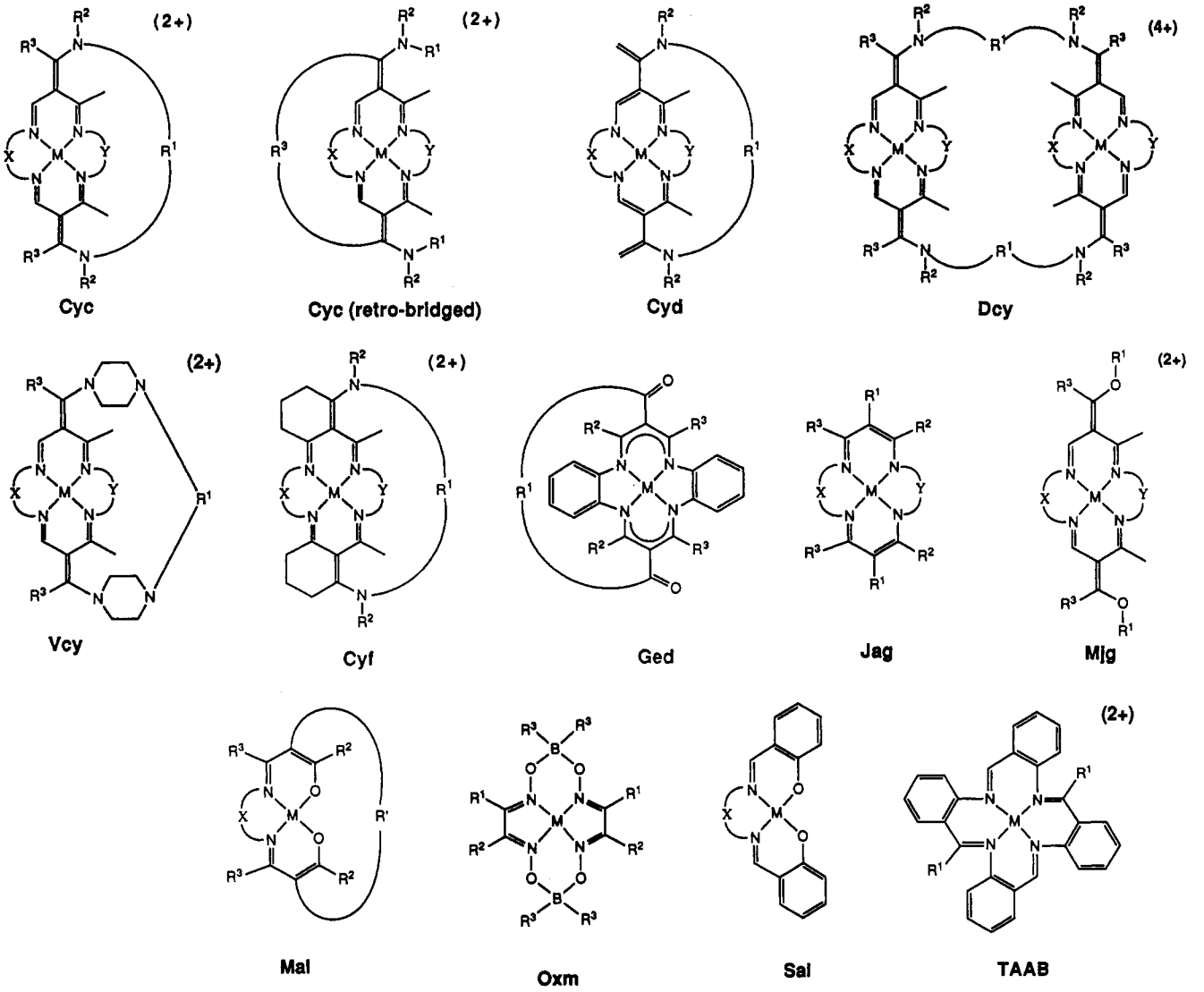

Figure 1. Structural formulas for the lacunar complexes discussed in this review. The abbreviations appearing beneath formulas are used in chemical formulas to identify the family of the ligand.

substitutent precedes number; Y-ring substituent follows (again, see Figure 1). When necessary, such an abbreviation will be explained in a footnote to the table in which it appears.

(b) If the ligand is *acyclic*, this number represents the terminal donor to terminal donor distance of the longest chain in the *parent ligand* (it does not traverse superstructure components) and it is enclosed in *braces*. Thus, for the familiar Schiff base of salicyl aldehyde and ethylenediamine, the symbol is {12}. The enclosure is also used to indicate any additional donor atoms beyond those in the prototypical parent ligand structure; e.g., for the corresponding Schiff base in which ethylenediamine is replaced by *N*-methyliminobis(1,3-propanediyldiimino), the symbol is {17NMe}.

3. The substituents on the parent ligand depend on the specific ligand system, as defined as in Figure 1, and are listed in increasing order of superscript: $R^1R^2R^3$. R^1 is generally used for the most common bridging position, and it should be noted, in particular, that the corresponding substituents in unbridged complexes are indicated as doubled—a notation that calls attention to the absence of the ring from that location; e.g., Me_2.

It is assumed that pairs of identical substituents are present at the R^2 and R^3 positions so that doubling is not specifically indicated.

Complicated substituents are sometimes indicated by sets of symbols enclosed in parentheses, usually explained specifically in the Table of Abbreviations. For example R^1 would be (C3NMeC3) if *N*-methyliminobis(1,3-propanediyl) were used as the bridging group.

$[Co((C3NMeC3)MePh[16]Cyc)(MeIm)(O_2)](PF_6)_2$ is a useful example. The three independent sets of parentheses inside the main brackets indicate three different ligands, one of which is complicated. The simple ligands are *N*-methylimidazole (MeIm, see Table of Abbreviations) and dioxygen. The complicated ligand is a [16]cyclidene (=[16]Cyc) with R^1 = *N*-methyliminobis(1,3-propanediyl), R^2 = methyl, and R^3 = phenyl. Similarly, $Co^{III}((C3NC3)MeMe[Me_216Me_2]Cyc)(NCS)_2^+$ is a specific example of a complex having the general formula $Co^{III}(R^1R^2R^3[\text{ring size}]\text{family})(\text{axial ligand})_2^+$.

II. Structural Correlations

Superficially similar lacunar complexes can have extraordinarily different abilities to bind dioxygen, and much of this variability can be attributed to structural effects. As a result, intensive structural studies (Table 2) have been undertaken on the lacunar dioxygen carriers and related complexes to elucidate the struc-

Table 1. Abbreviations Used in Formulas of Lacunar Complexes

abbreviation	name	abbreviation	name
	Ligand Families		
Cyc	cyclidene	Mal	β-diketone Schiff base
Cyd	deprotonated cyclidene	Mjg	methylated Jager
Cyf	cyclidene with fused cyclohexyl groups	Oxm	oxime
Dcy	dimeric cyclidene	Sal	salicylaldehyde Schiff base
Ged	Goedken macrocycle (di-benzo Jager)	TAAB	cyclic tetramer of *o*-aminobenzaldehyde
Jag	Jager	Vcy	vaulted cyclidene
	Terminal Substituents[a]		
Ac	acetyl	pCl	*p*-chlorophenyl
AcC	$CH_3(C{=}O)CH_2$—	Pe	2-phenylethyl ($C_6H_5C_2H_4$-)
bOMe	3,5-dimethoxyphenyl	pF	*p*-fluorophenyl
BzO	benzoyl	pOMe	*p*-methoxyphenyl
Bz	benzyl	Me	methyl
nBu	*n*-butyl	Mes	mesityl
tBu	*tert*-butyl	Neo	neopentyl
Dha	9,10-dihydroanthracenyl (substituted at both R^1 and R^2)	Pic	*o*-picolinyl
		MePic	*N*-methyl-*o*-picolinyl
Et	ethyl	Pz	pyrazolyl (Figure 2)
FAc	trifluoroacetyl	Ph	phenyl
FBzo	perfluorobenzoyl	Pr	propyl
Fl	7-fluoroindenyl (Figure 2)	ClAc	trichloracetyl
Hp	*n*-heptyl		
	Bridging Groups		
C6 (etc.)	$-(CH_2)_6-$	CPhCPhC	$-CH_2$-*m*-C_6H_4-CH_2-*m*-C_6H_4-CH_2-
C2C2	double bridge at R^1 and R^2 in Dcy	C3SC3	$-(CH_2)_3S(CH_2)_3-$
C7F1	9,9-di(propylfluorene) (Figure 2)	CPhOC4OPhC	$-CH_2$-*p*-C_6H_4-O-$(CH_2)_4$-*p*-C_6H_4-CH_2-
An	9,10-anthracenediyl	BzoOC3OBzo	-C(O)-*m*-C_6H_4-O-$(CH_2)_3$-O-*m*-C_6H_4-C(O)-
Cy	1,3-cyclohexylene	BzoOpXyOBzo	as preceding with central *p*-xylylene group
Dur	1,4-durenyl	NapOC4ONap	(Figure 2)
mXy	*m*-xylylene (also pXy, oXy)		
	Risers in Vaulted Cyclidenes		
Dpp	4,4′-bipiperidine-1,1′-diyl (Figure 2)	Pip	piperazine-1,4-diyl (Figure 2)
	Axial Ligands		
Bipy	bipyridine	Ac	acetone
Py	pyridine	$4HOCH_2Py$	4-(hydroxymethyl)pyridine
MeIm	*N*-methylimidazole	DMF	dimethylformamide
An	acetonitrile		

[a] Terminal and bridging groups are distinguished implicitly, but terminal groups at the R^1 position in unbridged cyclidenes are also identified by a subscript 2 (e.g. Ac_2).

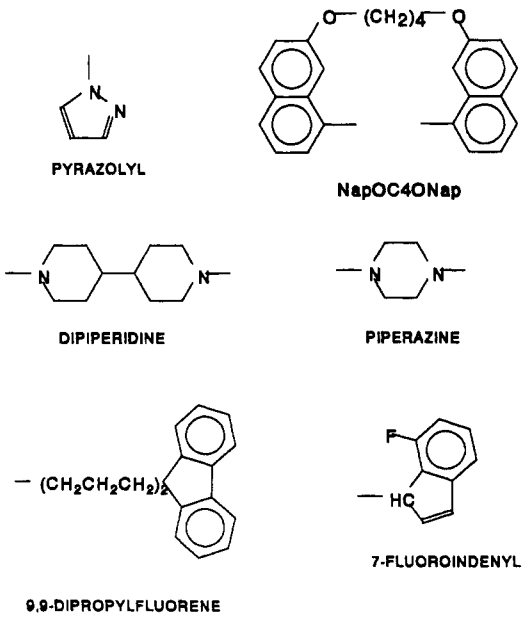

Figure 2. Identification of certain substituent groups for Table 1.

tural factors that determine dioxygen-binding ability and to distinguish electronic from spatial effects. Most attention has been paid to the cyclidene derivatives (and those closely related to them), but several other systems have been examined in less detail.

A. The Cyclidenes

A generalized structural formula for a lacunar cyclidene appears in Figure 1 (Cyc). The parent cyclidene macrocycle is defined to include the ring itself, which has been varied from 14 through 16 members (depending on X and Y) and the outwardly extending vinyl groups, along with their associated heteroatoms, the noncoordinated nitrogens. In a coordinated cyclidene, the four chelate rings are alternately saturated and unsaturated. In the unsaturated rings, conjugation extends from the donor nitrogens through the noncoordinated nitrogen atoms, which, in consequence, are planar (like the coordinated nitrogens). The unsaturated chelate rings are always 6-membered, and the variation in macrocyclic ring size is accomplished by altering the saturated chelate rings (X and Y) between 6- and 5-membered. The bicyclic character of the lacunar cyclidenes is produced by fusion of a second ring to the parent macrocycle at the extremity of the vinyl groups. In the majority of cases, the second ring links the noncoordinated nitrogen atoms (the R^1 position), but in the so-called retro-bridged cyclidenes the second ring connects the two R^3 positions; in the

Table 2. Structures of Lacunar Dioxygen Carriers and Their Cavity Dimensions

abbreviation	ref	width[a]	height	M-dev[b]
$Ni^{II}(Ac_2HMe[14]Jag)$	18	11.02	–	0.00
$Ni^{II}(Ac_2HMe[15]Jag)$	18	10.72	–	0.01
$Ni^{II}(Me_2Me[15]Mjg)$	18	7.23	–	0.05
$Ni^{II}(ClAc_2HMe[16]Jag)$	18	6.85	–	0.09
$Ni^{II}(Ac_2HMe[16Me_2]Jag)$	18	8.58	–	0.05
$Cu^{II}(H_2MeMe[16]Cyc)$	18	6.39	–	0.09
$Cu^{II}(Pz_2MeMe[16]Cyc)$	18	7.95	–	0.09
Cu^{II}(C3MeMe[16]Cyc)	19	4.90	4.27	0.17
Cu^{II}(C4MeMe[16]Cyc)	19	5.43	5.37	0.14
Ni^{II}(C5MeMe[16]Cyc)	19	6.42	5.65	0.08
Fe^{II}(C5HMe[16]Cyc)PyCO	20	6.27	5.88	0.05
Co^{III}(C5MeMe[16]Cyc)$(NCS)_2$	21	6.46	5.47	0.03
Ni^{II}(C6MeMe[15]Cyc)	22	7.12	4.63	0.03
Co^{II}(C6MeMe[16]Cyc)	23	6.74	5.13	0.06
Ni^{II}(C6MeMe[16MePic]Cyc)	50	6.94	4.82	0.08
Co^{III}(C6MeMe[16]Cyc)$(NCS)_2$	23	6.92	5.75	0.02
Co^{II}(C6MeMe[16]Cyc)ImO_2	24	6.76	5.91	0.08
Cu^{II}(C7MeMe[16]Cyc)	19	7.45	4.23	0.06
Cu^{II}((C3SC3)MeMe[16]Cyc)	19	7.52	3.81	0.04
Cu^{II}(C8MeMe[16]Cyc)	19	7.82	4.41	0.04
Ni^{II}(C8MePh[16]Cyc)	19	7.58	4.48	0.03
Co^{III}(C8MeMe[16]Cyc)$(NCS)_2$	24	7.69	5.54	0.01
Ni^{II}(C9MeMe[16]Cyc)	25	7.31	7.28	0.05
Ni^{II}(C10MeMe[16]Cyc)	25	6.81	6.88	0.09
Co^{III}(C11MeMe[16]Cyc)$(NCS)_2$	26	7.56	8.45	0.06
Ni^{II}(C12MeMe[16]Cyc)	19	5.80	9.92	0.10
Ni^{II}(C12MeMe[14]Cyc)	27	9.74	3.97	0.02
Fe^{II}(mXyHMe[16]Cyc)Cl	28	5.08	7.17	0.65
Fe^{II}(mXyMeMe[16]Cyc)Cl	28	7.26	5.02	0.54
Ni^{II}(mXyBzPh[16]Cyc)	29	7.27	4.82	0.04
Ni^{II}(mXyMeMe[$Me_2$16Me_2]Cyc)	30	7.32	4.38	0.03
Ni^{II}(mXyMePh[16]Cyc)	31	7.30	4.58	0.04
Ni^{II}(mXyNeoMe[16]Cyc)	31	7.26	4.55	0.02
Ni^{II}(pXyHMe[16]Cyc)	p	7.28	4.41	0.04
Ni^{II}(CyHMe[16]Cyc)	32	5.10	5.46	0.10
Ni^{II}((CPhOC4OPhC)MeMe [16]Cyc)	32	7.29	8.60	0.06
Co^{II}(C6Me(CH_2)[16]Cyd)	33	6.43	4.95	+
Co^{II}(C7Me[16]Cyf)	34	6.56	4.72	0.04
H_2[C6MeMe[16]Cyc]	35	–	–	–
H_5[(C3NHC3)HMe[16]Cyc]	35	–	–	–
$Co^{II}Co^{II}$(mXyHMe[16]Dcy)Cl	36	6.55	–	0.15
$Ni^{II}Ni^{II}$(mXyHMe[16]Dcy)	37	5.92	–	0.08
Ni^{II}(AnPipMe[16]Vcy)	38	5.77	8.48	0.08
Ni^{II}(pXyPipMe[16]Vcy)	39	6.32	8.16	0.04
Ni^{II}(DurDppMe[16]Vcy)	40	7.50	12.84	0.04
Ni^{II}(DurPipC8[16]Vcy)	41	6.94	8.28	0.05
Cu^{II}(H_2MeH{17NMe}Mal)	42	–	–	+
Cu^{II}((BzoOC3OBzo)MeH {17NMe}Mal)	42	6.29	5.84	+
Cu^{II}((BzoOC6OBzo)MeH {17NMe}Mal)	42	6.81	7.92	+
Ni^{II}(Ac_2MeH{12}Mal)	43	–	–	0.00
Ni^{II}(Ac_2MeMe{12}Mal)	43	–	–	0.00
Ni^{II}((BzoOC8OBzo)MeH{12}Mal)	44	9.40	6.72	0.00
Ni^{II}((BzoOC8OBzo)MeMe {12}Mal)	44	8.48	8.48	0.00
Co^{II}(DhaDhaF[14]Oxm)Py_2	45	–	–	0.00
Co^{II}(DhaDhaF{13}Oxm)Py_2	45	–	–	0.00
Co^{III}(MeMeF[14]Oxm)ClAn	46	–	–	0.01
Co^{III}(C12MeH{12}Oxm)ClPy	47	(7.68)	5.51	0.06
Ni^{II}((NapOC4Nap){24}Sal) Mol a	48	4.64	5.37	0.03
Mol b	48	4.90	6.75	0.04
Ni^{II}($(AcC)_2$[16]TAAB)	49	–	–	+

[a] Width definitions: Cyclidene and related systems—distance between outer nitrogen atoms (N3···N3); Malen and Salen—distance between ortho aromatic carbon atoms (e.g. C18···C38 in Figure 20; C116···C123 in Figure 23); oxime—distance between β carbon atoms of chain (though strictly this is not a width, as the chain passes to one side of the metal). [b] M-dev = Deviation of metal from coordination plane (normally of four nitrogen atoms); + = coordinated atoms not approximately planar; – = parameter not relevant to compound.

vaulted complexes, the bridging group rises equally from the R^1 and R^2 positions in the form of a cyclic moiety. Structural formulas for the subfamilies of cyclidenes are also shown in Figure 1 (Cyc, Cyd, Dcy, Vcy, Cyf).

For the cyclidenes, structures have been published for about 30 lacunar complexes, as well as seven related unbridged systems and two metal-free ligands. The unbridged complexes can themselves be dioxygen carriers, but are most important for the information they provide on basic structural relationships.

Structures have also been determined for a number of vaulted cyclidenes (Vcy). In these, rigid risers inserted between the parent cyclidene and the bridging group enlarge the cavity with the result that organic molecules can be enclosed therein, and guest–host complexation is added to their dioxygen-carrying capability.[38-40] Although these are, in a strict sense, lacunar complexes, they are distinguished from the main examples by their large cavities and are only considered briefly. The structures of two dimeric cyclidene complexes of Ni(II) and Co(II)[36,37] provide more substantial structural differences, and the unusual interaction of the cobalt(II) complex with O_2 is of considerable interest. Dimeric macrocyclic cobalt complexes synthesized by Martell and co-workers[51,52] bind oxygen between the two metal atoms, but such a behavior among dinuclear cyclidenes is unlikely because of relatively long obligatory separations between the metal ions. Martell's complexes are not considered here, because their O_2 binding sites are an integral part of the metal complex with the parent macrocycle or macrobicycle, rather than being created by the addition of a superstructure to a macrocyclic complex.

Within the lacunar cyclidenes (Figure 1), the following features, in the order of discussion to follow, have been altered among the published structures: (i) Metal ions have included nickel(II), cobalt(II) and (III), copper(II), and iron(II). (ii) The ring size of the parent cyclidene macrocycle ranges from 14 through 16. (iii) The bridge (R_1) has included polymethylene chains from trimethylene through dodecamethylene, aromatic groups, aliphatic cyclic groups, combinations of aliphatic and aromatic groups, and substitutional and isomeric derivatives. (iv) The substituents at bridge origin, R^2 and R^3, have been altered to change steric and electronic effects. (v) The center methylene positions on the saturated X and Y chelate rings in the [16]cyclidene system have been replaced by *gem*-dimethyl groups. (vi) The so-called "axial ligands", the groups coordinated to the metal ion that are not parts of the macrocycle vary from none to dioxygen, carbon monoxide, thiocyanate, chloride ion, and most commonly, the nitrogen bases pyridine and *N*-methylimidazole. Of these, changing the size of the parent cyclidene macrocycle (ii) and changing the group that bridges over the macrocycle (iii) exert the greatest influences on the structures. The metals and their oxidation states (i) are, of course, vital in conferring the ability to bind O_2, but have surprisingly small spatial consequences. In fact, protons can generate ligand stereochemistries very similar to those in the metal complexes. Similarly, substitution at R^2 and R^3 (iv) generally produces subtle electronic effects rather than obvious effects on the general features of the structures. Not surprisingly, understanding the effect of groups

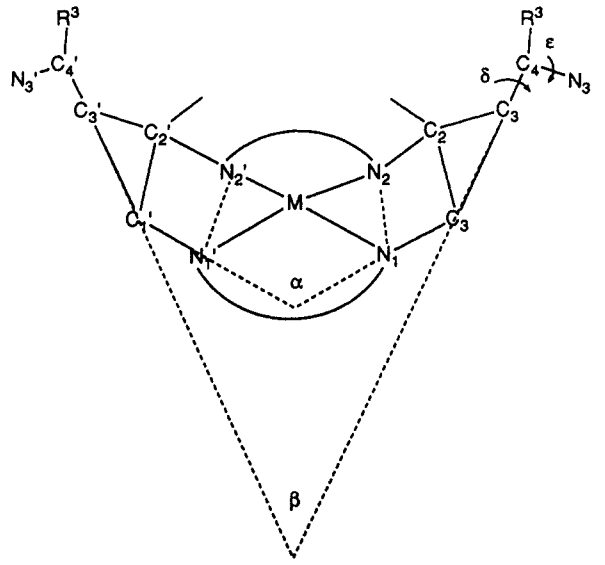

Figure 3. Structural parameters defining the cyclidene unit: α, angle between opposite $[N_1N_2C_1C_2]$ planes; β, angle between opposite $[C_1C_2C_3]$ planes; ($\gamma \simeq 0.5(\beta - \alpha)$); Δ, torsion angle $C_2C_3C_4N_3$; ϵ, torsion angle $C_3C_4N_3C$ (chain).

within the cavity (vi) proves to be critical to the understanding of dioxygen-binding ability. These effects depend greatly on the nature of the bridging group (iii).

Systematic structural correlations within the cyclidene family have been examined in three major papers, addressing the geometries respectively of unbridged systems,[18] of cyclidenes bridged by C3–C8 polymethylene chains,[19] and of those with longer chains.[25] Details of correlated distortions in the cyclidene unit are discussed in refs 18 and 19, including the variation in the angular parameters $\langle \alpha$ to $\epsilon \rangle$ identified in Figure 3. Here we focus on the overall effect on the cavity dimensions. Although van der Waals' contacts need to be considered in calculating how easily a ligand or guest will fit into the cavity, it is more convenient for simple comparisons to use distances between atom centers. The width of the cyclidene cavity can be straightforwardly specified by the distance between the outermost heteroatoms (noncoordinated nitrogens N3···N3′ in Figure 3); this distance is most directly controlled by the bridging group. In the narrower cyclidenes the C4···C4′ (Figure 3) atoms are slightly further apart, while with longer chains, they are slightly closer together, these differences relating to rotation about the vinyl group. This distance is also affected by torsion about the C–N bond (angle ϵ in Figure 3).

The height of the cyclidene cavity is less precisely defined because the bridge rarely passes directly above the metal, but for our purposes it is approximated by the distance from the metal to the central atom of the bridge (or central bond as appropriate), even though this direction is not perpendicular to the metal coordination plane. With planar bridges (xylyl groups), the obliquity of the ring must also be considered, because the heights at front and back of the cavity are different.

1. The Metal Ion

The dioxygen-carrying metal ions iron(II) and cobalt(II) are of main concern, and their study has revealed a close structural parallel to the well-known chemistry of porphyrins and heme proteins. The metal ions whose cyclidene complexes have been subjected to X-ray crystal structure determination are Fe(II), Co(II) and (III), Ni(II), and Cu(II). Structures have also been determined on two metal-free protonated ligand salts. Nickel(II) and copper(II) are included because ligand syntheses are accomplished by template reactions. For those cases where the metal ion essentially resides in the coordination plane, all metal–N distances are about 1.9 Å, with Ni^{II}–N the shortest (ca. 1.88 Å), and low-spin Fe–N the longest (1.99 Å[20]). The easily understood exception occurs for the chloro complexes of Fe(II)[28] which are high spin and, therefore, have substantially longer Fe–N distances (2.11–2.12 Å mean). This expansion is accommodated by displacement of the metal ion out of the N_4 plane by some 0.5 to 0.6 Å, resulting in a pyramidal coordination geometry, while maintaining the usual ligand shape. This pattern of structural behavior closely parallels that well-known for the metalloporphyrins and the heme proteins. Apart from the high-spin iron(II) examples, the metal ions are almost in plane (Table 2), the normal apparently random fluctuations being no more than 0.1 Å; larger deviations are correlated much more with the ligand geometry than with the nominal metal size. Thus, the cavities in the polymethylene-bridged complexes increase in width, as the bridge changes from C3 to C4 to C5, and the out of plane deviations for the metal ion decrease from 0.17 to 0.14 to 0.08 Å.

Two protonated metal-free lacunar ligands have also been characterized.[35] In one, two protons take the place of the central metal ion and the conformation is very close to that of the corresponding metal complexes. However, the other is pentaprotonated and assumes an entirely different everted geometry.

2. Size of the Cyclidene Ring

The size of the parent cyclidene macrocycle is easily controlled by varying the lengths of the saturated chains (X and Y in Figure 1), and remarkable structural effects have been observed despite the modest range of ring sizes so far examined (14, 15, and 16 atoms). The general result is that [16]cyclidenes adopt saddle-shaped conformations that are well suited to formation of lacunar derivatives while [14]cyclidenes are planar and not easily converted into lacunar derivatives. As one might suspect, [15]cyclidenes can exist in either form, and all of these molecular shapes are determined by the conformational selectivities of the saturated chelate rings.

The ring-size effects are least ambiguous for the unbridged complexes because those structures are unaffected by any possible distortions associated with bridge formation.[18] The overall structural pattern is determined by the conformational preference (energies) of the saturated chelate rings. The 5-membered rings tend to be gauche, while 6-membered chelate rings show almost equal preference for boat or chair conformations (and are sometimes disordered).

The combination of two 5-membered rings in [14]-cyclidenes leads to an essentially planar macrocycle, only buckled sufficiently to give gauche conformations to the $N(CH_2)_2N$ links. This is dramatized by the edge-on view of the macrocycle in Figure 4a, wherein the dimethylene chain is nearest the viewer. An important consequence is that the unsaturated chelate rings lie in the N_4 plane. In contrast, with two 6-membered chelate

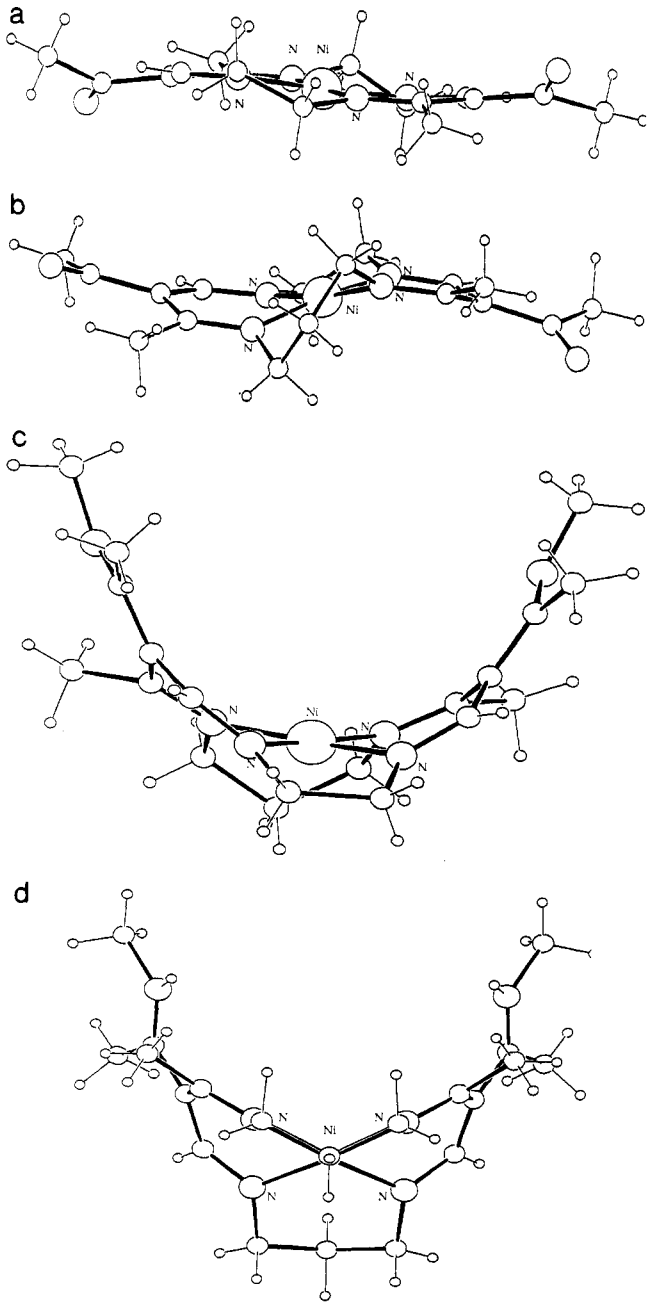

Figure 4. The effect of varying macrocycle ring size in unbridged cyclidene and related complexes (a) a [14] ring, Ni^{II}(Ac2HMe[14]Jag); (b) a flat [15] ring, Ni^{II}(Ac2HMe[15]-Jag); (c) a buckled [15] ring, Ni^{II}(Me2Me[15]Mjg) (252:3C) (d) a [16] ring, Ni^{II}(Tca2HMe[16]Jag).

rings, the presence of two chair or boat conformers for the saturated chelate rings causes the macrocycle to adopt a saddle shape. This constitutes an incipient lacuna and places the uncoordinated nitrogen atoms in ideal orientations for bridging. In Figure 4d the center methylene group of the near trimethylene chain is superimposed on the metal atom, emphasizing the boat form of that chelate ring. The second 6-membered ring appears in the lower part of the picture and is clearly in the chair conformation. Summarizing results from a number of studies, the ideal unconstrained width (N···N) for a [16]cyclidene appears to be in the range 6–7 Å.

In the [15]cyclidenes, the conformational preferences of the 5- and 6-membered chelate rings are in conflict, and unbridged examples have been found both with a

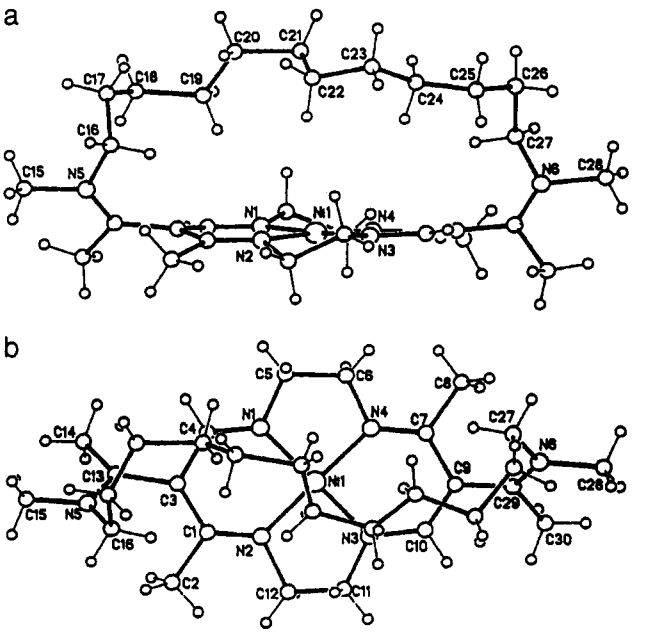

Figure 5. A cyclidene complex having a 14-membered cyclidene ring with $-(CH_2)_{12}-$ bridge, Ni^{II}(C12MeMe[14]Cyc).

planar conformation that is favored by the 5-membered chelate ring (Figure 4b) and with the saddle-shaped conformation preferred by the 6-membered chelate ring (Figure 4c). In Figure 4b the 6-membered saturated chelate ring is nearest the viewer and the disfavored skew conformation is clearly shown. Similarly, Figure 4c displays a high-energy eclipsed dimethylene conformation.

For the [16]cyclidenes, the formation of bridges does not affect the overall geometry; all take up saddle shapes, varying from shallow to steep, depending on the bridge length and the substituents (sections iii and iv). The [14]cyclidene maintains its planar array and is difficult to bridge, requiring exceptionally long chains. Figure 5 shows the structure of a $(-(CH_2)_{12}-)$-bridged [14]cyclidene.[27] The [14]cyclidene provides only the floor for the very shallow cavity. The one bridged [15]-cyclidene has a saddle rather than planar conformation and a comparatively short $-(CH_2)_6-$ bridging group.

The planarity of the [14]cyclidenes is accomplished by a deviation in diastereomeric structure as well. Although their formation reactions are identical to those for [15] and [16] rings, the ring-closing reaction causes isomerization from the usual *cis* to a *trans* location of the two methyl groups that are attached directly to the cyclidene ring. A steric response to this *trans* orientation of the relatively bulky methyl groups has the effect of directing the C12 bridge along a symmetrical path across the top of the metal atom (Figure 5B).

3. Variation of the Bridge (R^1)

The most powerful influence on the dioxygen-carrying ability of the lacunar complexes is the steric control exercised by the cavity itself, and this is mainly determined by the bridging group. Fine-tuning of the cavity size has been achieved using $-(CH_2)_n-$ chains of various lengths as bridges, and structures of lacunar complexes have been determined for all n in the range from 3 to 12 (n = 2 is too short to produce a lacunar complex).[19,25] Structures have also been determined for cyclidenes with more rigid bridges made up of *m*-

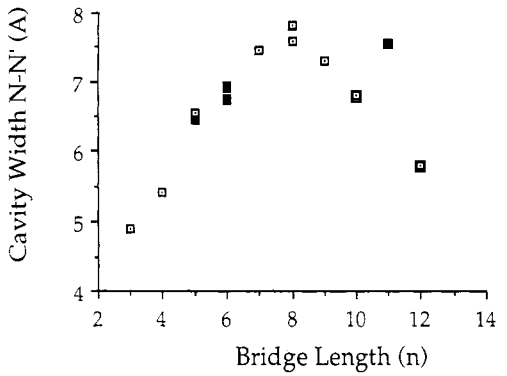

Figure 6. Correlation of cavity width with chain length for polymethylene-bridged cyclidenes complexes. Open squares indicate empty cavities and solid squares, occupied cavities.

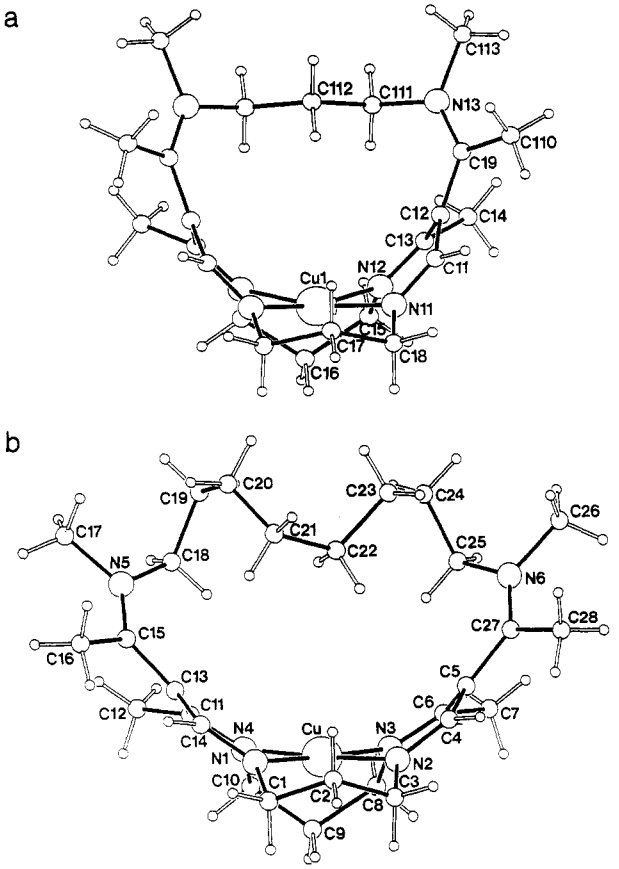

Figure 7. Narrow and wide polymethylene-bridged cyclidenes: (a) Cu^{II}(C3MeMe[16]Cyc) and (b) Cu^{II}(C8MeMe-[16]Cyc).

and *p*-xylylene, 1,3-cyclohexylene, and ($CH_2PhO(CH_2)_4OPhCH_2$) groups (Table 2).

For the polymethylene bridges, the width of the cavity has a remarkably precise linear correlation[26] with chain length for n = 3–8, the N···N distance (as defined in Figure 3) increasing from 4.9 to 7.8 Å (Figure 6). Figure 7, parts a and b, indicates the contrast between the narrowest and widest cavities, which are associated with, respectively, 3 and 8 carbon chains. Despite its intrinsic flexibility, the $-(CH_2)_8-$ chain stretches the cyclidene cavity beyond its ideal width of ca. 6.0 Å.[19,53] Correspondingly, the trimethylene bridge compresses the cavity from its ideal width to 4.9 Å. With the exception of the bridging groups themselves, all of these complexes (n = 3–8) have very similar structures. This is particularly true with regard to the points of departure

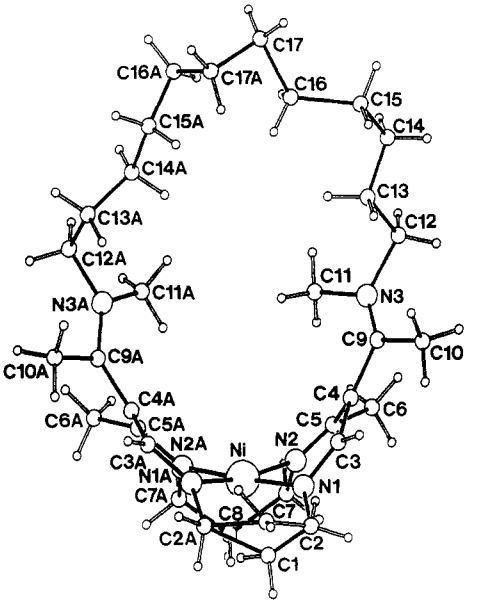

Figure 8. The $(-(CH_2)_{12}-)$-bridged cyclidene complex Ni^{II}-(C12MeMe[16]Cyc), showing the lid-on conformation of the outermost nitrogen atoms (contrast Figure 7b).

of the bridging group from the parent macrocycle. Because of its planar structure and orientation, the two remaining bonds of the noncoordinated nitrogen atoms point in distinctly different directions: one almost vertically and the other almost parallel to the N_4 plane. The bridges in all of these cyclidene complexes are attached at the parallel nitrogen linkages causing the bridge to be offset from the center of the N_4 plane, and representing what is called the "lid-off" isomer.

When n is 9–12, the cavity width gradually returns to its ideal value as the chain becomes more flexible.[25,26] This narrowing is accompanied by a conformational change from "lid-off" to "lid-on" at the outermost nitrogen atoms,[25] so that in the $-(CH_2)_{12}-$ species the chain points upward and the inward-pointing methyl groups block one side of the cavity (Figure 8; contrast Figure 7b). A remarkable aspect of this transition from the lid-off to the lid-on isomer is the gradual change in the orientation of the bridging groups. At C9, one side of the bridge is simply connected in the lid-off position while the other is disordered between the two structures. At C10, disorder also occurs, but in the lid-off component while one link is strictly lid-on.

The characteristic features of the aromatic bridges is their inflexibility, low roofs,[2,28–31] with metal to ring-center distances in the range 4.4–4.8 Å, and cavity widths approaching the widest found for polymethylene bridges. The one *p*-xylylene-bridged complex and most *m*-xylylene derivatives have N···N distances of ca. 7.2 Å (Figure 9). The *m*-xylylene-[28,32] and cyclohexylene-bridged species having R^2 = H exist in the lid-on conformation rather than lid-off form,[28] and this produces extremely narrow cavities (ca. 5.1 Å), barely wider than that found for the $-(CH_2)_3-$ bridge; these narrow lid-on complexes can also have exceptionally high cavities (7.2 Å for *m*-xylylene; 5.5 Å for cyclohexylene) (Figure 10).

The vaulted complexes combine inflexible aromatic roofs with rigid risers, but their greater height lifts the restriction imposed by the low roofs of the lacunar aromatic complexes (Figure 11A).[39] In the solid state,

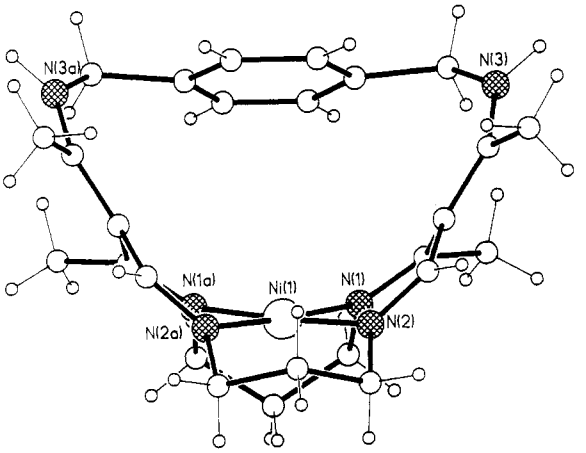

Figure 9. A *p*-xylylene-bridged cyclidene, Ni^{II}(pXyHMe-[16]Cyc).

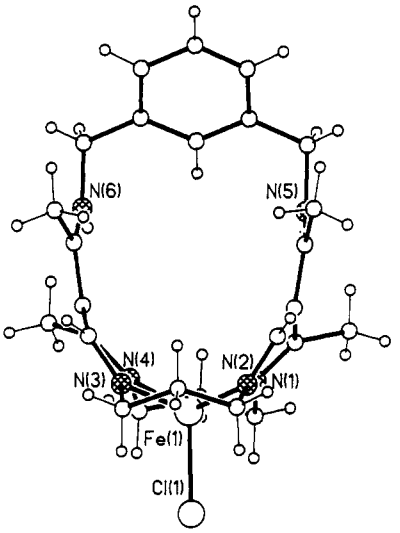

Figure 10. A lid-on *m*-xylylene-bridged cyclidene complex, Fe^{II}(mXyHMe[16]Cyc)Cl; contrast Figure 9.

it is characteristic of these complexes that the piperazine risers are pivoted inward so that they are almost mutually perpendicular, considerably restricting the cavity. A vaulted cyclidene also provides the only structure available on a "retro-bridged" cyclidene[41] (with the bridge spanning the R^3 positions) (Figure 11B).

4. The Substituents at R^2 and R^3

The standard substituents, $R^2 = R^3 = CH_3$, are present in the great majority of determined structures. Most other substituents have predominantly electronic rather than steric effects on the cavities, or influence its accessibility. Even the replacement[24] of the methyl at R^2 by neopentyl hardly changes the cavity dimensions. The exception to this generalization arises when R^2 = H, as described in the previous section. The changes described above seem specific to the cyclic xylylene and cyclohexylene bridges since the $(-(CH_2)_5-)$-bridged complex is hardly changed by replacing Me by H at R^2.

A more radical change in R^3 involves its deprotonation, converting the dication to a neutral complex.[33] The charge on the ligand and the presence of the vinyl group at R^3 leads to significant changes in the conjugation of the cyclidene system and, therefore, to the classification of the complex in a different structural group. The reduced C3–C4 (Figure 3) double-bond

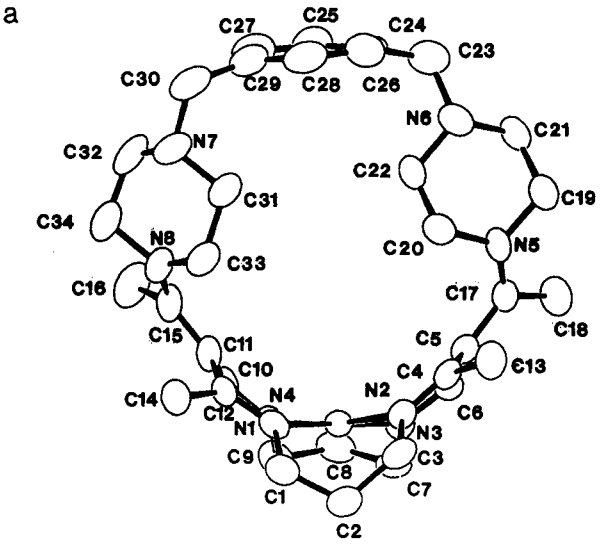

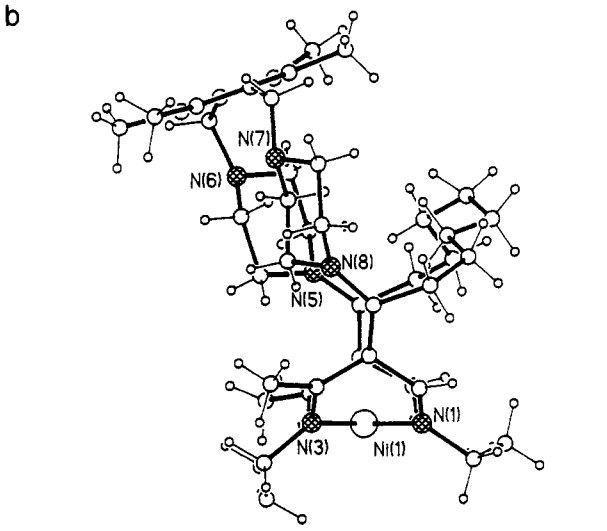

Figure 11. (a) A vaulted cyclidene, Ni^{II}(pXyPipMe[16]Vcy) and (b) vaulted and back-bridged cyclidene, Ni^{II}(DurPipC8-[16]Vcy).

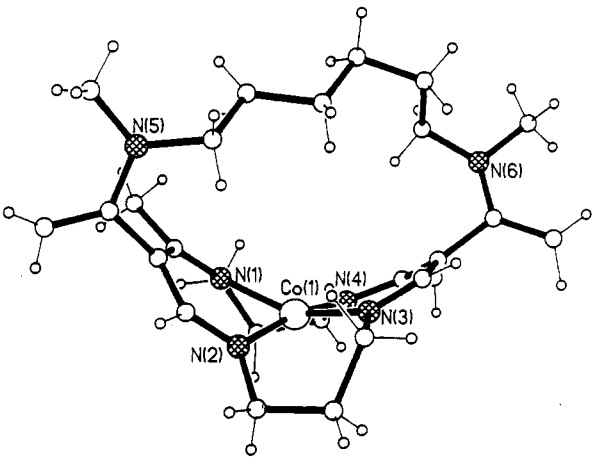

Figure 12. Structure of deprotonated cyclidene complex, Co^{II}(C6Me(CH_2)16]Cyd).

character allows one of these bonds to adopt a torsion angle of 75° rather than the usual 15–25°. The four donor nitrogens are nonplanar and the cavity is noticeably unsymmetrical, although its overall dimensions are not greatly altered (Figure 12).[33]

Still more radical is the fusion of a cyclohexyl ring between R^3 and the primary cyclidene backbone (Figure

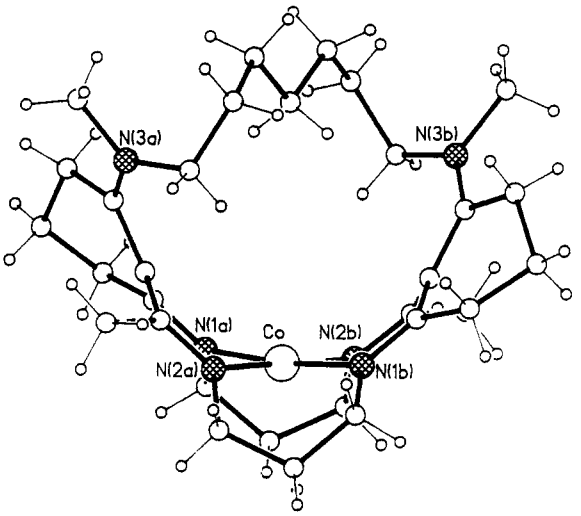

Figure 13. Structure of the cyclohexyl-fused cyclidene complex containing fused cyclohexyl groups, Co^{II}(C7Me[16]-Cyf).

13).[34] These rings fuse in "opposite directions" so that the symmetry of the complex is C_2, rather than C_s, and the ring proceeds diagonally across the structure, passing over the middle of the CoN_4 plane. The attachment of the C7 bridge is lid-off, but in a *trans* rather than the usual *cis* configuration.

5. Substituents on the Saturated Rings

Substituents have been attached to the saturated ring to either alter the steric bulk and hydrophilic/hydrophobic character of the cavity, or provide pendant groups for coordination to the metal ion as axial ligands. To add steric bulk, *gem*-dimethyl groups have been placed individually on rings X and Y and simultaneously on both rings;[30] the structure of the doubly substituted complex (Figure 14) shows that the Me_2 groups on the Y-ring effectively block the entrance to the cavity. When the bridge is aromatic (as here), its rigidity prevents the bridge from moving aside to accommodate a bound ligand. In order to accommodate an axial ligand, the X-ring must take up a chair conformation (unlike the boat form in Figure 14), leading to severe repulsions.

The attaching of a pendant group to either the X or Y rings poses synthetic problems because of isomer possibilities, only the *exo* isomer being suitable for coordination to the metal. Structural determination[50] confirmed one species as the *exo* isomer and the pendant group produced a model for the T state of hemoglobin (see Table 6).

6. Axial Ligands

The lacunar cyclidenes have provided a unique opportunity to study the interaction between small axial ligands and the cavities which contain them. The structures of complexes with intercavity ligands are important both from the standpoint of the influence of the cavity on the ligand binding and from that of the effects of the ligand on the shape of the cavity. Both are dependent on the rigidity of the system. The most rigid bridges are probably the *m*- and *p*-xylylene groups, and no crystal structures are known in which they are combined with bound ligands because of the failure of all attempts to crystallize these complexes with their cavities occupied. As described above, short polymethylene chains also produce small highly inflexible cavities. Indeed, the C3 bridge appears to prevent ligand binding completely;[54] the C4 bridge permits weak binding but, like the xylylene bridges, no complexes have been isolated with internal axial ligands. The C5 bridge yields a variety of 6-coordinate complexes having intracavity ligands, but the dimensions of the cavity are only slightly affected by the presence of the small ligand.[20] The strain appears to be applied mainly to the metal–ligand bond, producing strongly distorted bond angles and stretched bond distances. With the $(-(CH_2)_5-)$-bridged cobalt(III) bis(thiocyanate) complex[21] not only is the Co–N vector of the included NCS inclined at 5 °C from the normal to the $M-N_4$ plane, but the Co–N–C angle is only 141° (Figure 15). A similar distortion is found in the Fe–CO complex with a $-(CH_2)_5-$ bridge, in which the Fe–C–O angle is 170.6°.[20]

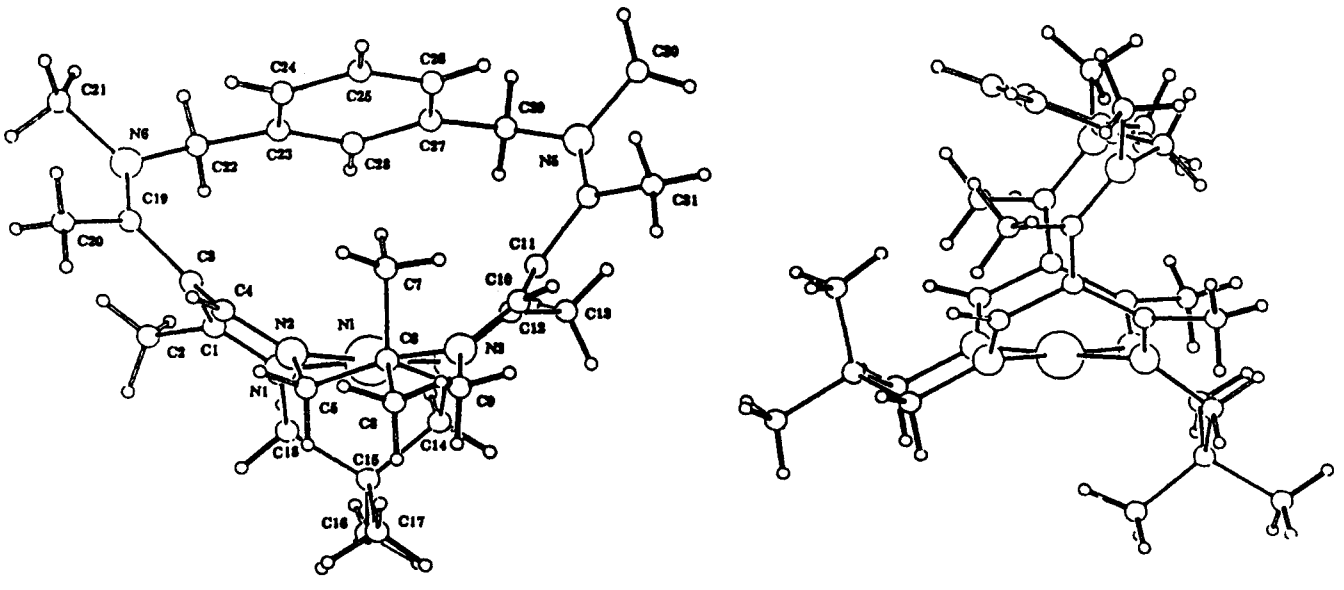

Figure 14. *gem*-Dimethyl substitution on both the X and Y rings, Ni^{II}(mXyMeMe[$Me_2$16Me_2]Cyc).

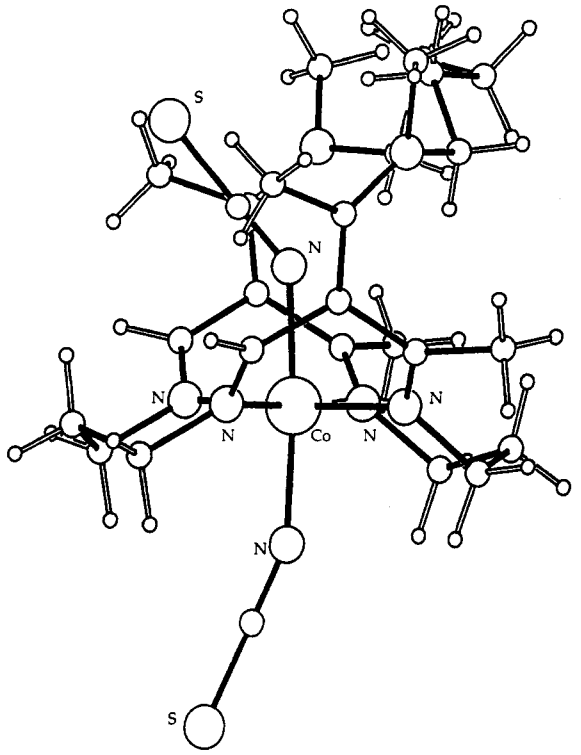

Figure 15. Distorted NCS^- groups inside and outside a small cyclidene cavity, Co^{III}(C5MeMe[16]Cyc)$(NCS)_2$.

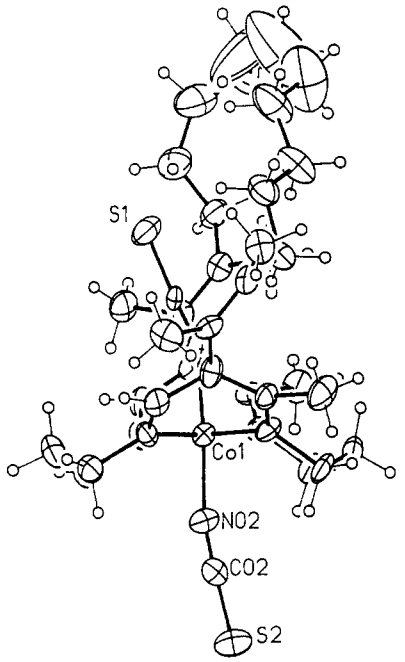

Figure 16. Distorted NCS^- groups inside and outside a cyclidene cavity bridged by a $-(CH_2)_{11}-$ chain, Co^{III}(C11MeMe-[16]Cyc)$(NCS)_2$.

In these complexes, the bridge conformation is virtually identical in unoccupied and occupied cavities. Thus, chains of moderately short length (C4 and C5) allow binding but provide inflexible cavities. Somewhat longer chains (C6 to C8) can adopt different low-energy conformations to facilitate binding,[15,53] while the longest chains will both alter their conformations and allow the cavity width to adjust itself to the ligand (Figure 16).[26]

The complexes in which O_2 itself is bound within the cavity have generally proved intractable to crystallographic characterization although one structure has been determined, as has one for a complex with CO bound to iron(II). However, for the case of cobalt(III), stable bis(isothiocyanato) complexes can readily be obtained. The binding of SCN^- within the cavity is significantly affected by steric effects, and itself influences the cavity geometry. It thus provides a valuable surrogate for bound O_2, without the instability inevitable for the latter complexes.

Before continuing with the main subject of ligand binding within the cavity, brief attention must be given to related considerations. Both Co^{II}– and Fe^{II}–cyclidene complexes require an externally coordinated base in order to function as dioxygen carriers. The constraints this imposes are generally minimal, although both X and Y chelate rings in the [16]cyclidene must assume the chair conformation in order to accommodate the external axial ligand; this is in contrast to the chair–boat conformations often observed for 4-coordinate cyclidenes. In complexes with NCS^-, it is clear from the geometry of the *external* NCS^- groups that its coordination to Co(III) is relatively flexible. Although the N–C–S angle is always close to 180°, the Co–N–C angle can be significantly smaller, in one case as low as 157° because of packing interactions (Figures 15 and 16).

Distortions due to the interactions within the cavity can be considerably greater than those observed for the external NCS groups, and this is shown for the C6- and C8-bridged complexes. Binding NCS^- within the cavity of the $(-(CH_2)_8-)$-bridged cyclidene changes the cavity width only marginally (N···N 7.69 Å), and the Co–N–C angle is 157°, showing only modest distortion.[23,24,53] The most significant effect is seen in the chain conformation. In the absence of a ligand, the chain folds inward, essentially minimizing the cavity volume and maximizing van der Waals contacts (Figure 17b); when a ligand is present, the chain unfolds, extending outward to reduce (and probably eliminate) repulsions between it and the NCS^- (Figure 17a). While first observed for the C6-bridged systems.[23,24] These changes were predicted for C7 and C8 on the basis of molecular modeling studies.[53] Subsequent experimental results confirmed the predictions of those modeling studies.

The two NCS^- complexes with longer bridges illuminate other steric effects in the cyclidene cavity. With a $-(CH_2)_{11}-$ bridge (Figure 16),[26] the cavity width (N···N) is 7.56 Å, almost as large as that for the empty $-(CH_2)_8-$ complex and much larger than expected from interpolation between $-(CH_2)_{10}-$ and $-(CH_2)_{12}-$ (ca. 6.3 Å) (Figure 6). Thus, with this flexible chain, the cavity can expand to the optimum size for binding a ligand (of course with an energy penalty that is absent for the "prestretched" $-(CH_2)_8-$ complex). The $-(CH_2)_{11}-$ chain itself shows a similar attachment (half lid-on and half lid-off) to those of the $n = 9$ and 10 bridges,[25] and it passes over the top of the mildly distorted NCS^- group (Co–N–C angle 156°).

The most significant structure of all those determined for the cyclidenes is undoubtedly that of the O_2 adduct,[24] Co(C6MeMe[16]Cyc)(MeIm)$(O_2)^{2+}$. This fully confirms the expectations derived from the investigation of many other compounds in its geometry and ligand organization (Figure 18). The Co–O–O angle is 121°,

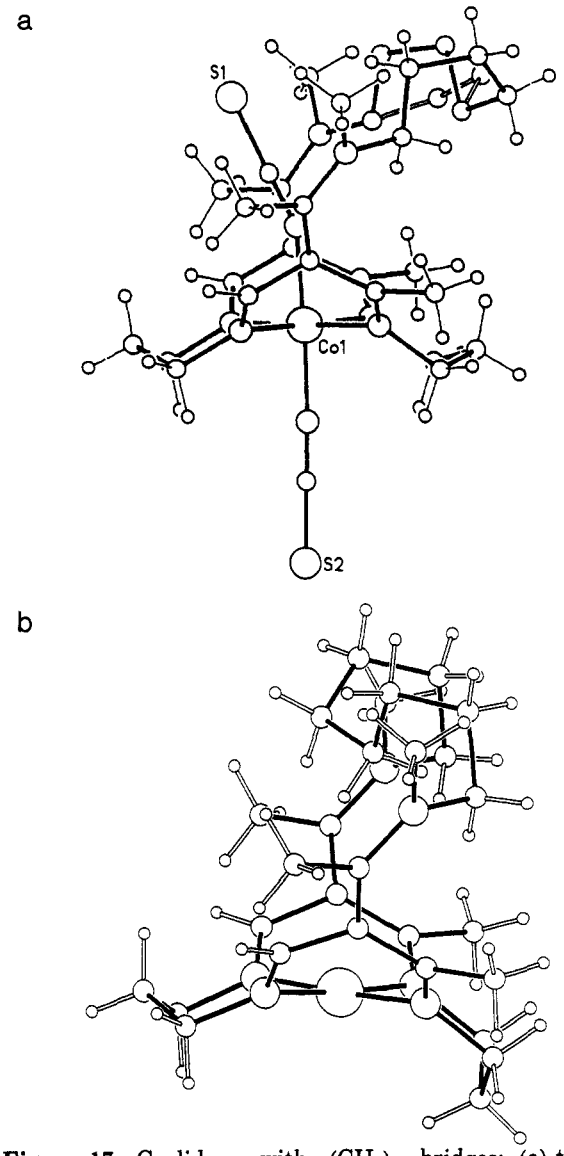

Figure 17. Cyclidenes with $-(CH_2)_8-$ bridges: (a) the Co-$(NCS)_2$ complex, Co^{III}(C8MeMe[16]Cyc)$(NCS)_2$; (b) Cu complex without additional ligands, Cu^{II}(C8MeMe[16]Cyc) (cf. Figure 7b).

and O–O distance 1.32(2) Å, as expected for a coordinated superoxide.[55] The cavity is unaltered in width on coordination, but the bridge folds away from the ligand, in exactly the same fashion as for the $-(CH_2)_8-$ bis(thiocyanato) complex. The longer polymethylene bridges generally combine partial disorder with high thermal motion for their central atoms. This is particularly true for bridges with an even number of atoms, where the molecule often lies across a pseudomirror plane. In many cases, only the general conformation can be established and (as with this $-(CH_2)_6-$ bridge), it does not have a unique geometry.

B. Non-Cyclidene Lacunar Complexes

No other lacunar systems have been studied structurally in anything approaching the depth achieved for the cyclidenes. However these other systems provide interesting comparisons, highlighting the special features of the cyclidenes.

1. Malen Complexes

This family of ligands is derived from β-diketone and 1,3-dialdehyde (or diketone) Schiff bases and the

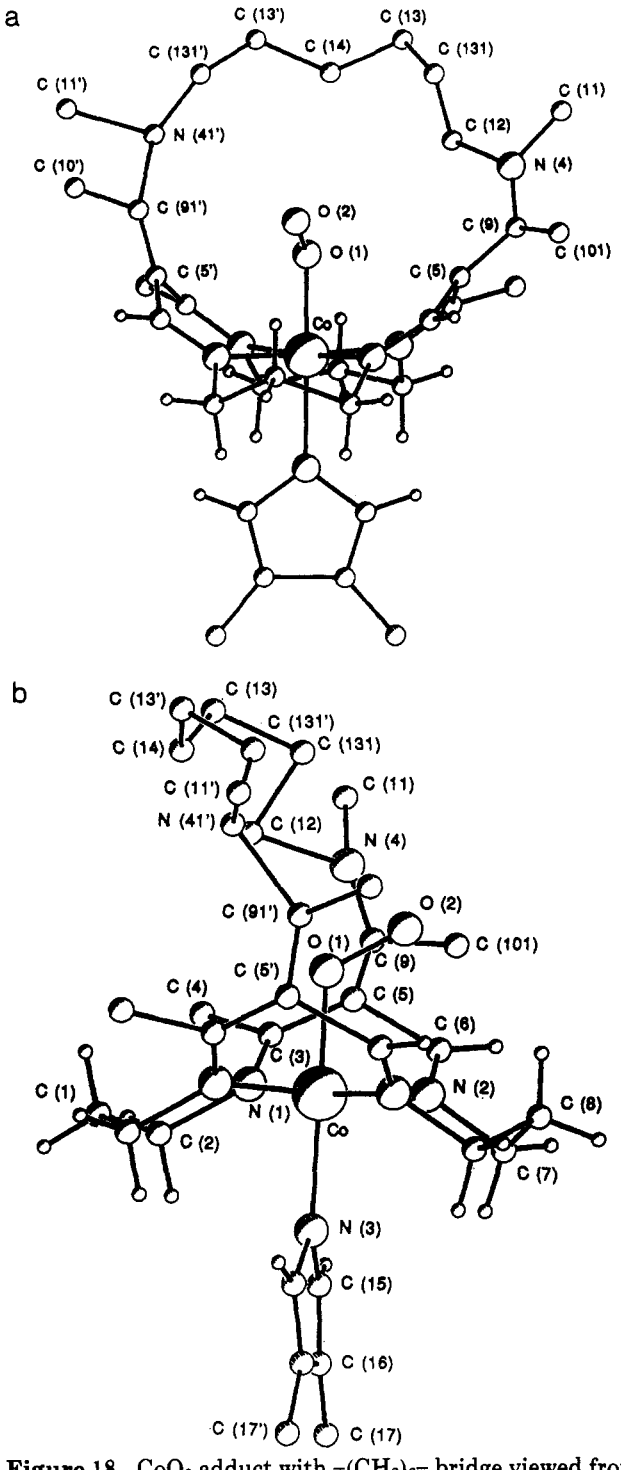

Figure 18. CoO_2 adduct with $-(CH_2)_6-$ bridge viewed from the front (a) and the side (b) of the cavity, Co^{II}(C6MeMe-[16]Cyc)ImO_2.

simplest example is that formed by ethylenediamine and 2 mol of acetylacetone, a ligand long abbreviated as acacen. We assign the root Mal to these derivatives because malonaldehyde is the simplest 1,3-dicarbonyl compound; therefore the ethylenediamine Schiff base of acetylacetone is a dimethyl-substituted derivative abbreviated as H_2MeMe{12}Mal. The structures of seven lacunar, or related, Mal complexes (Figure 1) have been reported. Unbridged complexes (R^1 = Ac) are essentially planar, although an interesting effect has been noted.[43] When both R^2 and R^3 are Me, repulsion between these groups and the terminal acetyl causes the latter to twist into a position perpendicular to the

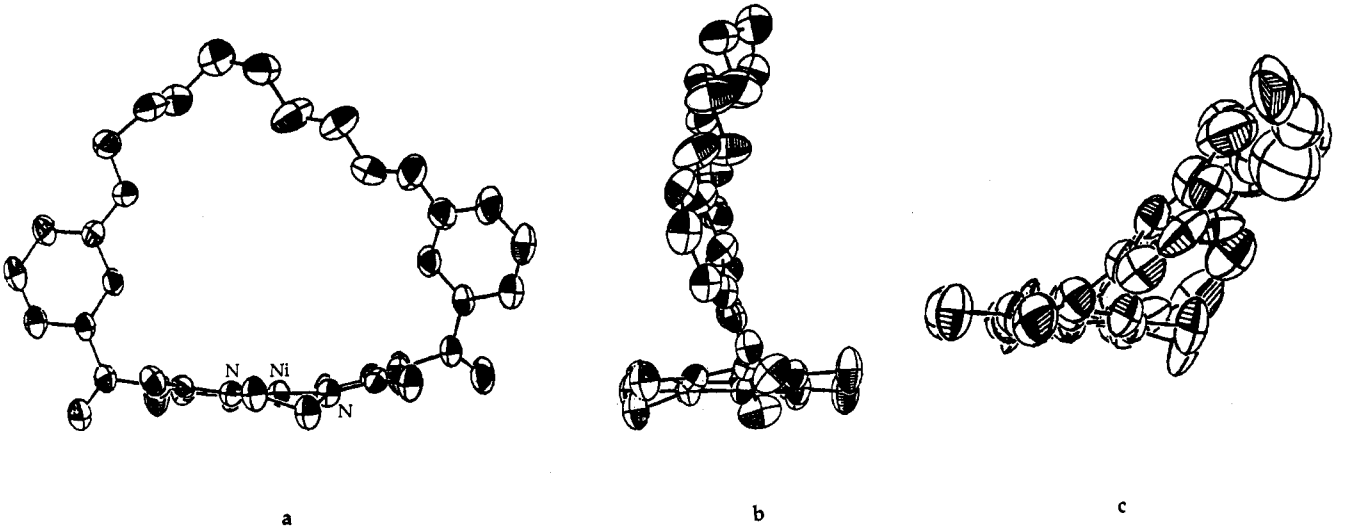

Figure 19. Structural variation in lacunar malen complexes (a), (b) two views of a complex with R^3 = Me, giving a vertically oriented bridge, Ni^{II}(BzoOC8OBzo)MeMe{12}Mal); (c) side view of the complex with R^3 = H (otherwise identical), Ni^{II}(BzoOC8OBzo)MeH{12}Mal).

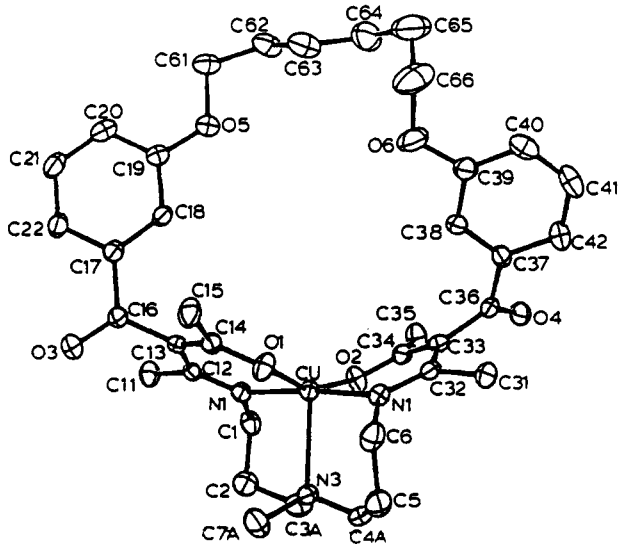

Figure 20. Mal complex with an internal axial base, Cu^{II}-((BzoOC6OBzo)MeH{17NMe}Mal).

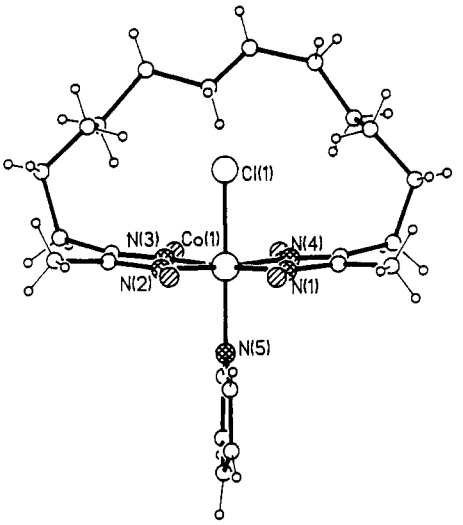

Figure 21. Lacunar oxime complex, Co^{III}(C12MeH{12}Oxm)-ClPy.

main ligand plane; exactly the same effect is found with a long bridge at R^1, leading to an interesting conformational variation (Figure 19).[44] Depending on the substituent at R^3, the bridge either stands straight up, or leans at an oblique angle (as a wall rather than a bridge). Clearly this provides a basis for designing Schiff base ligands in which a bridging group is suspended above a metal ion site.

A second favorable ligand design feature of the Mal ligands is the ease with which the fifth donor atom can be built into the structure. Replacing the C2 X-ring by a $-(CH_2)_3N(Me)(CH_2)_3-$ bridge, which passes across the metal atom, facilitates amine coordination at an axial position. This has the remarkable effect on the primary ligand of producing a *trans* orientation of imine and oxygen donors, rather than the *cis* arrangement that exists for the tetradentate ligands (Figure 20).

2. Oxime Complexes

Retey[47] first reported a bridged bis(α-dioxime) complex that constituted a sort of lacunar complex, but the bridge was confined to one side of the complex. An early structure shows the resulting geometry (Figure 21, bridging hydrogens are not shown). The oxime derivatives of greatest interest differ from simple bis-(α-dioxime) complexes by replacing the bridging hydrogen in the parent macrocycle by a bridging BF_2^+ group (Figure 1, Oxm). Recent structural work on these oxime derivatives has involved only nonlacunar systems.[45,46,56,66] In a recent structural variant the presence of 9,10-dihydroanthracene in the R^1 and R^2 positions greatly enhances the steric bulk of the ligand (Figure 22, Co–N bonds to axial pyridines have been omitted for clarity).

3. Salen Complexes

Salen was the ligand in the first synthetic dioxygen carrier; it is the Schiff base of ethylenediamine and salicylaldehyde (Figure 1, Sal). The aromatic rings of the salen complex have considerable potential for substitution, and unbridged substituted complexes have been investigated in other work, but in the studies considered here only the parent aldehyde has been employed. The lacunar complexes are produced using a lengthy X-ring to form a bridge across the cavity,

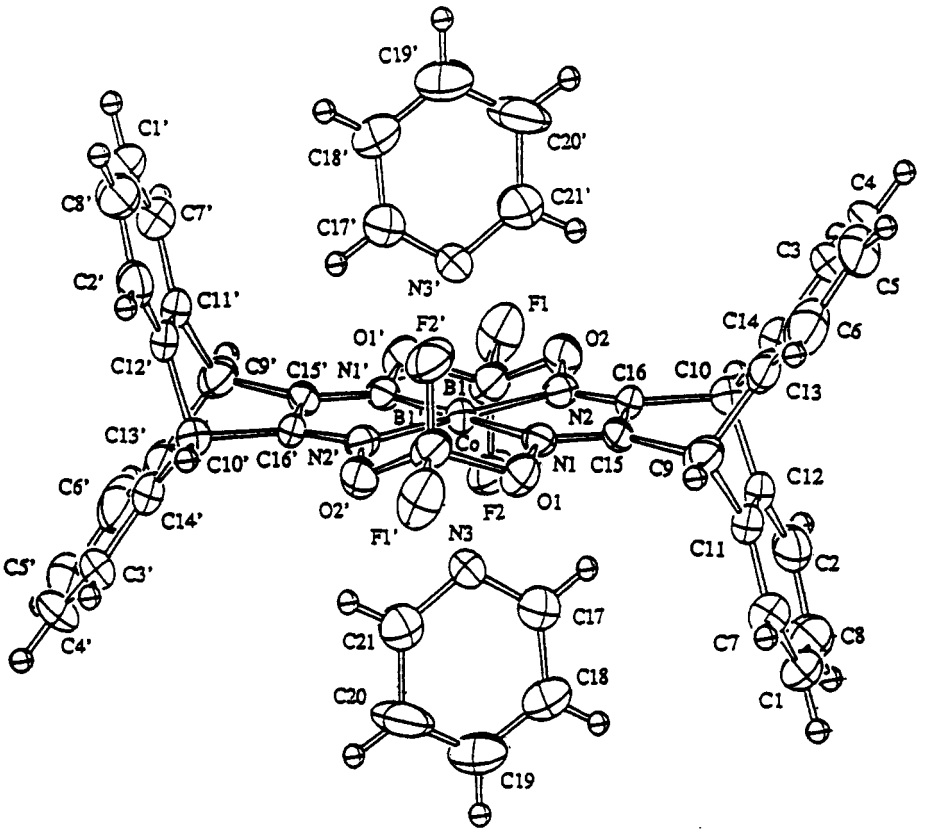

Figure 22. Unbridged oxime with 9,10-dihydroanthracene substituents, $Co^{II}(Dha_2F\{13\}Oxm)Py_2$.

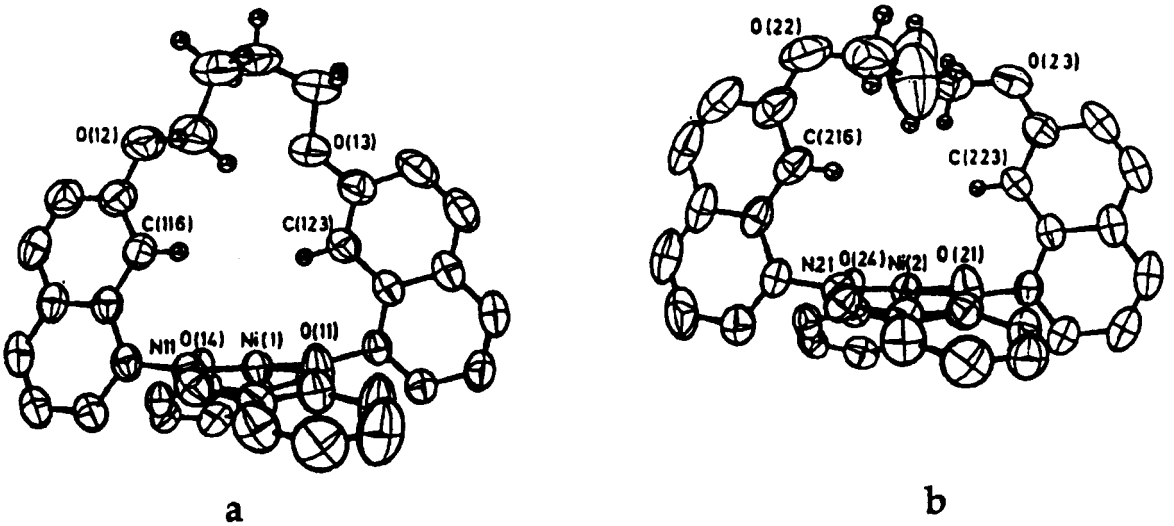

Figure 23. Lacunar salen complex, $Ni^{II}(\{(NapOC4ONap)24\})$.

suspended on naphthyl risers, giving a relatively large cavity; one structure has been determined.[48] Remarkably, the crystal contains two independent molecules which have very different bridge geometries, reminiscent of the bridge reorientation found for the long-chain cyclidenes (Figure 23).

4. TAAB (Anhydro Tetramer of o-Aminobenzaldehyde) Complexes

Lacunar complexes derived from the TAAB macrocycle (Figure 1, TAAB) have been prepared, containing both simple polymethylene chains[57] as bridging groups and more complex ones, but the only structure[49] so far reported is of an unbridged complex (Figure 24). This has a most interesting saddle shape with alternate aromatic rings bent up and down, reminiscent of the cyclidene system although rather flatter.

III. Synthesis and Properties of Lacunar Dioxygen Carriers

A. Synthesis of Lacunar Dioxygen Carriers

The design and synthesis of the lacunar dioxygen carriers is mainly a problem in organic synthesis, but with a number of special features either associated with the role of the metal ion in the synthesis or in the peculiar requirements of the target molecules. Most of the lacunar ligands were produced by the modification of known ligands, often with the use of the metal ion as a template and with special attention being given to

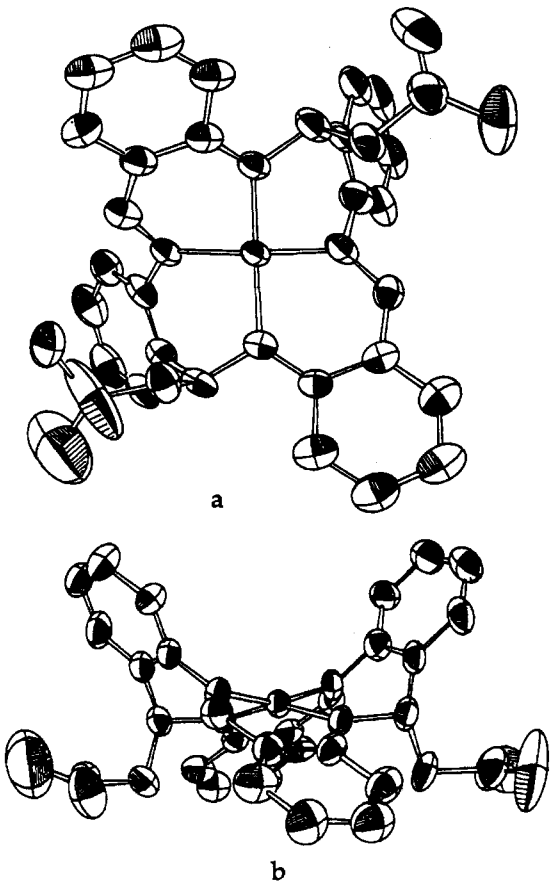

Figure 24. Structure of Ni(TAAB)$(CH_2COCH_3)_2$ (a) viewed from above the coordination plane and (b) looking toward the edge of the coordination plane.

creating the permanent void in the final structure. In condensed phases, truly flexible molecular structures tend to collapse on themselves thereby closing any cavity that might have been proposed in their design. The principles of molecular organization[58] assist in the molecular design.

The neutral, bicyclic lacunar cyclidene ligand is derived from the well-known family of dianionic tetraazamacrocyclic ligands developed by E. Jaeger and his students.[59,60] The critical reaction is the conversion of an appended carbonyl function into a vinyl ether group by reaction with a very strong alkyl cation source, such as methyl fluoro sulfate or methyl trifluoromethane sulfonate (Scheme 1).[1,29,61] The resulting functional group, ostensibly a vinyl ether, behaves rather like a carboxylic ester and addition–elimination reactions readily occur so that the alkoxy group is readily replaced by such groups as amine residues.[1,61,62] Further, the product of reaction with the amine is, like carboxamides, relatively unreactive and constitutes a stable product for further study or applications. The similarity of the functions to carboxylate derivatives is rationalized on the assumption that the double bond at the reactive site is conjugated to the strongly electron-withdrawing metal ion. The second ring closure, which produces the lacuna, is a template reaction using the nickel(II) ion.

The natural saddle shape of the [16]cyclidenes facilitates ring closure (Scheme 1) with diamines varying in length from 1,3-propanediamine to, at least, 1,12-dodecanediamine, and a variety of alkyldiamines containing other heteroatoms or aromatic rings.[1,25,29,30,32,54,63,64] The [15]cyclidenes, in their saddle

Scheme 1

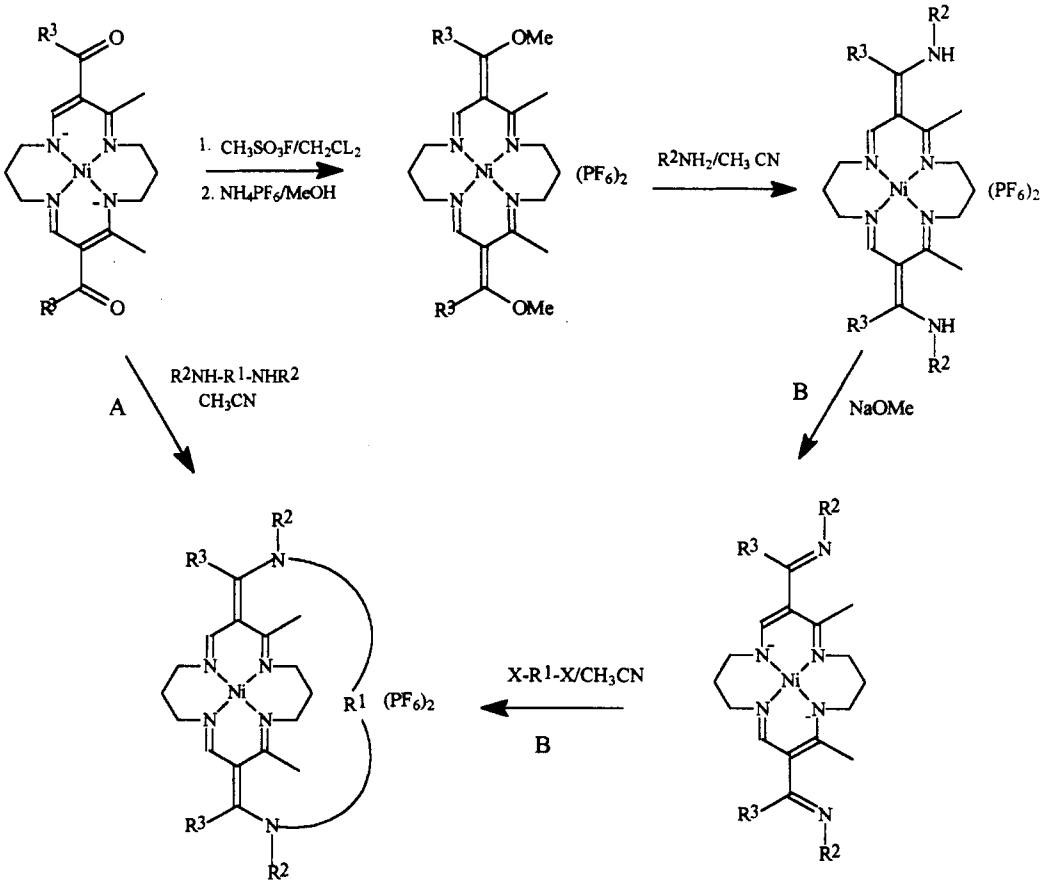

Scheme 2

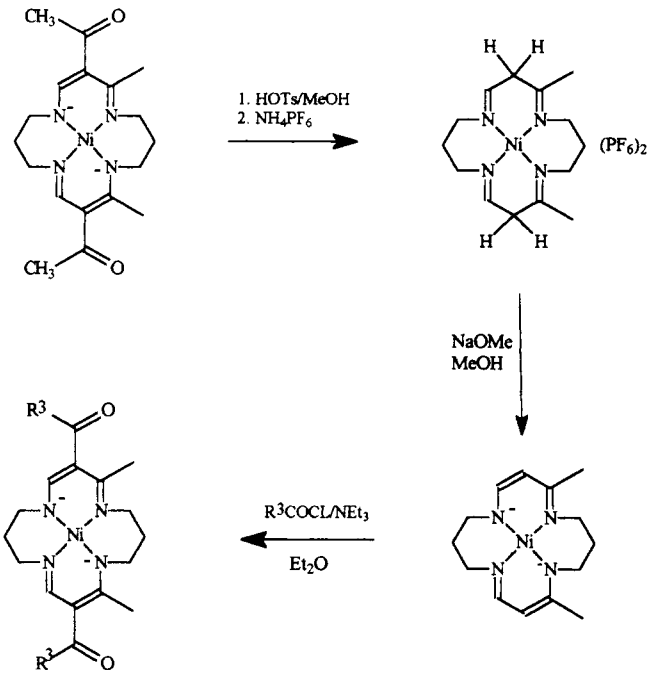

conformation, share the advantage for ring closure of the 16-membered rings and the same procedures apply.[22] However, [14]cyclidenes are planar and very long bridges are necessary in order to close the second ring.[27] In fact, advanced designs making use of risers and supporting substituents, as developed for the lacunization of Schiff base complexes (see below) would be appropriate to [14]cyclidenes.

Two routes to ring closure are equally available (Scheme 1). The obvious route involves reaction of the methylated Jaeger complex with a diamine having either primary or secondary amine groups.[22,29,63] The second proceeds by way of the reaction product with 2 mol of an alkylamine, methylamine being most often used. The intermediate unbridged amine derivative is then ring closed using an α,ω-dibromide or ditosylate.[1,29,54] The pathway most suitable for any given derivative is a matter of experiment. Either procedure may be used to place specific alkyl groups in the R^2 position.

The group R^3 is varied by a more lengthy procedure (Scheme 2) in which the original Jaeger complex is altered.[29] The usual synthesis of these complexes leads to the diacetyl derivative and the acetyl groups can be removed by nucleophiles in acidic media. The deacetylated product is then acylated in order to provide the R^3 group of choice. From that point, the synthesis follows Scheme 1. If the bridge is to proceed from the R^3 position instead of R^1, a diacyl species must be used to produce a bridged Jaeger complex as an intermediate, essentially as shown in Scheme 2.[41]

Because of the extensive dioxygen chemistry of the Schiff base ligands, they have been converted into lacunar forms. The first to be studied were those of the salen type, Schiff bases of salicylaldehyde with diamines.[48] Those investigators reasoned that a properly designed diamine would force the connecting group between the amino functions to suspend over the metal ion, leaving below it a protected cavity within which O_2 might bind. Their implementation is shown in the structure given in Figure 23 wherein the important concepts of separate *risers* and *bridging groups* is well illustrated. The naphthalene moieties serve the function as risers in a range of related bridging diamines whose bridging groups vary.

The Schiff base ligands derived from β-diketones and α,ω-primary amines have been bridged by reaction at the γ positions[42,44,65] as shown in Scheme 3, and the reaction is a template process using nickel(II) for the tetradentate ligands and copper(II) for the pentadentate ligands. The bridging groups were designed to raise the bridge above the metal ion as the spanning group proceeded across the space above the metal ion. The risers were based on *m*-hydroxybenzoic acid, with the spanning group linking the hydroxyl oxygens of opposing risers, and polymethylene or xylylene groups serving the spanning function. As described in the preceding section on structures, alkyl groups at the R^2 and R^3 positions are necessary in order to cause the bridge to rise vertically above the coordination plane (Figure 19). This is a common problem for relatively planar parent ligands; special consideration must be given to fixing the bridge in a perpendicular orientation.

To date, lacunar α-dioxime complexes have only been synthesized with bridges between substituents on a single α-dioxime moiety, although a number of possibilities exist for spanning *trans*-oriented structural points. Retey[47] prepared tetraketones having pairs of keto groups in α locations and then derived his bridged tetraoximes from those key intermediates. Lance[45,46,56,66] improved the tetraoxime synthesis and extended this work to include macrocycles with BF_4^+ groups connecting adjacent oxime oxygens, as shown in Scheme 4. A preliminary publication has reported a bridged Goedken macrocycle.[67]

B. Electrochemical Properties of Lacunar Complexes

1. Cyclidene Complexes

There has long been a realization that the dioxygen affinities of cobalt(II) dioxygen carriers increase as the electron density at the cobalt center increases, as manifested in the electrode potential for the cobalt(III)/cobalt(II) couples.[68,69] A similar correlation between

Scheme 3

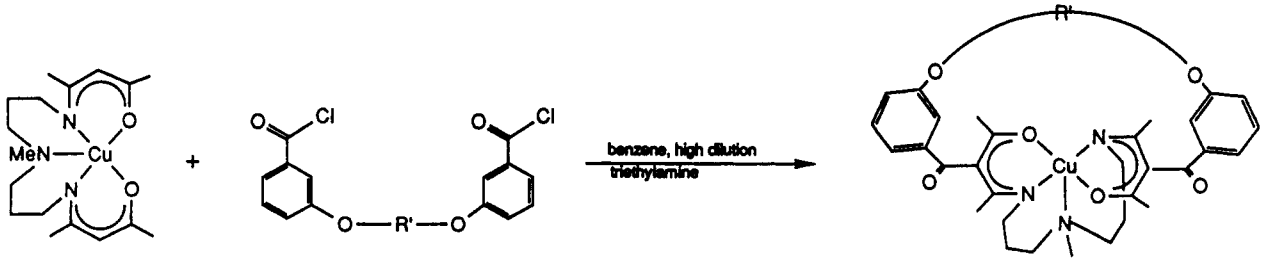

Scheme 4

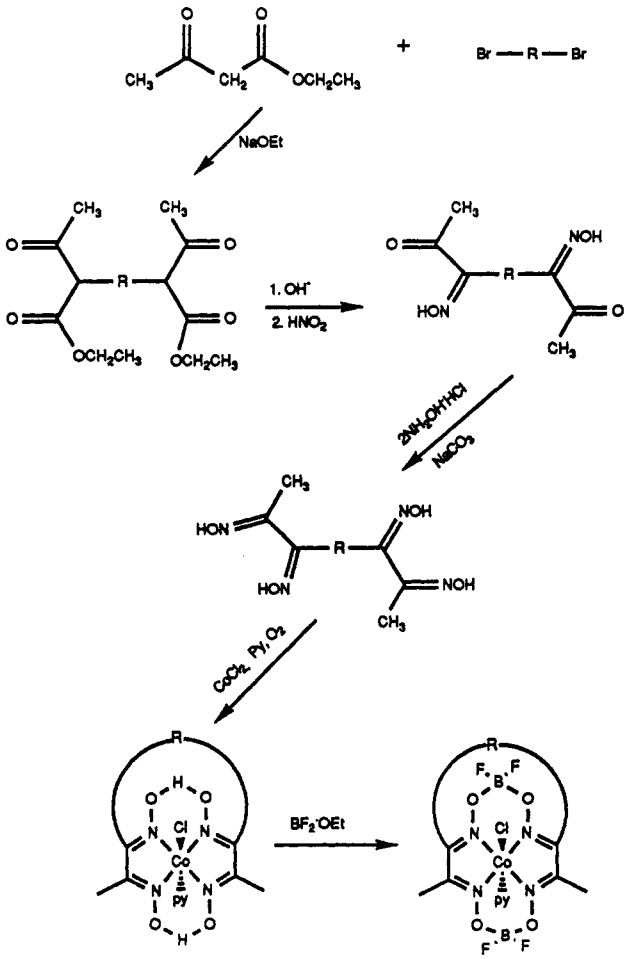

the electrode potential and the electron density is expected for most metal ions and the greatest amount of data is available for the nickel complexes, since that metal ion is invariably used in the template synthesis of the cyclidene. For the divalent iron, cobalt, and nickel cyclidene complexes (Table 3), the first redox process is often associated with the M^{3+}/M^{2+} couple and the difficulty of oxidation proceeds Ni > Co > Fe. For the cyclidenes the substituent effect is greatest for R^3 (Figure 1); replacing H by CH_3 changes the potential for Ni(mXyMeR^3[16]Cyc) by 160 mV, and that for Ni(C6MeR^3[16]Cyc), by 190 mV. Changing R^3 from the electron-donating CH_3 to electron-withdrawing phenyl results in similar changes: Ni(mXyMeR^3[16]Cyc), 160 mV; Ni(C6MeR^3[16]Cyc), 140 mV; Co(C6MeR^3[16]Cyc), 140 mV; Fe(mXyMeR^3[16]Cyc), 140 mV. The substituent on the bridge nitrogen atoms R^2 also affects the electrode potential. For Fe(mXyR^2Me[16]Cyc), the change is 60 mV on going from hydrogen to methyl; for Ni(C6R^2Me[16]Cyc), 120 mV; and for Ni(mXyR^2Me[16]Cyc), 150 mV.

Changing the ring-size for the parent macrocycle is expected to have electronic consequences, the smaller ring providing the greater electron density.[76] For comparable nickel complexes the potential of the [15]cyclidene is about 100 mV less positive than that for the [16]cyclidene. It also appears that locating the bridge at the R^3 position rather than at R^1 has a significant effect on the redox potential.

The influence of variation in the bridging group and cavity size on the half-wave potentials of the complexes

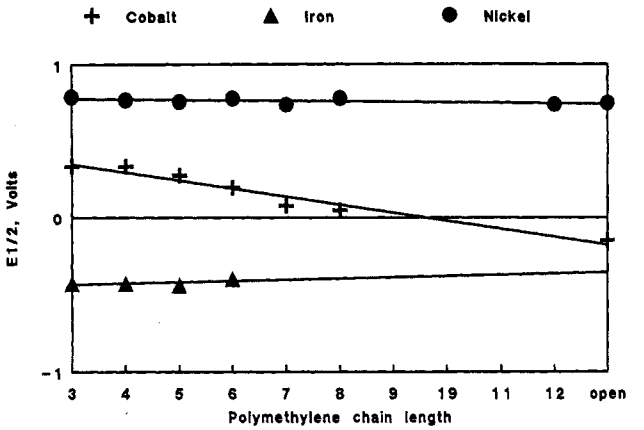

Figure 25. Variation of $E_{1/2}$ with bridge length for M^{II}(CnMeMe[16]Cyc) in acetonitrile solutions containing 0.1 M NBu_4BF_4, vs $Ag/AgNO_3$ reference electrode.

is of much interest since dioxygen affinity is extremely responsive to this structural variable. Figure 25 shows this dependence for the R^1MeMe[16]cyclidene complexes of iron, cobalt, and nickel in acetonitrile solution. The final points in the cobalt and nickel graphs are for the unbridged species having Me_2 for R^1. Clearly the potentials for the nickel and iron complexes are insensitive to cavity size, but a modest change of almost a half of a volt is observed for the cobalt complexes whose cavities range from too small to accept a ligand (C3) to completely open (no bridge). In the absence of additional chemical interactions, related changes in electronic structure would be expected for all three metals. Consequently, the failure of the potentials for the iron and nickel couples to respond to changes in cavity size leads to the conclusion that the electron density at the metal center is not changed as the bridge is changed. This conclusion requires the concomitant conclusion that changes in dioxygen affinity with bridging group are not traceable to electronic sources, despite the fact that the metal ion does alter its in plane/out of plane status slightly as the bridge length changes (Table 2).

It is necessary to explain the dependence of the redox potential of the $cobalt^{III}/cobalt^{II}$ couple on cavity size in the absence of an electronic effect. The critical studies by Chavan et al.[70] have shown that the binding of the sixth ligand within the cavity is the origin of this effect. This sixth ligand cannot bind if the cavity is very small (C3 and possibly C4), but it binds relatively strongly as the cavity size increases from C5 through C8. This sixth ligand binding stabilizes the oxidized state and lowers the potential for the process. In further support of this rationale, $E_{1/2}$ does not change with ring size in the noncoordinating solvents acetone[70] or methylene chloride.[26] The oxidized cobalt(III) complex has the low-spin d^6 electronic configuration which requires a sixth ligand for stabilization. The oxidized nickel(III) complex has a d^7 configuration which is Jahn–Teller distorted and not so critically dependent on binding of the sixth ligand. While essentially valid, this explanation is simplified since the oxidized center also varies with chain length. That is, when the sixth ligand does not bind, the ligand, rather than the metal ion, may be oxidized. This has the consequence that the ligand is more susceptible to oxidative destruction for structures where ligands cannot easily enter the cavity.

Table 3. Electrochemical Data for Lacunar Complexes M^{3+}/M^{2+} Couple

	sol[a]	ref	$E_{1/2}$	ΔE_p		sol[a]	ref	$E_{1/2}$	ΔE_p
Co^{II}(C12MeMe[14]Cyc)	An	27	−0.065	230	Ni^{II}(C7HMe[16]Cyc)	An	72	0.82	60
Co^{II}(Me_2MeMe[15]Cyc)	An	70	−0.20	abs	Ni^{II}(C7HPh[16]Cyc)	An	29	0.92	65
Co^{II}(C6MeMe[15]Cyc)	An	70	0.21	abs	Ni^{II}(C7MeMe[16]Cyc)	An	72	0.74	70
Co^{II}(C7MeMe[15]Cyc)	An	70	0.12	abs	Ni^{II}(C7MePh[16]Cyc)	An	29	0.90	70
Co^{II}(C8MeMe[15]Cyc)	An	70	0.007	abs	Ni^{II}(C8HMe[16]Cyc)	An	72	0.84	86
Co^{II}(C12MeMe[15]Cyc)	An	22	−0.03	70	Ni^{II}(C8HPh[16]Cyc)	An	29	0.95	60
Co^{II}(mXyMeMe[15]Cyc)	An	22	0.28	70	Ni^{II}(C8MeMe[16]Cyc)	An	72	0.78	80
Co^{II}(Me_2MeC7[16]Cyc)	An	41	0.29	70	Ni^{II}(C8MePh[16]Cyc)	An	29	~0.90	irr
Co^{II}(Me_2MeC5[16]Cyc)	An	41	0.19	70	Ni^{II}(C12MeMe[16]Cyc)	An	70	0.74	abs
Co^{II}(Me_2MeC6[16]Cyc)	An	41	0.19	100	Ni^{II}(mXyBzMe[16]Cyc)	An	29	0.82	70
Co^{II}(Me_2MeC7[16]Cyc)	An	41	0.29	70	Ni^{II}(mXyBzPh[16]Cyc)	An	29	0.99	80
Co^{II}(Me_2MeMe[16]Cyc)	An	70	−0.15	abs	Ni^{II}(mXyHC7[16]Cyc)	An	41	1.03 E_{pa}	irr
Co^{II}(Me_2MePh[16]Cyc)	An	16	−0.09	abs	Ni^{II}(mXyHMe[16]Cyc)	An	72	0.925	67
Co^{II}(Pr_2HC7[16]Cyc)	An	41	0.34	80	Ni^{II}(mXyHPh[16]Cyc)	An	29	~0.92	irr
Co^{II}(C3MeMe[16]Cyc)	An	54	0.34	70	Ni^{II}(mXyMebOMe[16]Cyc)	An	29	0.92	70
Co^{II}(C4MeMe[16]Cyc)	An	70	0.34	abs	Ni^{II}(mXyMeH[16]Cyc)	An	29	0.94	80
Co^{II}(C4MePh[16]Cyc)	An	16	0.50	abs	Ni^{II}(mXyMeMe[16Me2]Cyc)	An	30	0.82	90
Co^{II}(C5MeMe[16]Cyc)	An	70	0.28	abs	Ni^{II}(mXyMeMe[16]Cyc)	An	72	0.78	70
Co^{II}(C5MePh[16]Cyc)	An	16	0.44	abs	Ni^{II}(mXyMeMe[$Me_2$16Me_2]Cyc)	An	30	0.82	90
Co^{II}(C6MeMe[16]Cyc)	DCM	33	0.15	abs	Ni^{II}(mXyMeMe[$Me_2$16]Cyc)	An	30	0.80	80
Co^{II}(C6MeMe[16]Cyc)	An	70	0.20	abs	Ni^{II}(mXyMePh[16]Cyc)	An	29	0.94	70
Co^{II}(C6MePh[16]Cyc)	An	16	0.34	abs	Ni^{II}(mXynBuMe[16]Cyc)	An	72	0.79	60
Co^{II}(C7MeMe[16]Cyc)	An	70	0.08	abs	Ni^{II}(mXyPhBz[16Me_2]Cyc)	An	30	1.02	100
Co^{II}(C7MePh[16]Cyc)	An	16	0.24	abs	Ni^{II}(mXyPhBz[$Me_2$16Me_2]Cyc)	An	30	1.02	90
Co^{II}(C8MeMe[16]Cyc)	An	70	0.05	abs	Ni^{II}(mXyPhBz[$Me_2$16]Cyc)	An	30	1.02	75
Co^{II}(C9MeMe[16]Cyc)	DCM	26	0.05	80	Ni^{II}(pXyMeMe[16]Cyc)	An	72	0.81	60
Co^{II}(C10MeMe[16]Cyc)	DCM	26	0.05	100	Co^{II}(C6Me(CH_2)[16]Cyd)	DCM	33	−0.58	abs
Co^{II}(C11MeMe[16]Cyc)	DCM	26	0.06	95	Ni^{II}(C6Me(CH_2)[16]Cyd)	DCM	33	−0.39	abs
Co^{II}(C12MeMe[16]Cyc)	DCM	26	0.03	95	$Fe^{II}Fe^{II}$(C2HMe[16]Dcy)	An	73	−0.18 E_{pa}	
Ni^{II}(C8MeMe[15]Cyc)	An	70	0.65	abs	$Fe^{II}Fe^{II}$(C2HMe[16]Dcy)	An/Im	73	−0.47 E_{pa}	
Ni^{II}(mXyMeMe[15]Cyc)	An	22	0.71	75	$Fe^{II}Fe^{II}$(C2HMe[16]Dcy)	An/Py	73	−0.18 E_{pa}	
Ni^{II}(mXyHMe[15]Cyc)	An	22	0.85	80	$Fe^{II}Fe^{II}$(C3HMe[16]Dcy)	An	73	−0.12	70
Ni^{II}(C12MeMe[15]Cyc)	An	70	0.53	abs	$Fe^{II}Fe^{II}$(C3HMe[16]Dcy)	An/Im	73	−0.55	70
Ni^{II}(Bz_2HMe[16]Cyc)	An	62	0.830	85	$Fe^{II}Fe^{II}$(C3HMe[16]Dcy)	An/Py	73	−0.22	70
Ni^{II}(H_2HMe[16]Cyc)	An	62	0.870	80	$Fe^{II}Fe^{II}$(C4HMe[16]Dcy)	An	73	−0.13	90
Ni^{II}(Me_2HC6[16]Cyc)	An	41	0.89	90	$Fe^{II}Fe^{II}$(C4HMe[16]Dcy)	An/Im	73	−0.55	90
Ni^{II}(Me_2HC7[16]Cyc)	An	41	0.89	70	$Fe^{II}Fe^{II}$(C4HMe[16]Dcy)	An/Py	73	−0.22	90
Ni^{II}(Me_2HC8[16]Cyc)	An	51	0.92	60	$Fe^{II}Fe^{II}$(C7FlHMe[16]Dcy)	An/Py	73	−0.08	100
Ni^{II}(Me_2HMe[16]Cyc)	An	62	0.800	80	$Fe^{II}Fe^{II}$(mXyHMe[16]Dcy)	An	73	−0.32	90
Ni^{II}(Me_2MeC5[16]Cyc)	An	41	0.67	70	$Fe^{II}Fe^{II}$(mXyHMe[16]Dcy)	An/Im	73	−0.48	90
Ni^{II}(Me_2MeC6[16]Cyc)	An	41	0.60	70	$Fe^{II}Fe^{II}$(mXyHMe[16]Dcy)	An/Py	73	−0.13	90
Ni^{II}(Me_2MeC7[16]Cyc)	An	41	0.68	abs	$Ni^{II}Ni^{II}$(C2C2Me[16]Dcy)	An	74	0.900	92
Ni^{II}(Me_2MeMe[15]Cyc)	An	70	0.58	abs	$Ni^{II}Ni^{II}$(C2HMe[14]Dcy)	An	74	0.760	105
Ni^{II}(Me_2MeMe[16]Cyc)	An	62	0.745	70	$Ni^{II}Ni^{II}$(C2HMe[16]Dcy)	An	74	0.935	87
Ni^{II}(Me_2MePh[16]Cyc)	An	16	0.84	abs	$Ni^{II}Ni^{II}$(C3HMe[16]Dcy)	An	74	0.894	61
Ni^{II}(nBu_2Me[16]Cyc)	An	62	0.810	75	$Ni^{II}Ni^{II}$(C4HMe[16]Dcy)	An	37	0.87	63
Ni^{II}(tBu_2HMe[16]Cyc)	An	62	0.845	75	$Ni^{II}Ni^{II}$(C5HMe[16]Dcy)	An	37	0.85	65
Ni^{II}(Pr_2HC7[16]Cyc)	An	41	0.89	70	$Ni^{II}Ni^{II}$(C7FlHMe[16]Dcy)	An	37	0.91	90
Ni^{II}(C3HMe[16]Cyc)	An	16	0.88	abs	$Ni^{II}Ni^{II}$(C7HMe[16]Dcy)	An	37	0.85 E_{pa}	
Ni^{II}(C3MeMe[16]Cyc)	An	54	0.79	80	$Ni^{II}Ni^{II}$(C8HMe[16]Dcy)	An	37	0.82	50
Ni^{II}(C4HMe[16]Cyc)	An	72	0.84	71	$Ni^{II}Ni^{II}$(DurHMe[16]Dcy)	An	37	0.890	70
Ni^{II}(C4HPh[16]Cyc)	An	29	0.90	80	$Ni^{II}Ni^{II}$(DurMeMe[16]Dcy)	An	37	0.780	80
Ni^{II}(C4MeMe[16]Cyc)	An	72	0.77	60	$Ni^{II}Ni^{II}$(mXyHMe[16]Dcy)	An	74	0.904	50
Ni^{II}(C4MePh[16]Cyc)	An	29	0.91	60	$Ni^{II}Ni^{II}$(pXyHMe[16]Dcy)	An	37	0.88	80
Ni^{II}(C5HMe[16]Cyc)	An	72	0.85	70	Co^{II}(Bzo_2MeMe[14]Ged)	An	75	−0.22	97
Ni^{II}(C5HPh[16]Cyc)	An	29	0.92	60	Co^{II}(FAc_2MeMe[14]Ged)	An	75	−0.044	98
Ni^{II}(C5HtBu[16]Cyc)	An	29	0.75	60	Co^{II}($FBzo_2$MeMe[14]Ged)	An	75	0.012	120
Ni^{II}(C5MeMe[16]Cyc)	An	72	0.76	60	Co^{II}(DhaDhaF[14]Oxm)Py_2	DCM	45	−0.26	200
Ni^{II}(C5MePh[16]Cyc)	An	29	0.91	70	Co^{II}(MeMeF[14]Oxm)	An	66	0.48 E_{pa}	irr
Ni^{II}(C6HC6[16]Cyc)	An	41	0.9	irr	Co^{II}(MeMeF[14]Oxm)	An/Py	66	−0.12	100
Ni^{II}(C6HC7[16]Cyc)	An	41	0.96	irr	Co^{II}(PhPhF[14]Oxm)	An	66	0.036	70
Ni^{II}(C6HC8[16]Cyc)	An	41	1.06	140	Ni^{II}(Me_2AcH{12}Mal)	An	43	0.72	80
Ni^{II}(C6HHp[16]Cyc)	An	29	0.92	85	Ni^{II}(Me_2AcMe{12}Mal)	An	43	0.61	80
Ni^{II}(C6HMe[16]Cyc)	An	72	0.895	76	Ni^{II}(Me_2HH{12}Mal)	An	43	0.46 E_{pa}	irr
Ni^{II}(C6HPh[16]Cyc)	An	29	0.94	75	Ni^{II}(Me_2HMe{12}Mal)	An	43	0.40 E_{pa}	irr
Ni^{II}(C6HtBu[16]Cyc)	An	29	0.78	60	Ni^{II}((MeOBzo)2MeH{12}Mal)	An	44	0.74	70
Ni^{II}(C6MeH[16]Cyc)	An	29	0.97	60	Ni^{II}((MeOBzo)2MeMe{12}Mal)	An	44	0.63	80
Ni^{II}(C6MeMe[16]Cyc)	An	72	0.775	67	Ni^{II}((BzoOC8OBzo)MeH {12}Mal)	An	44	0.74	90
Ni^{II}(C6MePh[16]Cyc)	An	29	0.92	70					
Ni^{II}(C7FlHMe[16]Cyc)	An	72	0.94	65	Ni^{II}(BzoOC8OBzo)MeMe {12}Mal)	An	44	0.64	70
Ni^{II}(C7HC8[16]Cyc)	An	41	0.98 E_{pa}						

[a] Unless otherwise indicated, measurements were made on acetonitrile solutions containing 0.1 M NBu_4BF_4 with a $Ag/AgNO_3$ (0.1 M) reference electrode; abs means that the parameter was not reported in the reference; irr means irreversible; DCM is dichloromethane.

Table 4. ESR Parameters[24] Fit to Pilbrow/Smith Model:[6] 1.5 M MeIm/Acetonitrile or Py/Acetonitrile Glass at 196 °C[a]

	g_x	g_y	g_z	A_x	A_y	A_z	$\langle A \rangle$	$\alpha \pm 0.3$
Co^{II}(Me$_2$MeMe[16]Cyc)MeImO_2	2.010	2.090	1.993	5.5	20.1	9.0	11.5	31.1
Co^{II}(Me$_2$MePh[16]Cyc)MeImO_2	2.010	2.091	1.993	6.4	18.8	8.6	11.3	29.2
Co^{II}(C4HPh[16]Cyc)MeImO_2	2.012	2.096	1.993	6.1	20.0	8.4	11.5	30.0
Co^{II}(C4MeMe[16]Cyc)MeImO_2	2.008	2.086	1.991	6.4	19.7	8.9	11.7	29.6
Co^{II}(C4MeMe[16]Cyc)PyO_2	2.010	2.086	1.993	5.9	19.5	8.7	11.4	29.8
Co^{II}(C4MePh[16]Cyc)MeImO_2	2.011	2.097	1.993	6.4	19.7	8.3	11.5	30.2
Co^{II}(C5HPh[16]Cyc)MeImO_2	2.011	2.091	1.993	6.2	19.8	8.6	11.4	29.0
Co^{II}(C5MeMe[16]Cyc)MeImO_2	2.010	2.091	1.995	7.2	19.3	8.6	11.7	30.8
Co^{II}(C5MeMe[16]Cyc)PyO_2	2.011	2.091	1.993	5.6	20.7	8.9	11.7	29.7
Co^{II}(C5MePh[16]Cyc)MeImO_2	2.012	2.093	1.994	6.8	19.0	8.4	11.4	28.4
Co^{II}(C6HPh[16]Cyc)MeImO_2	2.009	2.087	1.993	6.9	18.1	8.4	11.1	29.5
Co^{II}(C6MeMe[16]Cyc)MeImO_2	2.009	2.088	1.992	6.1	19.6	8.9	11.6	31.6
Co^{II}(C6MeMe[16]Cyc)PyO_2	2.009	2.087	1.992	5.3	19.8	8.8	11.3	31.3
Co^{II}(C6MePh[16]Cyc)MeImO_2	2.009	2.089	1.993	6.6	18.0	8.3	11.0	30.6
Co^{II}(C7HPh[16]Cyc)MeImO_2	2.009	2.087	1.993	6.6	18.7	8.6	11.3	28.7
Co^{II}(C7MeMe[16]Cyc)MeImO_2	2.011	2.090	1.995	6.6	19.5	8.7	11.6	28.7
Co^{II}(C7MeMe[16]Cyc)PyO_2	2.010	2.088	1.993	6.4	19.5	8.8	11.6	30.0
Co^{II}(C7MePh[16]Cyc)MemO$_2$	2.009	2.086	1.992	7.0	18.3	8.4	11.2	28.0
Co^{II}(C8HPh[16]Cyc)MeImO[2]	2.009	2.088	1.992	7.1	18.4	8.4	11.3	27.8
Co^{II}(C8MeMe[16]Cyc)MeImO_2	2.009	2.086	1.992	6.3	19.2	8.4	11.3	27.0
Co^{II}(C8MeMe[16]Cyc)PyO_2	2.010	2.089	1.991	5.7	20.3	8.7	11.6	27.7
Co^{II}(C8MePh[16]Cyc)ImO2	2.009	2.088	1.992	6.2	18.5	8.4	11.0	28.4
Co^{II}(C9MeMe[16]Cyc)MeImO_2	2.010	2.090	1.994	6.5	19.2	8.5	11.4	27.2
Co^{II}(C9MeMe[16]Cyc)PyO_2	2.009	2.090	1.991	5.9	20.2	8.8	11.6	27.8
Co^{II}(C10MeMe[16]Cyc)MeImO_2	2.011	2.090	1.994	6.6	19.1	8.4	11.4	27.7
Co^{II}(C10MeMe[16]Cyc)PyO_2	2.010	2.090	1.991	6.0	20.0	8.7	11.6	29.5
Co^{II}(C11MeMe[16]Cyc)MeImO_2	2.009	2.088	1.993	6.3	19.2	8.4	11.3	29.1
Co^{II}(C11MeMe[16]Cyc)PyO_2	2.009	2.089	1.991	6.3	19.8	8.8	11.6	29.6
Co^{II}(C12MeMe[16]Cyc)MeImO_2	2.011	2.091	1.995	6.3	19.3	8.4	11.3	28.8
Co^{II}(C12MeMe[16]Cyc)PyO_2	2.009	2.090	1.991	5.9	20.4	8.8	11.6	30.2
Co^{II}(mXyMeMe[16]Cyc)MeImO_2	2.010	2.089	1.992	5.6	19.4	8.1	11.6	32.5
Co^{II}(DurPipMe[16]Vcy)MeImO_2	2.009	2.086	1.993	5.4	19.3	8.6	11.1	30.3
Co^{II}(DhaDhaF[14]Oxm)PyO_2[45]	2.006	2.069	2.017	5	11	10	9	

[a] Units on A are $cm^{-1} \times 10^4$.

The dinuclear complexes of the ditopic bis(cyclidene) complexes give very similar electrochemical behavior to their mononuclear counterparts, but a small splitting in the potentials of the pairs of metal atoms has been resolved.[74] $\Delta E_{1/2}$ values as large as 105 mV were observed. The corresponding dicobalt complexes that have been studied gave irreversible couples with peak potentials similarly located to those of the mononuclear complexes.[36]

2. Non-Cyclidene Lacunar Complexes

In order to provide a basis for extending earlier electrode potential/dioxygen affinity correlations to other lacunar complexes, values are recorded in Table 3 for the Mal, Oxm, and Goedken families of complexes. These ligands all differ from the cyclidenes in that the coordinated form of the ligand is anionic in each case. The Goedken complexes are somewhat similar in structure to precursors of the cyclidenes, but their most electron-rich members exhibit negative electrode potentials (−220 mV vs some +300 mV for cobalt cyclidenes), a result in keeping with the net −2 charge assigned to the ligands. The Mal ligands produce a range of redox potentials, but all tend to be more cathodic than comparable cyclidenes. Similarly, the oximes also exhibit potentials more negative than those of the cyclidenes, falling in the same region as those of the Goedken derivatives. Simplistically, one might predict that, all else being equal, the order of dioxygen affinities might be Mal > Goedken ≃ Oxm > Cyc. As shown in sections that follow, this is not the case.

C. Spectroscopic Properties

1. ESR Spectroscopy

ESR spectroscopy is particularly useful for the identification and study of the dioxygen adducts of cobalt because both the 5-coordinate cobalt(II) precursor complexes and the 1:1 cobalt–dioxygen adducts have distinctive ESR spectra.[6,7] These provide a most rapid and convenient qualitative identification of dioxygen adducts, something that is not possible for the dioxygen adducts of other metal ions.[7,77] ESR spectra are useful in examining the electronic structures of the cobalt–dioxygen complexes.[6,78–80]

The ESR spectral parameters are summarized in Tables 4 and 5 for the O_2 adducts of the lacunar cobalt(II) complexes. Computer simulation has facilitated detailed assignment of the parameters (α, A_i, and g_i, where $i = x, y, z$) for many cyclidene complexes, and these appear in Table 4. Figure 26 shows an example of the observed and simulated ESR spectra. While the spectra of the complexes often appear very similar, good spectral resolution and simulation permit the evaluation of small differences. Experimental parameters are reported in Table 5 for the other cobalt(II) lacunar dioxygen adducts whose spectra have been analyzed in less detail.

The parameter α (see Figure 27) is of particular interest because it is a measure of the Co–O–O angle, which equals α + 90. From an X-ray structure determination on [Co(C6MeMe[16]Cyc)(1-MeIm)(O_2)]-[PF_6], the Co–O–O bond angle was found to be 121 ± 1°, giving an α of 31 ± 1°. This result agrees well with

Table 5. Empirical ESR Parameters for Lacunar Cobalt(II) Dioxygen Carriers: Most Values for 1.5 M MeIm/ Acetonitrile Glass at 196 °C

	ref	$g_\parallel$	$g_\perp$	$A_\parallel$, G	$A_\perp$, G
Co^{II}(C12MeMe[14]Cyc)$MeImO_2$	27	2.119	2.022	19	14
Co^{II}(C6MeMe[15]Cyc)$MeImO_2$	22	2.087	1.999	18.0	12.0
Co^{II}(C7MeMe[15]Cyc)$MeImO_2$	22	2.086	2.000	18.5	12.1
Co^{II}(C8MeMe[15]Cyc)$MeImO_2$	22	2.086	1.999	17.8	11.6
Co^{II}(C12MeMe[15]Cyc)$MeImO_2$	22	2.087	1.998	18.2	12.5
Co^{II}(mXyMeMe[15]Cyc)$MeImO_2$	22	2.089	2.000	18.8	12.5
Co^{II}(Me_2HC7[16]Cyc)$MeImO_2$	41	2.078	2.012	18	10
Co^{II}(Me_2MeC7[16]Cyc)$MeImO_2$	41	2.081	2.014	18	8
Co^{II}(nPr_2HC7[16]Cyc)$MeImO_2$	41	2.085	2.014	18	9
Co^{II}(Me_2MeC8[16]Cyc)$MeImO_2$	41	2.086	2.010	18	10
Co^{II}(Me_2MetBu[16]Cyc)$MeImO_2$	13	2.093	2.016	20	9
Co^{II}(C6HtBu[16]Cyc)$MeImO_2$	13	2.094	2.020		
Co^{II}(C6MeH[16]Cyc)$MeImO_2$	13	2.081	2.008	18	10
Co^{II}(mXyMePh[16]Cyc)$MeImO_2$	13	2.088	2.012	16	8
$Co^{II}Co^{II}$(mXyHMe[16]Dcy)$MeImO_2$	36	2.05	1.98	16.7	
Co^{II}(Bzo_2MeMe[14]Ged)PyO_2	75	2.091	1.998	19.9	12.9
Co^{II}(FAc_2MeMe[14]Ged)PyO_2	75	2.081	2.002	16.1	11.8
Co^{II}($FBzo_2$MeMe[14]Ged)PyO_2	75	2.078	1.944	18.9	10.5
Co^{II}(($MeOBzo)_2$MeH{17NMe}Mal)$MeImO_2$	13	2.004	2.100	15.0	20.5
Co^{II}((BzoOC6OBzo)MeH{17NMe}Mal)$MeImO_2$	13	1.997	2.096	15.0	20.5
Co^{II}((BzoOpXyOBzo)MeH{17NMe}Mal)$MeImO_2$	13	1.999	2.092	15.4	20.7
Co^{II}({(NapOC6ONap)26}Sal)$MeImO_2$	81	2.090	1.987	18.6	
Co^{II}({(NapOpXyONap)26}Sal)$MeImO_2$	81	2.091	1.985	18.2	
Co^{II}(MeMeF[14]Oxm)PyO_2	66	2.01 (g)			
Co^{II}(C10MeF[14]Oxm)PyO_2	66	2.01 (g)			

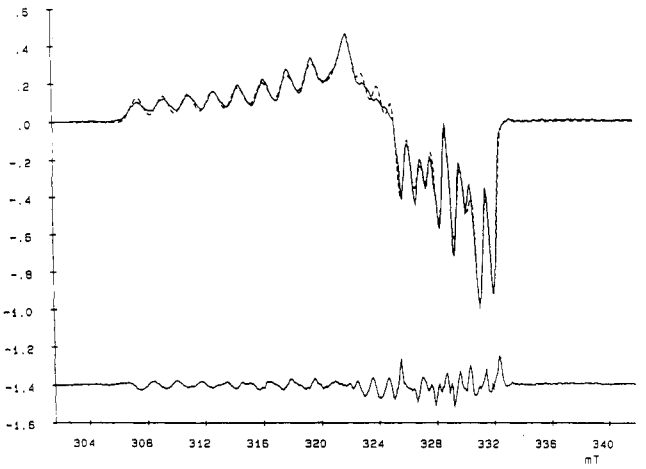

Figure 26. Observed and simulated ESR spectra for a typical cobalt lacunar [16]cyclidene dioxygen adduct: Co(C6MeMe-[16]Cyc)(MeIm)O_2^{2+} in acetone/1-methylimidazole at 77 K.

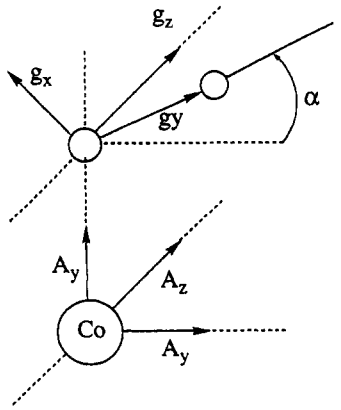

Figure 27. Coordinate system for Zeeman and hyperfine terms of ESR spectrum.

the value of 31.6 ± 0.3° that was obtained from ESR simulation (Table 4). The values of α for the dioxygen adducts of the (cyclidene)cobalt(II) complexes[24] correlate with the peak potentials obtained by cyclic voltammetry in noncoordinating solvents (acetone, methylene chloride),[26,70,82] but not with dioxygen affinities; this suggests that α is more sensitive to electronic than steric effects while the opposite is true for the dioxygen affinities of the polymethylene-bridged cyclidenes of cobalt(II) (Figure 28).

For [Co(CnMeMe[16]Cyc)(B)(O_2)]$^{2+}$ variations in parameters between B = pyridine (py) and 1-methylimidazole (MeIm) have been attributed to differences in the σ- and π-donating properties of the bases.[24] Changes in the substituents R^2 and R^3 exert similar influences on the ESR hyperfine parameters, presumably by electronic interactions. Intricate variations of individual Zeeman and/or hyperfine parameters with bridge length R^1 have been observed, but the origins of the subtle relationships remain unclear. For example, A_z, g_x, and g_z all show alternations as n is increased with even-membered bridging groups, giving lower values than neighboring odd-membered groups. Similar alternating patterns have been reported for the O–O stretching vibrations of cobalt–dioxygen adducts[83] and the ^{13}C NMR spectra of the carbon atoms associated with the unsaturated portions of the cyclidene in the nickel(II) complexes.[25,84] In general, these even–odd alternations have been attributed to differences in the strain energies of the R^1 bridge that arise from the dissymmetry of the middle two carbon atoms in the even-membered polymethylene bridges.

2. NMR Spectroscopy

NMR spectroscopy has been especially useful in determining the structures and/or conformations of the lacunar complexes with ligands of interest but with diamagnetic metal ions such as nickel(II). Complete assignments of the ^1H and ^{13}C NMR spectral bands were achieved by a combination of 2D experiments[85] and ^{13}C enrichment.[38] At room temperature, proton NMR shows that the two *N*-methyl groups of unbridged Ni(Me_2MeMe[16]Cyc) exchange rapidly, while at lower

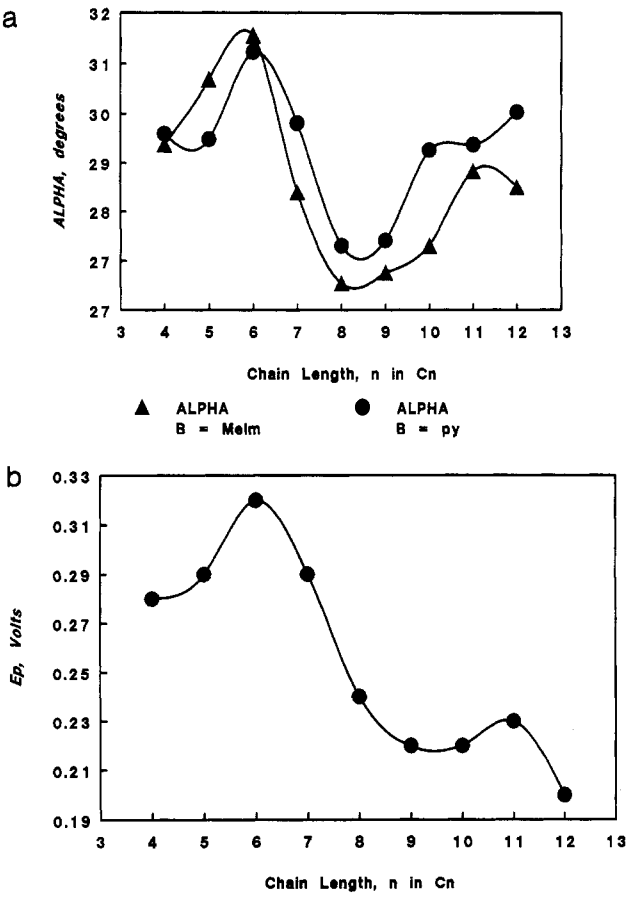

Figure 28. Variation of the CoO_2 angle α with the length of the polymethylene bridge that spans the lacuna in cobalt cyclidene complexes and its correlation with cyclovoltammetric peak potentials. Panel a shows a graph of α versus bridge chain length. Panel b shows a graph of CV peak potential for Co(CnMeMe[16]Cyc) in methylene chloride.

temperatures restricted rotation occurs,[62] in keeping with the stability of lid-on and lid-off conformations for the bridged species. Similarly, the unbridged species shows a slowing in the flexing of the unsaturated chelate rings as temperature is lowered. The NMR spectra of the complexes having *gem*-dimethyl groups in their saturated chelate rings[30] show that one of the methyl pair is in close proximity to the nickel ion, perhaps blocking an axial coordination site, a factor that is important in the dioxygen-binding chemistry of the iron and cobalt complexes of these ligands. It will be recalled, from the section on structures, that the polymethylene bridges from C3 through C8 have lid-off configurations and that a gradual transition to a lid-on configuration occurs at C9 and C10 with a pure lid-on form for C12. NMR studies have shown a parallel behavior in solution.[25] Assignments have also been made for the ligand atom resonances in the complexes of the Mal family[44] and the Oxm family[66] of lacunar dioxygen carriers.

3. Infrared Spectroscopy

The stretching frequencies for the O–O bond[86] in the iron(II) and cobalt(II) C6MeMe[16]Cyc complexes (assignments confirmed by isotopic substitution)[83] both occur at 1141 cm^{-1}, very close to the values reported for the Schiff base complex $Co(H_2MeMe\{12\}Mal)$,[87] 1143 cm^{-1}, and cobalt tetraphenylporphyrin[88] in the presence of *N*-methyl imidazole, 1144 cm^{-1}. Replacing the R^3 = Me group with phenyl caused a shift of the vibrational mode to 1157 cm^{-1} for both metal cyclidenes, and the frequency shows an even–odd alternating increase as the polymethylene chain length increases.[83]

IV. Dioxygen Affinities

The ability of a dioxygen carrier to perform a given function depends on the matching of its intrinsic dioxygen affinity with the requirements it must serve. For example, the affinity of the myoglobin in red muscle tissue exceeds that of the hemoglobin in the blood so that O_2 can be delivered by the hemoglobin to the myoglobin where it is stored until it is used. The equilibrium constant for the binding of O_2 to the metal atom, K_{O_2}, provides the precise measure of dioxygen affinity. The equilibrium constant is usually expressed as formation and reported in units of reciprocal pressure ($Torr^{-1}$) since the relative concentration of O_2 is most simply expressed in terms of the partial pressure of O_2 with which the solution is equilibrated. The units may be converted to those of concentration by application of the solubility of O_2 to the equilibrium equation. In many papers the dioxygen affinity is reported as P_{50}, the pressure at which half of the available dioxygen carrier is bound to O_2 because that number is intuitively meaningful and because it is the reciprocal of the equilibrium constant $1/K_{O_2}$.

This report summarizes the dioxygen affinities of lacunar dioxygen carriers and the lacuna is believed to play three roles that directly affect their affinities. In the first, the cavity size influences the dioxygen binding affinity through steric interactions, and that is discussed at great length in sections that follow. A second role of the small cavity or lacuna is to limit the kind of ligand that can enter and bind to the metal ion at the sheltered site inside the lacuna. Size is the obvious limiting factor and this is exploited by using relatively large axial bases such as imidazole, substituted imidazoles, and pyridine. Invariably, these ligands bind to the cobalt(II) outside the cavity, even in the case of the vaulted cyclidenes. A second factor associated with selective binding at the coordination site within the cavity appears to be solvation. The importance of axial ligand solvation is inferred from the failure of attempts to produce complexes with chloride and other halides within the cavity, although thiocyanate readily enters, as discussed in the section describing crystal structure results.[21] The third role of the lacuna is to determine the environment in the immediate vicinity of the bound dioxygen. The majority of the structures known to date provide relatively nonpolar hydrophobic surroundings, but examples have been reported with polar and charged groups in the bridge that spans the cavity.

A. Cobalt(II) Cyclidene Complexes

The many dioxygen affinities for cobalt(II) cyclidene complexes that are summarized in Table 6 confirm the long-established expectation that dioxygen affinities of transition metal dioxygen carriers can be controlled by both steric and electronic means. The data are organized in terms of structural features, solvents, axial bases, and concentrations, but the largest number of measurements have been made in a common solvent system composed of 1.5 M *N*-methylimidazole in acetonitrile.

Table 6. Dioxygen Affinities for the Lacunar Complexes

	ref	sol[f]	base	[B], M	T, °C	K_{O_2}	T, °C	K_{O_2}	T, °C	K_{O_2}	T, °C	K_{O_2}	T, °C	K_{O_2}
Co^{II}(C12MeMe[14]Cyc)	27	An	MeIm	1.5	−32.4	0.62	−22.9	0.11	−17.6	0.050				
Co^{II}(C5MeMe[15]Cyc)	22	An	MeIm	1.5	20	0.003								
Co^{II}(C6MeMe[15]Cyc)	22	An	MeIm	1.5	20	0.52								
Co^{II}(C7MeMe[15]Cyc)	22	An	MeIm	1.5	20	1.32								
Co^{II}(C8MeMe[15]Cyc)	22	An	MeIm	1.5	20	5.2								
Co^{II}(Me_2HC7[16]Cyc)	41	An	MeIm	1.5	−20.2	0.015	−14.4	0.0081	−10.0	0.0047	0	0.0020		
Co^{II}(Pr_2HC7[16]Cyc)	41	An	MeIm	1.5	−14.8	0.014	0	irrev						
Co^{II}(Me_2MeC8[16]Cyc)	41	An	MeIm	1.5	−37.6	0.020	−33.2	0.0099	−25.0	0.0037				
Co^{II}(C4HPh[16]Cyc)	24	An	MeIm	1.5	−19.3	0.0018	−10.2	0.0011						
Co^{II}(C4MeMe[16]Cyc)	13	An	MeIm	1.5	−40	0.0020								
Co^{II}(C4MePh[16]Cyc)	24	An	MeIm	1.5	−40	0.005								
Co^{II}(C5HMe[16]Cyc)	24	An	MeIm	1.5	−30	0.210	−19.3	0.050	−12.8	0.025	−10.0	0.019	−0.6	0.0066
Co^{II}(C5HPh[16]Cyc)	24	An	MeIm	1.5	−10.2	0.017	−1.5	0.0079	8.6	0.0026	18.6	0.0012		
Co^{II}(C5MeMe[16]Cyc)	24	An	MeIm	1.5	−20	0.66	−10.1	0.215	1.0	0.058	10.1	0.0186	20.0	0.0094
Co^{II}(C5MeMe[16]Cyc)	24	H_2O	MeIm	2.5	4.8	0.17	10.0	0.11	15.3	0.055	25.0	0.027	29.8	0.013
					37.0	0.009								
Co^{II}(C5MePh[16]Cyc)	24	An	MeIm	1.5	−10	0.09	0	0.025	10	0.0097	20	0.0031	1.5	0.0015
Co^{II}(C6BzMe[16]Cyc)	24	An	MeIm	1.5	20.0	0.144								
Co^{II}(C6BzPh[16]Cyc)	24	An	MeIm	1.5	5.6	0.54	20.0	0.13						
Co^{II}(C6HMe[16]Cyc)	24	An	MeIm	1.5	−19.3	1.7	−15.0	0.97	−10.1	0.49	0.0	0.14	2.1	0.12
Co^{II}(C6HMe[16]Cyc)	24	H_2O	MeIm	2.5	1.6	0.97								
Co^{II}(C6HPh[16]Cyc)	24	An	MeIm	1.5	−10.0	1.3	−5.0	0.64	1.0	0.41	5.0	0.24	10.0	0.12
					15.0	0.071	20.0	0.025						
Co^{II}(C6HtBu[16]Cyc)	13	An	MeIm	1.5	−0.4	~200								
Co^{II}(C6MeH[16]Cyc)	24	An	MeIm	1.5	−25.0	0.16	−20.0	0.083	−15.4	0.042	−10.0	0.026	0.0	0.010
Co^{II}(C6MeMe[16Pic]Cyc)	50	An	*a*		−38.8	0.022	−30.4	0.010	−29.9	0.005	−19.9	0.004	−10.0	0.001
Co^{II}(C6MeMe[16Pic]Cyc)	50	Ac	*a*		−22.2	0.006	−20.0	0.004	−19.5	0.004	−11.8	0.002	−10.0	0.0014
					−5.0	0.0009								
Co^{II}(C6MeMe[16Pic]Cyc)	50	H_2O	*a*		2.0	0.003								
Co^{II}(C6MeMe[16]Cyc)	50	An	An		−34.4	0.062	−27.5	0.043	−20.0	0.026	−10.2	0.006	−4.8	0.005
Co^{II}(C6MeMe[16]Cyc)	50	Ac			−36.3	0.010	−30.9	0.006	−27.5	0.005	−21.0	0.005		
Co^{II}(C6MeMe[16]Cyc)	24	DMF	MeIm		−22.5	0.012								
Co^{II}(C6MeMe[16]Cyc)	24	DMF	MeIm	2.5	1.0	2.8	10.0	1.1						
Co^{II}(C6MeMe[16]Cyc)	24	An	MeIm	1.5	−10.1	4.6	1.0	1.3	2.1	0.98	15	0.25	20.0	0.16
Co^{II}(C6MeMe[16]Cyc)	24	An	Py	1.5	0.0	0.065	5.0	0.034	10.0	0.020	15.0	0.012		
Co^{II}(C6MeMe[16]Cyc)	24	H_2O	MeIm	2.5	3.3	7.7	6.3	5.3	8.3	4.8	10.0	4.5	14.8	2.2
					19.7	1.6								
Co^{II}(C6MeMe[16]Cyc)	50	Ac	Py	1.0	−20	0.68	−10.0	0.19						
Co^{II}(C6MenBu[16]Cyc)	24	An	MeIm	1.5	20.0	0.23								
Co^{II}(C6MenPr[16]Cyc)	24	An	MeIm	1.5	20.0	0.24								
Co^{II}(C6MePh[16]Cyc)	24	An	MeIm	1.5	0.0	0.85	0.50	0.51	10.0	0.31	15.0	0.17	20.0	0.101
					25.0	0.065	30.0	0.032						
Co^{II}(C6MePh[16]Cyc)	24	H_2O	MeIm	2.5	6.0	2.4	6.6	2.3	14.0	0.74				
Co^{II}(C6PePh[16]Cyc)	24	An	MeIm	1.5	5.0	0.28	20.0	0.13						
Co^{II}(C7HMe[16]Cyc)	24	An	MeIm	1.5	−10.0	2.46	0.0	0.80	5.0	0.41	10.0	0.23	15.0	0.15
Co^{II}(C7MeMe[16]Cyc)	24	An	MeIm	1.5	0.0	4.5	10.0	1.4	14.9	0.93	19.4	0.62	25.0	0.26
					30.0	0.16								
Co^{II}(C7MeMe[16]Cyc)	24	An	MeIm	0.15	2.3	1.7	5.0	1.4	8.4	1.0	11.6	0.66	15.4	0.44
					20.4	0.24								
Co^{II}(C7MePh[16]Cyc)	24	An	MeIm	0.15	5.0	2.3	10	0.94	15	0.51	20	0.27	25	0.16
Co^{II}(C8HMe[16]Cyc)	24	An	MeIm	1.5	0.0	1.7								
Co^{II}(C8MeMe[16]Cyc)	24	An	MeIm	1.5	0.0	5.92	4.9	3.34	10.0	1.95	15.0	1.1	20.0	0.65
					25.0	0.45	29.8	0.25						
Co^{II}(C9MeMe[16]Cyc)	26[e]	An	MeIm	1.5	0	3.37	5.0	2.05	10.0	1.13	15.0	0.67	20.0	0.59
Co^{II}(C10MeMe[16]Cyc)	26[e]	An	MeIm	1.5	0	1.61	5.0	0.82	10.0	0.53	15.0	0.29	20.0	0.17
Co^{II}(C11MeMe[16]Cyc)	26[e]	An	MeIm	1.5	0	1.12	5.0	0.65	10.0	0.35	15.0	0.23		
Co^{II}(C12MeMe[16]Cyc)	26[e]	An	MeIm	1.5	0	0.70	5.0	0.35	10.0	0.23				
Co^{II}(mXyMeMe[16]Cyc)	22	An	MeIm	1.5	−30	0.0012								
Co^{II}(mXyMeMe[16]Cyc)	24	3:1:1	APW		−39.0	0.0019								
Co^{II}(mXyMePh[16]Cyc)	89	An	MeIm	1.5	−30	0.012								
Co^{II}(mXyHMe[16]Cyc)	24	An	MeIm	1.5	−40.0	0.0085								
Co^{II}(CyMeMe[16]Cyc)	24	An	MeIm	1.5	−10.0	0.025								
Co^{II}(C5MeMe[$Me_2$16]Cyc)	24	An	MeIm	1.5	−10	0.046								
Co^{II}(C6MeMe[$Me_2$16]Cyc)	24	An	MeIm	1.5	−2.4	1.0	0.0	0.86	9.2	0.27	17.6	0.16	25.0	0.090
Co^{II}(C6MeMe[$Me_2$16Me_2]Cyc)	24	An	MeIm	1.5	20.0	0.170								
Co^{II}(C8MeMe[16Me_2]Cyc)	24	An	MeIm	1.5	20.0	1.75								
Co^{II}(C8MeMe[$Me_2$16]Cyc)	24	An	MeIm	1.5	12.1	1.2								
Co^{II}((C3NMeC3)HMe[16]Cyc)	24	An			−20	0.054	−15	0.0051						
Co^{II}((C3NMeC3)HMe[16]Cyc)	24	An	MeIm	1.5	−20	0.114	−15	0.053	−10	0.027	−5	0.016	0	0.0099
					10	0.0064								
Co^{II}((C3NMeC3)HMe[16]Cyc)	24	An	*d*		−20	0.011	−15	0.0017						
Co^{II}((C2OC2)MeMe[16]Cyc)	24	An	MeIm	1.5	5.0	0.092	20.0	0.027						
Co^{II}((C2CMe_2C2)MeMe[16]Cyc)	24	An	MeIm	1.5	−20.0	0.102	0.0	0.027						
Co^{II}((CPhCPhC)MeMe[16]Cyc)	24	An	MeIm	1.5	−4.4	1.2	6.3	0.33	9.2	0.23	15.5	0.14	20.3	0.070
Fe^{II}((5tBumXy)MeMe[16]Cyc)	24	3:1:1	APW	1.5	−34.7	0.010								
Co^{II}(C7Me[16]Cyf)	34	An	MeIm	1.5	−35	0.015	−23	0.0066	−16.5	0.0024				
Co^{II}(DurPipMe[16]Vcy)	90	H_2O	*c*		0.0	0.070								

Table 6 (Continued)

	ref	sol[f]	base	[B], M	T, °C	K_{O_2}	T, °C	K_{O_2}	T, °C	K_{O_2}	T, °C	K_{O_2}	T, °C	K_{O_2}
Co^{II}(DurPipMe[16]Vcy)	90	H_2O	*b*		0.0	0.074								
Co^{II}(DurPipMe[16]Vcy)	91	An			−16.3	0.075	−7.9	0.053	10.5	0.051	8.5	0.036		
Co^{II}(DurPipMe[16]Vcy)	91	An	MeIm	1.5	1.0	31								
Co^{II}(Bzo_2MeMe[14]Ged)	76	Tol	Py	0.01	5	1.12	10	0.60	20	0.23	28	0.074	35	0.050
Co^{II}(FAc_2MeMe[14]Ged)	76	Tol	Py	0.01	−15	1.58	−5	0.46	5	0.11	15	0.58		
Co^{II}($FBzo_2$MeMe[14]Ged)	76	Tol	Py	0.01	−21	0.089	−15	0.044	−5	0.015	5	0.0075		
Fe^{II}(Me_2MeC7[16]Cyc)	41	An			−38.7	0.0055								
Fe^{II}(Me_2MeC8[16]Cyc)	41	An			−41.0	0.219	−34.9	0.118	−29.5	0.046	−25.0	0.032	−20.7	0.019
Fe^{II}(C5MePh[16]Cyc)Cl	41	Ac	Cl		−19	0.030								
Fe^{II}(C5MePh[16]Cyc)Cl	28	Py			0.0	0.010								
Fe^{II}(C5MePh[16]Cyc)Cl	28	Ac			−19	0.030								
Fe^{II}(C5MePh[16]Cyc)Py	28	3:1:1	APW		−31	>100								
Fe^{II}(C6MeMe[16]Cyc)Cl	28	Ac			−40	>200								
Fe^{II}(mXyBzMe[16]Cyc)Py	28	3:1:1	APW		−34.7	0.016	−34.0	0.013	−30.0	0.0088	−26.5	0.0057	−27.0	0.0050
					−19.5	0.0030								
Fe^{II}(mXyBzPh[16]Cyc)	28	H_2O	MeIm	1.5	0.0	0.031								
Fe^{II}(mXyBzPh[16]Cyc)	28	An	MeIm	1.5	0.0	0.016								
Fe^{II}(mXyBzPh[16]Cyc)	28	MeOH	MeIm	1.5	0.0	0.041								
Fe^{II}(mXyBzPh[16]Cyc)Cl	28	Ac	MeIm	1.5	0.0	0.0086								
Fe^{II}(mXyBzPh[16]Cyc)	28	Tol	MeIm	1.5	0.0	0.022								
Fe^{II}(mXyBzPh[16]Cyc)Py	28	3:1:1	APW		−37.7	0.55	−32.3	0.20	−21.3	0.050	−10.1	0.0091	−10.2	0.0095
					0.0	0.0025								
Fe^{II}(mXyMeHp[16]Cyc)Py	28	3:1:1	APW		−20	0.120								
Fe^{II}(mXyMeMe[16]Cyc)Cl	28	4:1	PAc		−41.5	0.015								
Fe^{II}(mXyMeMe[16]Cyc)	28	Ac	MeIm	1.5	−41.5	1.7								
Fe^{II}(mXyMeMe[16]Cyc)Py	28	4:1	PAc		−41.5	0.08								
Fe^{II}(mXyMeMe[16]Cyc)Py	28	3:1:1	APW		−41.5	0.16								
Fe^{II}(mXyMepCl[16]Cyc)Py	28	3:1:1	APW		−34.5	0.076	−29.8	0.034	−19.1	0.0073	−9.4	0.0022		
Fe^{II}(mXyMepF[16]Cyc)Py	28	3:1:1	APW		−29.8	0.026	−23.0	0.0101	−15.4	0.0037	−6.6	0.0013		
Fe^{II}(mXyMePh[16]Cyc)Cl	28	An	MeIm	1.5	0.0	0.053								
Fe^{II}(mXyMePh[16]Cyc)Cl	28	Tol	MeIm	1.5	0.0	0.0067								
Fe^{II}(mXyMePh[16]Cyc)Py	28	3:1:1	APW		−40.5	0.125	−39.2	0.119	−30.0	0.032	−29.1	0.025	−20.0	0.011
					−12.0	0.0045								
Fe^{II}(mXyMepOMe[16]Cyc)Py	28	3:1:1	APW		−41.3	0.0325	−34.2	0.013	−29.5	0.0065	−32.0	0.0046	−23.8	0.0030
					−15.7	0.0014	−9.8	0.00089						
Fe^{II}(mXyPhBz[16Me_2]Cyc)Cl	30	3:1:1	APW		−24.5	0.36	−20.0	0.21	−15.0	0.101	−10.0	0.067	0.0	0.018
Fe^{II}(mXyPhBz[$Me_2$16]Cyc)Cl	30	3:1:1	APW		−45.0	0.016	−42.2	0.013	−40.0	0.011	−35	0.0061	−30.0	0.003
Co^{II}(($MeOBzo)_2$MeH{12}Mal)	92	Tol	Py	2%	−15	2.6								
Co^{II}(($MeOBzo)_2$MeH-{17NMe}Mal)	92	Tol			−20	12.4								
Co^{II}(($MeOBzo)_2$MeMe{12}Mal)	13	Tol	Py	2%	−15	2.9								
Co^{II}((BzoOC6OBzo)MeMe-{17NMe}Mal)	69	Tol			−10	6.0	0	1.66	5	1.07	10	0.68	15	0.39
					25	0.15								
Co^{II}((BzoOpXyOBzo)MeMe-{17NMe}Mal)	69	Tol			−20	0.059	−10	0.0271	0	0.0093	5	0.0067	10	0.0047
					25	0.0011								
Co^{II}((BzoOC8OBzo)MeH-{12}Mal)	93	Tol	Py		27	0.00943								
Co^{II}((BzoOC8OBzo)MeMe-{12}Mal)	93	Tol	BPy		−11.2	7.06								
Co^{II}(C10MeF[14]Oxm)	66	An	MeIm	0.14	−20	0.468	−15	0.268	−10	0.151	−5	0.088	0	0.052
Co^{II}(C10MeF[14]Oxm)	66	An	Py	0.14	−15	0.0176	−10	0.0095	−5	0.0069	0	0.0036		
Co^{II}(DhaDhaF[14]Oxm)Py_2	45	Tol			−90	2 × 10−4								
Co^{II}(MeMeF[14]Oxm)	66	An	MeIm	0.14	−20	0.206	−15	0.119	−10	0.069	−5	0.041	0	0.025
Co^{II}(MeMeF[14]Oxm)	45	An	Py	0.14	−20	0.0145	−15	0.0101	−10	0.0056	−5	0.0038	0	0.0019
Co^{II}({(NapOC6O-Nap)26}Sal)MeIm	81	Tol	MeIm	0.01	−55.3	0.096	−39.1	0.007						
Co^{II}({(NapOpXyO-Nap)26}Sal)MeIm	81	Tol	MeIm	0.01	−56.2	0.012								

[a] Chelated pyridine is axial base. [b] Medium is 0.1 M aqueous KCl. [c] Medium is 1.0 M KCl. [d] Solution contains 1 equiv of *p*-toluic acid. [e] Unpublished data from Chia and Busch; paper only gives thermal parameters and sample equilibrium constants. [f] Solvents: APW, 3:1:1 acetone/pyridine/water; An, acetonitrile; Ac, acetone; Tol, toluene; DMF, dimethylformamide.

When compared to such long-known dioxygen carriers as cobalt(II) salen or acacen, cobalt(II) cyclidenes have large dioxygen affinities. However, large dioxygen affinities are common among lacunar dioxygen carriers and the dioxygen affinities of the cobalt cyclidenes are about average when compared with others of this group (see below).

1. Dioxygen Affinity and Cavity Size

The dioxygen affinities of the cyclidene complexes correlate with cavity size which is largely determined by the width of the natural cleft that creates the cavity.[24,26,28,94] When the length of the bridging group is increased, the cavity width follows suit. Depending on the bridging group, the height of the bridge above the metal ion may also be important. In the cyclidene systems, a major role of the cavity is to lower the dioxygen affinity; i.e., for a given environment at the binding site and electronic influence on the metal ion, the cavity size may either permit the complex to display its maximum dioxygen affinity or, through steric constraints, produce a systematic decrease in that

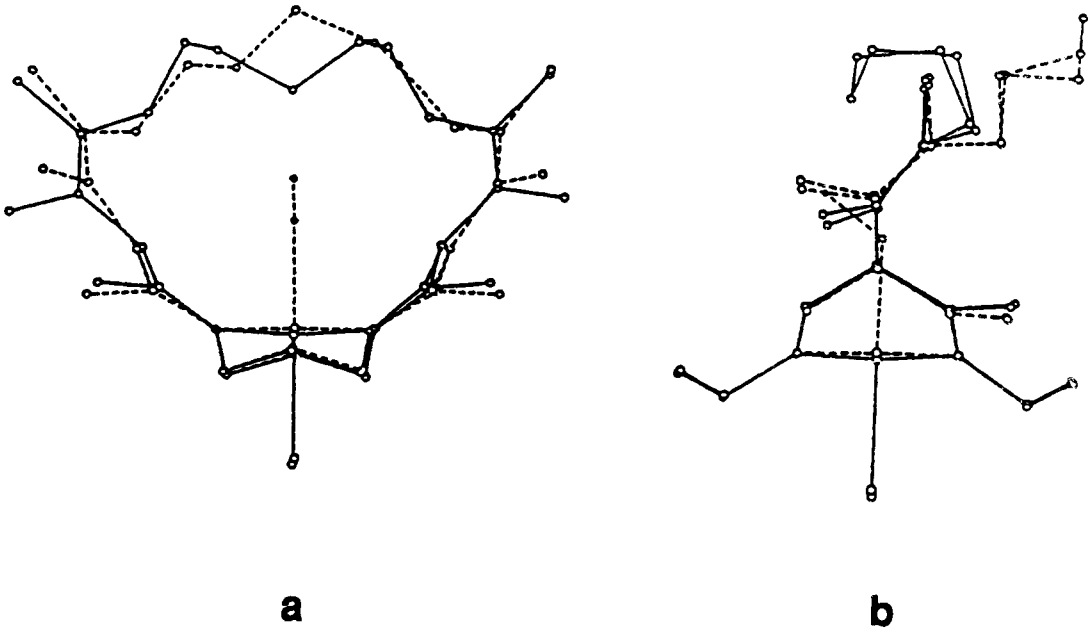

Figure 29. Dual conformations of heptamethylene chain to accommodate filled and empty cavities in lacunar cyclidene complexes.[53]

affinity. The largest dioxygen affinities have been observed for the vaulted cyclidenes of cobalt(II) (Table 6), and those cavities are so large that they can also accommodate small organic substrates in addition to the O_2 molecule. For example in acetonitrile/1.5 M MeIm at 1 °C, the vaulted complex has a K_{O_2} of 31 $Torr^{-1}$ while the maximum value of K_{O_2} found for a polymethylene-bridged cyclidene of cobalt(II) under the same conditions is 5.9 $Torr^{-1}$.

Polymethylene-bridged species have been studied with bridge lengths varying from trimethylene, C3, through dodecamethylene, C12, and the corresponding cobalt dioxygen carriers are properly classified into four groups, depending on the chain length, because of profound difference in the structure/function relationships. The C3-bridged species is in a class by itself because it does not bind small ligands within its cavity.[54]

There is a structural similarity among all of the polymethylene-bridged species having chain lengths equal to or less than C8. The bridge conformations begin at the planar nitrogen atoms by moving parallel to the MN4 coordination plane in what has been called the lid-off configuration (Figures 7–9). However, despite this similarity, two distinct structural behaviors are observed among them (Table 2). The inflexibility of the complexes with the shorter chain species, C4 and C5, leads to strong repulsion between the cavity members and small ligands that bind inside, leading to greatly diminished affinities. In contrast, the *dual conformation complexes* having bridge lengths ranging from C6 through C8 accommodate an incoming ligand, such as O_2 by interchanging between two conformations (or sets of conformations), one of which is well adapted to binding a small molecule within the cavity while the other folds the center parts of the bridge into the cavity and thereby minimizes the volume occupied by the complex (Figure 29).[53]

The gradual transformation in the diastereomeric bridge position from lid-off to lid-on that occurs as the bridge length is increased beyond C8 is accompanied by a smooth decrease in dioxygen affinity (Figure 30).

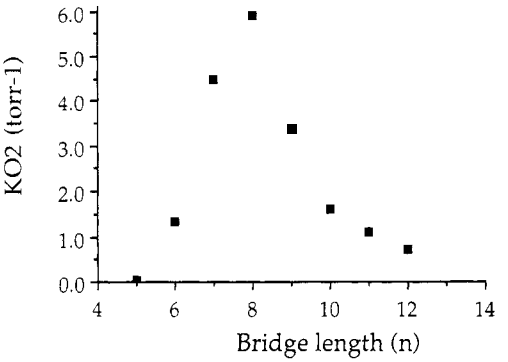

Figure 30. Correlation of bridge length and O_2 affinity for Co(CnMeMe[16]Cyc)MeIm at 0 °C in acetonitrile/1.5 M 1-methylimidazole.

a. Bridge Lengths C4 through C8. The complexes in this group are the most typical and best behaved of the cyclidene family and the structural relationships are the most straight forward. For complexes with $R^3 = R^2 =$ Me and $R^1 =$ Cn the dioxygen affinity varies systematically on varying n from 4 to 8 (Table 6), and that variation parallels a corresponding increase in the width of the cavity of the lacunar complex (Figure 6).[11,24] Figure 31 dramatizes this unusual structural control of a functional molecular parameter, showing clearly how the equilibrium constant varies over approximately 5 orders of magnitude as the bridge length changes. This figure summarizes the data for the three series for which four or five different chain lengths are available while all other structural variables are maintained constant. The equilibrium constants for each family correspond to the same temperature, but temperatures vary from family to family in order to maximize the number of data displayed. As demonstrated in the section on structure, the cavity width increases smoothly as the chain length increases from trimethylene through octamethylene. Figure 31 shows that the extent to which the affinity increases is strongly attenuated in the vicinity of the maximum limit at octamethylene. Since longer bridges lead to decreasing O_2 affinities (see next section) octamethylene represents a true

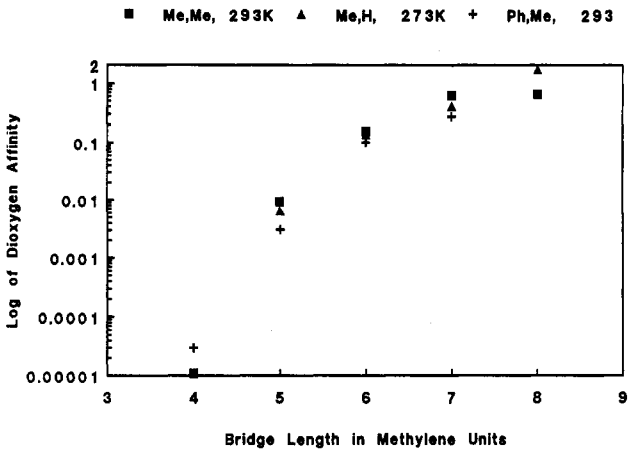

Figure 31. Variation of O_2 affinities for cobalt(II) cyclidene complexes with cavity sizes.

maximum in dioxygen affinity for the cobalt complexes of [16]cyclidenes (Figure 30).

b. Bridge Lengths C9 through C12. Dioxygen affinities are reduced for bridge lengths exceeding octamethylene, an effect which has been correlated with the width of the cavity surrounding the dioxygen binding site. Up to this point, these comparisons have basically involved the empty cavity species because the cavity widths remain essentially unchanged upon occupancy for the bridged species having chains ≤ C8. The correlation between the cavity widths (Figure 6) and the dioxygen affinities (Figure 30) for longer chains, however, must arise differently. The presence of a thiocyanate ligand inside the cavity expands the width of the 6-coordinate undecamethylene-bridged cobalt(III) complex to a value similar to that of the octamethylene-bridged complex. In contradistinction, other observations showed that the widths of vacant cavities do not significantly differ from the widths of filled cavities for bridge lengths ≤ $(CH_2)_8$. This constitutes a distinct behavior of the longer bridged complexes. They are flexible enough to expand their cavities when a small molecule is coordinated to the metal center. The decrease in dioxygen affinity as the chain length increases (n = 8–12) must therefore arise from the energy barrier for this expansion, as a combination of the energy needed to distort the cyclidene unit and that to reorient the chain. The magnitude of the steric effects on dioxygen affinities is similar on the two sides of the graph (Figure 30) so that the affinities for long-chain complexes with a particular cavity width are only slightly larger than those for the corresponding short-chain complexes.

c. Other Bridging Groups. The presence of rings as parts of the bridging group has characteristic effects on affinities. The most studied *m*-xylylene group gives rise to binding constants about equal to those found for tetramethylene-bridged analogues. Similarly, the shortest chain across the cavity in the 1,3-cyclohexylene bridged species is five carbons, but the dioxygen affinity of the corresponding cobalt complex is only one-tenth that of the pentamethylene-bridged species. This does, however, far exceed the affinity of the *m*-xylylene derivative; the latter being at the lower limit of available measurements (~0.001 $Torr^{-1}$) at −40 °C, whereas the former displays a binding constant of 0.025 $Torr^{-1}$ at −10 °C.

In contrast, opening the cavity with large bridges composed partly of small rings has the effect of producing large O_2 affinities. The bridge *m*-CH_2-C_6H_4-*m*-CH_2-C_6H_4-CH_2- (with nine atoms in its shortest chain) gives affinities about a factor of 2 smaller than a hexamethylene-bridged complex. Thus one sees a reduction in cavity size upon the incorporation of each benzene ring that amounts to about 1.5 atom equivalents when viewed in terms of the affinities of polymethylene bridged complexes.

From very limited data (four points) it appears that the presence of a protonated amine in the center of a 7-atom bridging group reduces the O_2 affinity by a factor between 3 and 5.[24] Since the addition to the structure of a strong hydrogen bond would be expected to enhance the dioxygen affinity,[95-96] the effect is attributed to the presence of the tetrahedral charged nitrogen with its bulky methyl group. In contrast, the replacement of the central methylene group in the pentamethylene-bridged species with an oxygen atom is accompanied by an increase in O_2 affinity by a factor of about 2.5 to 3. Putting a bulky *gem*-dimethyl group in the central position in a pentamethylene bridge decreases the affinity by a similar factor. Thus the protonation of the tertiary amine group, in the cyclidene case, appears to produce more of a steric effect than of a hydrogen-bonding effect. Further, the presence of a adjacent positive charge would have been expected to increase the binding because of the superoxide character of the bound O_2. When the equilibrium constant for binding of the bis(3-aminopropyl)methylamine-bridged complex is compared to that of the heptamethylene derivative, a still more surprising result is found. The presence of the NMe group reduces the dioxygen affinity by a factor approaching 100-fold. The most probable rationale for this large effect is that heptamethylene and other 7-atom-bridged species belong to the *dual conformation* group of cyclidene dioxygen carriers, wherein an "open-cavity" conformation is especially favorable for the binding of small molecules within the lacuna. It appears that the substituent disfavors the "open-cavity" conformation. Perhaps lone-pair solvation favors the orientation of the *N*-methyl group toward the cavity, thereby crowding the bound O_2.

d. Bridge Relocation—Retro-Bridged Cyclidenes. The bridging group can be relocated at the R^3 position (see Figures 1 and 11b), and the influence on the binding of dioxygen has been well studied.[41] Retro-bridged complexes have been synthesized with from 5 to 8 methylene groups and they have provided a clear demonstration of the steric source of the increase in dioxygen affinity with bridge length. The shift in half-wave potentials shows that the cobalt becomes increasingly difficult to oxidize as the bridge length increases. This electronic effect should lead to a decrease in O_2 affinity with increasing chain length, contrary to the experimental results.

Comparison with the corresponding complexes in which the bridge is in the usual R^1 location is complicated by a striking additional steric effect. The dioxygen affinity is greatest for the maximum bridge length but only when there is a single alkyl substituent on the pendant nitrogen atom, i.e., either R^1 or R^2 must be hydrogen. At −20.2 °C, K_{O_2} for the heptamethylene retro-bridged complex having R^1 = Me and R^2 = H is

0.015 $Torr^{-1}$ while that of the corresponding complex, differing only in that R^2 is also Me, is too small to measure (<0.0005 $Torr^{-1}$). As presented below, for the more common case where R^1 = bridging group, the replacement of the NH hydrogen by a second Me group is accompanied by a substantial increase in O_2 binding constant. This steric effect is probably traceable to the repulsion between the methyl of the appended nitrogen atom and the R^4 methyl group that is a substituent on the parent cyclidene ring. It is suggested that this interaction directs one *N*-Me group inward, impairing access to the cavity.

Within these limitations, it remains of interest to compare retro-bridged with regularly bridged cyclidene complexes. First of all, for the traverse across the cleft to produce the lacuna, the retro-bridged polymethylene chain must have two more methylene groups to have a chain of the same number of atoms (i.e., for R^1 bridges two nitrogen atoms contribute to chain length). Secondly, having departed from the vinyl site, all atoms in the chain are tetrahedral in structure, whereas the two nitrogen atoms in the regular bridge are trigonal planar. Now (Table 6) at 0, −10, and −20 °C the O_2 affinities of the mono-*N*-methyl-substituted C7 retro-bridged complex are 0.002, 0.0047, and 0.015 $Torr^{-1}$ while those of the regularly bridged C5 derivative having R^3 = Me and R^2 = H are 0.0066, 0.019, and 0.050 Torr-1, at 0, −10, and −20 °C, respectively. Thus, the best retro-bridged derivative has lower affinities for dioxygen than the corresponding R^1 bridged species—and the latter is not the best for its class of structures.

2. Effects of Substituents R^2 and R^3 on Dioxygen Affinities

The effects of R^2 and R^3 on dioxygen affinities of the cobalt^{II}[16]cyclidene complexes are also revealed in Table 6. Considering first complexes with R^3 = Me, the dioxygen affinities of complexes with an electron-donating methyl group attached to the nitrogen atoms of the superstructure (the R^2 position) are always greater than those having hydrogen atoms at R^2, but the magnitude of this effect depends strongly on the length of the bridging R^1 polymethylene group. For the relatively short C5 bridge the ratio of the equilibrium constants (K_{O_2} for R^2 = Me)/(K_{O_2} for R^2 = H) averages about 12, decreasing to 9 at C6, 6 at C7 and finally to 3 for C8. When the same structural variations are considered for the examples where R^3 = Ph, the same general behavior is observed but the effect is diminished by a factor greater than 2. The effects of $PhCH_2$ or $PhCH_2CH_2$ at the R^2 position are very similar to those of methyl groups.

In the R^3 position on the vinyl group of the cyclidene ring, replacing the vinyl hydrogen atom with a methyl group increases the dioxygen affinity dramatically. For example for the C6-bridged species having R^2 = Me, at −10 °C, K_{O_2} = 0.026 for the complex with R^3 = H while K_{O_2} = 4.6 for R^3 = Me, a ratio of approximately 180. In contrast, replacing a Me at the R^3 position with a Ph group shows less dramatic but more complicated changes, increasing K_{O_2} by a small factor when R^2 is methyl and showing a similar decrease when R^2 is hydrogen. The effects of an n-Bu or an n-Pr group are similar, but some 50% larger than those of a methyl group.

The effects described above for the R^2 and R^3 substituents can be ascribed to the electron-donating abilities of the substituents. Because of the conjugated systems in the cyclidene ligands, the electron-donating abilities of the R^2 and R^3 groups have an immediate effect on the electron density at the cobalt center, which in turn affects the dioxygen affinity of any given cyclidene complex. As described above, the electrode potentials of the Ni(III,II) couples of nickel cyclidene complexes reflect the electron-donating abilities of the ligand. The electrochemical data on the nickel complexes shows that both H and Ph are electron withdrawing when compared to methyl groups at the R^3 positions (Table 3). This simple electronic argument accounts very well for most of the effects of the R^2 and R^3 substituents on the dioxygen affinities of the cobalt^{II}-[16]cyclidene complexes. However, the striking increase in sensitivity toward electron-donating groups as the bridging group is shortened, which is found for dioxygen affinities, is not mirrored in the electrochemical data. Since shorter bridges act sterically to diminish the dioxygen affinity, the enhanced sensitivity of the dioxygen affinity to electronic effects may be viewed in analogy to the *selectivity–reactivity principle*. When the dioxygen affinity is diminished sterically, the influence of electronic factors is enhanced; i.e., the less the reactivity (lower dioxygen affinity), the greater the selectivity (electronically).

A trend which cannot be completely explained arises from the contrasting behavior of phenyl and methyl groups at the R^3 position when R^2 is hydrogen. For pentamethylene-bridged complexes, the dioxygen affinities show almost no change when phenyl and methyl are interchanged at the R^3 position, but for the hexamethylene-bridged complexes K_{O_2} is some 2–3 times greater for the phenyl derivatives than for the methyl counterpart. While no adequate explanation is at hand, we suspect that the behavior may be associated with the substantial acidity of the proton R^2 (on nitrogen). Thus hyperconjugative effects might emphasize different resonance forms for the delocalized chelate rings in the phenyl and methyl derivatives.

In sharp contrast to the size of an R^1 group, which controls the dimensions of the cavity and the dioxygen affinity, the R^2 and R^3 substituents are expected to have no substantial steric effects on dioxygen affinity, an assumption that is consistent with the preceding discussion. It is obvious that the size of R^2 will have little effect on K_{O_2} since R^2 is far away from the cavity. Even though R^3 is located at the entrance of the cavity, it is likely that its steric effects are also small because the R^3 groups point outward and away, continuing the general tapering shape of the cavity. The hydrophobic character of bulkier groups at the R^3 site may effectively extend the cavity volume, providing additional shielding for the small ligand therein. Since dioxygen affinities are known to increase with solvent polarity, such a hydrophobic effect would be expected to act counter to the observations.

3. Steric Effects of gem-Dimethyl Groups on the Saturated Chelate Rings

gem-Dimethyl substitutents place an axial methyl group slightly below and otherwise directly in the entry into the lacuna (Figure 14).[30] For lid-off bridges, the

proximity to that position differs substantially, depending on whether the *gem*-dimethyl group is located under the bridge (closed side of lacuna) or on the open side of the lacuna. The latter is most likely to interfere with O_2 binding.[30] For the C6-bridged complex having a *gem*-dimethyl group on the closed side of the lacuna, or the presence of both *gem*-dimethyl groups, is virtually without effect. More limited data indicates that for the C8-bridged species a *gem*-dimethyl group on the closed side substantially enhances the dioxygen affinity. The obvious rationalization is that its steric demand forces a preorganized conformation that facilitates O_2 binding. As discussed below, studies on the iron complexes show that substituents at these positions have profound effects on the interaction between dioxygen and the coordinated metal ion when the bridging group is *m*-xylylene.

4. Influence of the Ring Size of the Parent Cyclidene

The overall shape of the cyclidenes is greatly affected by the size of the parent macrocycle. As detailed in the sections on structure, the conformations of the saturated chelate rings control the shape of the unbridged complexes. The greater stabilities of the chair and boat conformations of the 6-membered chelate rings of the [16]cyclidene, over the skew conformations, produces a deep saddle or U-shaped macrocycle, both in the presence or absence of a bridging group. In contrast, the dimethylene chains of the [14]cyclidenes lead to a relatively planar shape—the so-called Z-shaped complex, while [15]cyclidenes may adopt either a planar or saddle conformation, but either the 5-membered or the 6-membered chelate ring must have a disfavored conformation. That is of little consequence from the structural standpoint if a bridging group forces a U-shape on the structure. The consequences on dioxygen binding are, however, substantial. The strain on the [15]cyclidene produces a widening of the lacuna with the result that O_2 affinities are, except for C5, larger than those of the corresponding [16]cyclidenes, the difference increasing with increasing cavity size.[22] The dioxygen affinity of Co^{II}(C12MeMe[14]Cyc) is greater than that of the corresponding C4[16]cyclidene complex, but less than that of the C5 derivative, and about the same as Co^{II}(C5HMe[16]Cyc). Since electron density arguments suggest that binding to the complex of [14]cyclidene would be favored over that to a corresponding [16]cyclidene, it must be concluded that the presence of a bridge, even as long as C12, strongly disfavors O_2 binding to the [14]Cyc derivative. Molecular modeling suggests[27] that O_2 binding would require pushing the bridge aside, rather like drawing a bowstring, doming the parent macrocycle away from the O_2.

5. Other Effects on Dioxygen Affinities

The K_{O_2} values in Table 6 show that the cobalt(II) complexes [16]cyclidenes follow the general rule that the more polar the solvent and/or the stronger the axial base, the higher the O_2 affinity. For example, the K_{O_2} values for the MeMeC6[16]cyclidene complex in 2.5 M 1-methylimidazole at 10 °C are 4.5 $Torr^{-1}$ in H_2O, 1.06 $Torr^{-1}$ in DMF, and 0.52 $Torr^{-1}$ (interpolated; 1.5 M MeIm) in CH_3CN. The K_{O_2} values for $[Co^{II}$(MeMeC6-[16]Cyc)$]^{2+}$ in MeCN at −10 °C are 0.006 $Torr^{-1}$ with

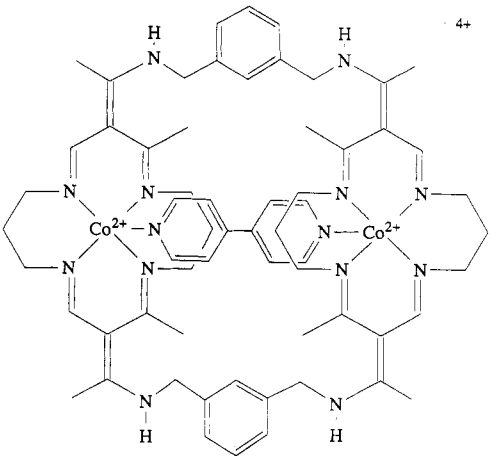

III

Figure 32. Coordinated 4,4′-bipyridine guest in cavity of ditopic dicobalt cyclidene.

no other axial ligand, 0.19 $Torr^{-1}$ in 1 M pyridine (acetone solvent) and 4.6 $Torr^{-1}$ with 1.5 M 1-methylimidazole (CH_3CN solvent). As axial ligands favoring the dioxygen adducts of [16]cyclidenes, the species fall in the following sequence: acetone < DMF < CH_3CN < H_2O < Py < MeIm. (Position of H_2O determined from data on the vaulted cyclidene complexes.)

6. Dinuclear Cobalt Cyclidenes

The dicobalt(II) complexes of ditopic cyclidene ligands have large flexible cavities,[36] but the metal ions are constrained to separations too great to permit simultaneous binding of both cobalt atoms to a single molecule of O_2. From the large cavity, a high affinity would be expected, and the possibility exists that the two cobalt atoms might each bind an O_2 molecule. Indeed, at −45.2 °C, upon exposure to 0.1 Torr of O_2, the ESR signal due to the deoxy complex of the dimethylene-bridged ligand first sharpens up and then converts into that of the 1:1 dioxygen adduct. From these and additional studies it has been concluded that one of the two cobalt atoms is very rapidly oxidized to cobalt(III). The cobalt(III) complex, with its two axial ligands then serves as an unusual bridging group for the remaining "lacunar" cobalt(II) which subsequently forms a relatively stable O_2 adduct. Thus the mixed-valence complex is a reasonably good dioxygen carrier, whereas the dicobalt(II) complex is very rapidly autoxidized, even at low temperatures. In the absence of strong axial ligands (e.g., in acetone or methylene chloride solutions), both cobalt atoms reversibly form dioxygen adducts.

The dinuclear complex having *m*-xylylene bridging groups forms an interesting guest–host complex (Figure 32) wherein a 4,4′-bipyridine molecule enters the cavity and binds to both cobalt(II) atoms.[36] This complex is readily oxidized to the mixed-valence compound which has been characterized in solution, and, remarkably, even at low temperatures (−37 °C), the dicobalt(II)/guest–host complex is rapidly autoxidized to the mixed-valence complex which then acts as a reasonably stable dioxygen carrier.

B. Iron(II) Cyclidene Complexes

The iron(II) cyclidene complexes are remarkable as the only well-established iron(II) dioxygen carriers,

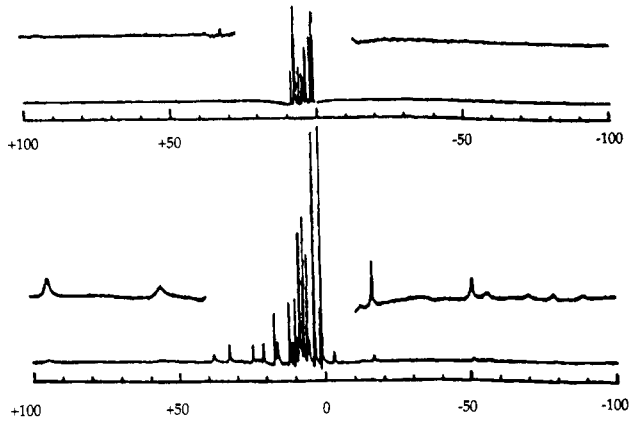

Figure 33. (Lower spectrum) ^{1}H NMR spectrum of Fe^{II}(mXyBzPh[16]Cyc) in pyridine at 253 K and (Upper spectrum) spectrum of same solution after exposure to 752 Torr O_2 for 200 s.

other than those occurring in nature and various derivatives of the porphyrin ring, which is a natural O_2-binding prosthetic group. Proof that reversible dioxygen binding occurs in these systems rests on multiple tests.[14,28,97] Minimally, the electronic spectral changes used to measure equilibrium constants are reversible, and the immediate product of complete reaction with dioxygen is diamagnetic, as revealed by solution magnetic susceptibility measurements and ^{1}H NMR spectroscopy (Figure 33).[14,28] Further, the Mossbauer parameters for the dioxygen adducts of the iron cyclidenes are very similar to those of the similar adducts of iron porphyrins.[97,98] Analysis of the algebraic relationships has shown that the presence of mixtures of complexes having different axial ligands will produce data that conforms to the functional form for normal dioxygen binding equilibria, but the calculated equilibrium constants will be average values.[99]

The iron(II) cyclidenes are also remarkable for the range of autoxidation rates that have been observed (see below) in contrast to the corresponding cobalt(II) complexes. The iron complexes require extensive shielding by bulky substituents in order to retard the autoxidation rate sufficiently to facilitate the study of binding equilibria by direct measurements. Also the dioxygen affinities of iron complexes far exceed those of the corresponding cobalt complexes, a factor that may interfere with reversibility even in the absence of autoxidation. As a result of these tendencies, most measurements have been made of iron(II) [16]cyclidene complexes with small cavities, in order to reduce the O_2 affinity, specifically *m*-xylylene which also greatly reduces the autoxidation rate. The C4-bridged complex autoxidizes very rapidly even at −40 °C, an observation attributed to the slight shielding of the dioxygen binding site from the environment or external reagents.[14,28]

A few values for Fe^{II}(C5MePh[16]Cyc)Cl allow direct comparison with cobalt(II) (Table 6). At 0 °C with Py as an axial ligand (in pyridine solvent), K_{O_2} = 0.010 $Torr^{-1}$ for the iron(II) complex. Interpolating, the corresponding cobalt(II) complex would be expected to have a K_{O_2} of about 10^{-4} $Torr^{-1}$. Even this large difference may underestimate the differences in affinities since there is reason to suspect that both pyridine and chloride act as axial ligands in the case of this iron complex.[99] In acetone solution with no added

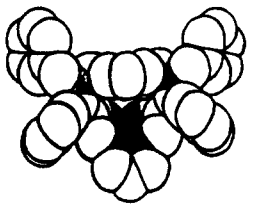

Figure 34. Space-filling representation of the X-ray structure of the nickel complex of mXyBzPh[16]Cyc (Ni and N atoms shaded for clarity).

base, the binding constant for the iron(II) complex is 0.030 $Torr^{-1}$ at −19 °C. In contrast, it has been demonstrated that the solvent 3:1:1 acetone/pyridine/water (henceforth APW) results in complete replacement of axial chloride by pyridine and K_{O_2} has been estimated to be >100 $Torr^{-1}$ at −31 °C. The temperature ranges over which these measurements were made was limited by competing autoxidation.

Fe^{II}(mXyMeMe[16]Cyc)Cl, in APW at low temperature, was used in the first convincing demonstration of reversible dioxygen[100] binding by an iron cyclidene complex. The dioxygen affinity of 0.016 $Torr^{-1}$ at −34.7 °C gave large changes in spectra as O_2 was added and removed and the low temperature retarded autoxidation. From the values given above for the C5-bridged species, it is apparent that a wide range of dioxygen affinities is potentially available with the iron cyclidene complexes.

The substituents R^2 and R^3 have more profound effects on the binding behavior of the iron complexes than was observed with those of cobalt. The more dramatic effects relate to the retardation of autoxidation, and these will be discussed in a later section. However, that effect has facilitated the measurement of the equilibrium constants for dioxygen binding at relatively high temperatures for some of these complexes. Most of the data on Fe^{II}(mXyMeMe[16]Cyc) was obtained at low temperatures (<−30 °C), but replacement of the R^3 methyl group with a phenyl group makes temperatures some 30° higher accessible to equilibrium measurements (Table 6). Moreover, substitution of a benzyl group for the methyl group at R^2 produces a species that is sufficiently stable for equilibrium measurements at room temperature and above.[101] The steric bulk surrounding the O_2 binding site in that species is well illustrated for the closely similar nickel complex in Figure 34; for comparison, see Cyc structure in Figure 1 and a related crystal structure in Figure 14. The binding constants for the species approximated by Figure 34, Fe^{II}(mXyBzPh[16]Cyc), show a solvent dependence that is not readily explained (toluene ≃ 1-methylimidazole > acetonitrile > acetone > methanol), failing to correlate with such characteristics as polarity or hydrophobicity. As observed for the cobalt counterparts, phenyl groups reduce the dioxygen affinities by a small factor, and electron-withdrawing groups on the phenyl produce additional small decreases. The fully methylated retro-bridged complexes of iron(II) bind dioxygen reversibly and give substantial binding constants.

The presence of *gem*-dimethyl groups as components of the saturated chelated rings has profound effects for the *m*-xylylene-bridged iron(II) cyclidenes.[30] When such a group is beneath the bridge and away from the large opening into the lacuna, the dioxygen affinity is

enhanced by a factor of about 4, and this has been explained, by molecular modeling. The bulky substituents force the bridge upward, increasing the size of the cavity slightly. Conversely, placement of the group on the other chelate ring locates a methyl group directly in front of the large opening (Figure 14) and this decreases the dioxygen affinity greatly (a factor of 0.01 or less). Steric interactions between a methyl group and the bound O_2 account for the dramatic effect. The presence of two pairs of *gem*-dimethyl groups effectively stops O_2 binding entirely.

C. Non-Cyclidene Lacunar Dioxygen Carriers

All non-cyclidene lacunar dioxygen carriers are cobalt(II) derivatives. The most interesting lacunar Schiff base complexes are the pentadentate Mal complexes Co^{II}((BzoOCnOBzo)MeMe{17NMe}Mal) because the parent ligand provides all needed ligating atoms as well as the protected cavity within which O_2 binds (Figure 20).[65] The dioxygen affinities for the optimal C6-bridged species are extraordinarily high for this family of Schiff base complexes of cobalt(II).[5,102] The complexes are also outstanding in their resistance to autoxidation, with half-lives of the order of hours at 50 °C. The O_2 affinity of the *p*-xylylene-bridged complex is about a factor of 100 lower than that of the C6-bridged complex, a difference attributed to the large steric hindrance due to the rigid bridge. Work with nonlacunar $Co^{II}(MeOBzo)_2MeH${17NMe}Mal) gave evidence for both μ-peroxo dimer and 1:1 O_2 adduct formation and a much greater rate of autoxidation.

Each part of the bridging group in these complexes play a significant role. The acyl groups function both as risers to lift the spanning group above the metal ion and as electron-withdrawing groups, to stabilize the complex toward autoxidation. The effectiveness of the acyl substituents in the latter role is demonstrated by the fact that an alkyl group at this position produces a half-life of autoxidation in pyridine/toluene at −10 °C of about 200 s, whereas the acyl-containing lacunar complex is stable for many minutes at 50 °C. Comparing optimized structures (C6-bridged Mal and C8-bridged cyclidene) the cyclidene has, by a small factor, the greater dioxygen affinity.

The known lacunar Schiff base complexes derived from salicylaldehyde (Sal, Figure 23)[48,81] have very low dioxygen affinities, 0.096 $Torr^{-1}$ for the example having its risers spanned by a C6 link and 0.012 $Torr^{-1}$ for the example spanned by *p*-xylylene, both at −55 °C. However, optimization has not been attempted. It is probably significant that the *p*-xylylene linkage produces substantial reductions in dioxygen affinity for both the Sal and Mal families of Schiff base complexes.

The macrocyclization of the long known bis(α-dioxime) complexes by replacing the two hydrogen bridges with BF_2^+ and other covalent linkages has provided a very promising family of ligands for the formation of lacunar dioxygen adducts.[45,46,66,103,104] To date only a cis-bridged derivative has been synthesized.[47,56,66] For these complexes, competition for the lacunar site between axial base and O_2 shows the ineffectiveness of this geometry. However, some indication of relative dioxygen affinities has been obtained. The value in acetonitrile/*N*-methylimidazole at 0 °C of 0.052 $Torr^{-1}$ is about 100 times less than the value for Co^{II}(C8MeMe[16]Cyc) under the same conditions (Table 6). A provocative conclusion is that the dioxygen affinities of the iron(II) oxime complexes should be of convenient magnitude. The early report[105] that a ligand having the same bulky groups conferred on iron(II) the ability to reversibly bind dioxygen led to the synthesis and characterization of the hindered oxime macrocycle shown in Figure 21.[45] A crystal structure has shown that this superstructure is not very protective of the metal center in the α-dioxime derivatives. As in the case of other cobalt(II) oxime complexes, axial ligand binding competed with dioxygen coordination. In acetonitrile glasses, both in the presence and absence of axial bases, the dioxygen adduct was readily observed at 77 K. However, in liquid toluene, the extent of binding was very slight, even at the very low temperature of −90 °C, where a binding constant of $\sim 2 \times 10^{-4}$ $Torr^{-1}$ was estimated from the ESR signal. It should be pointed out that this result is the opposite of what would have been predicted from the electrochemical data; the anomaly derives from the axial ligand competition, a factor that would be eliminated by an effective lacunar structure.

In summary, to date the relative O_2 affinities of the lacunar cobalt(II) complexes appear to be in the order: cyclidene > Mal > Oxm > Sal. However, not all of these families have been optimized.

V. Autoxidation

All known dioxygen carriers undergo autoxidation in solution, but reduction processes will restore the ability of many of them to bind O_2. For example, about 1% from the 1.5–3% of mammalian hemoglobin[106] that is autoxidized each day is restored.[107] However, the intervention of irreversible pathways leads to permanent inactivation or destruction of certain dioxygen carriers, commonly accompanied by ligand oxidation. Because of its universal occurrence, autoxidation ranks second only to the O_2-binding process in importance in the chemistry of transition metal dioxygen carriers. Despite the importance of autoxidation, the subject has not been extensively reviewed with the first major review having just appeared.[12] Therefore, the foundations of autoxidation are reviewed here more extensively than are the other much reviewed basic aspects of the chemistry of lacunar dioxygen carriers.

Although dioxygen[108–110] is a 4-equivalent oxidant, mechanistic studies commonly reveal only one- and two-electron processes, and these are related to the thermodynamics of the overall redox system. Only relatively strong reductants are expected to be oxidized by the one-electron reaction of O_2 to form O_2^- because of the negative potential of the O_2/O_2^- couple. In contrast, the potential for the two-electron reduction of O_2 is highly positive in both acid and neutral solutions, and autoxidation is thermodynamically favorable for many dioxygen carriers, specifically those with potentials less positive than about 0.7 V vs SHE.

A. Autoxidation of Iron(II) Compounds

Essentially all discrete molecular iron(II) compounds are of interest in the context of autoxidation, but interest

tends to focus on the natural dioxygen carriers, hemoglobin (Hb) and myoglobin (Mb), their prosthetic groups, the iron porphyrins, with their many modifications, together with their only well-established entirely synthetic models, the iron(II) cyclidenes. The resistance to autoxidation for an iron(II) complex depends on structural features that hamper a succession of decreasingly effective autoxidation mechanisms. Two of these mechanisms are now reasonably well established.

1. Peroxo-Bridged Mechanism

The longest known mechanism for autoxidation of iron(II) dioxygen carriers follows a two-electron pathway, involving the formation of a peroxo-bridged dinuclear iron(III) intermediate, $LFe^{III}(O_2^{2-})Fe^{III}L$ (Scheme 5). This critical intermediate can form only if two iron atoms can be bound to the dioxygen unit simultaneously.

Scheme 5

$$LFe^{II} + O_2 \leftrightarrow LFe^{III}(O_2^{-}) \quad (1)$$

$$LFe^{III}(O_2^{-}) + Fe^{II}L \leftrightarrow LFe^{III}\text{–}O_2\text{–}Fe^{III}L \quad (2)$$

$$LFe^{III}\text{–}O_2\text{–}Fe^{III}L \leftrightarrow 2LFe^{IV}O \quad (3)$$

$$LFe^{IV}O + Fe^{II}L \leftrightarrow LFe^{III}\text{–}O\text{–}Fe^{III}L \quad (4)$$

The μ-peroxo mechanism is not limited to iron porphyrins but has been proposed for the reactions of dioxygen with many types of iron(II) compounds, including simple salts. The autoxidation of iron(II) perchlorate and chloride obey the same rate law, rate $= k[Fe]^2[O_2]$.[111,112] The autoxidation reactions of many cobalt(II) complexes appear to follow a similar mechanism, differing in the critical fact that the μ-peroxo complex is stable and shows no tendency to cleave. Analogous μ-peroxo dimer formation occurs in the reaction of O_2 with chromium(II) complexes[113] and ruthenium porphyrins.[114]

The oxidation state of each metal atom increases by one unit upon formation of the dinuclear μ-peroxo complex, and the cleavage of this intermediate to form the oxo complex requires a further increase in the metal ion oxidation state, for an overall change of +2. The occurrence of the O–O bond cleavage step appears to correlate with the accessibility of the higher oxidation states. Thus the bulk of the studies on this mechanism and its intermediates have been with iron, and the ferryl and other iron(IV) species have become well known in recent years.[114–126] In contrast, cobalt(II) complexes most often form relatively stable dinuclear derivatives and the autoxidation reactions of cobalt(II) complexes typically stop at the μ-peroxo dimer. Chromium exemplifies the situation for metals having well-established high oxidation states. Oxochromium(IV) and oxochromium(V) species have been isolated and characterized;[127–131] some of the high-valent derivatives were formed by reaction of chromium(II) complexes with molecular dioxygen.[132–134]

The peroxo-bridged mechanism for the autoxidation was proposed, apparently independently, on the bases of studies on iron porphyrins[135] and on iron salts dissolved in organic solvents[111] (Scheme 5). The second-order rate law for the autoxidation of iron(II) chloride in solvents such as alcohols, glycols, and dmso and the fact that the oxidation of the substrate benzoin showed a parallel kinetic profile led Hammond and Wu[111] to the model. Further, the volume of O_2 consumed suggested the oxidation of solvent, and in the case of alcohols, aldehydes were detected. These observations led to the suggestion that a peroxo-bridged intermediate first formed and then cleaved into an oxoiron(IV) intermediate.

Caughey first proposed the mechanism shown in Scheme 5 for porphyrin complexes[136] on the basis of the following observations. The product of the reaction was found to be an oxo-bridged complex. The mechanism does not require water, and hydrogen peroxide is not produced. Excess pyridine inhibits the autoxidation, an observation suggesting that pyridine might compete with O_2 for a coordination site. Most importantly, kinetic studies had shown that the autoxidation of (2,4-protoporphyrin IX dimethyl ester)iron(II) in benzene/pyridine/ethanol at 25 °C is second order in iron and first order in dioxygen at low pyridine concentrations, a result completely consistent with a reaction involving a dinuclear intermediate.[137] Among the strongest indications of the validity of the peroxo-bridge mechanism[138] is the success of the often used strategy for the synthesis of hemoglobin and myoglobin models that provides steric protection at the iron site to prevent formation of the Fe–OO–Fe intermediate.[139–141]

The existence of the critical intermediates in the peroxo-bridged mechanism has been established by elegant studies. With iron porphyrins[142,143] a transient 1:1 dioxygen complex has been detected and found to combine with a second iron(II) complex to form the dinuclear peroxo-bridged species. The μ-peroxo dimer of iron(*meso*-tetrakis(*m*-tolylporphyrin)) was originally characterized by Balch et al. using ^1H NMR in toluene at −80 °C[143,144] and more recently by spectroscopic and chemical studies.[145] Conversion of the μ-peroxo dimer to the μ-oxo dimer has also been studied.[143,144] According to the mechanism, the O–O bond of the peroxo group of unhindered porphyrins undergoes homolytic cleavage, followed by rapid reaction of the cleavage product with iron(II) porphyrin, leading to the stable iron μ-oxo dimer. When the formation of the Fe–O–Fe unit is sterically prevented, a mononuclear hydroxoiron(III) product is formed.[146] The addition of *N*-methylimidazole to the μ-peroxoiron complexes of *meso*-tetrakis(*m*-tolylporphyrin) and tetraphenylporphyrin in toluene at −80 °C is followed by the formation of the ferryl complex, which is indefinitely stable under those conditions.[144,147] The d^4 iron(IV) in this ferryl complex was characterized as having an $S = 1$ ground state, on the basis of its magnetic moment of 2.9 Bohr magnetons. Corresponding properties have been reported for a related dialkyloxyiron(IV) porphyrin.[148] The Fe=O stretching vibration for Fe(TMP)=O has been recorded at 841 cm^{-1} in dichloromethane at −85 °C.[144,149] Interestingly, the reaction of the ferryl group with iron(II) to form the μ-peroxo dimer is reversible, either photochemically[150] or by the stabilization of the iron(II) species in certain cases.[142]

The μ-peroxo-bridged autoxidation mechanism is prevented in heme proteins by the protective confinement of the iron(II) porphyrin prosthetic group within a globular protein. Therefore, hemoglobin and myoglobin must undergo autoxidation by an alternative mechanism. Three mechanisms have been considered, each involving a one-electron rate-determining step.

2. One-Electron Mechanisms

The simple fact that hemoglobin and myoglobin are autoxidized requires at least one mechanism in addition to the μ-peroxo route. While other two-electron pathways are conceivable, the importance of the III,II redox couples in iron and cobalt chemistry and the frequent detection of superoxide as an autoxidation product provide strong indications of the importance of one-electron mechanisms. As the following discussion will show, these mechanisms proceed by one-electron pathways, but they simultaneously enjoy the thermodynamic advantages of two-electron processes. Stanbury, Haas, and Taube[151] showed how this can happen. The standard electrode potential for O_2/O_2^- is -0.16 ± 0.02 V with 1 M O_2 as the standard state,[152,153] suggesting that only reduced species with potentials more negative than -0.16 V would react spontaneously with O_2 by one-electron mechanisms. A process involving two one-electron steps can overcome this problem, if the second step involves the superoxide produced in the first step. In fact, rapid disproportionation of the superoxide to hydrogen peroxide and dioxygen would effectively convert the reaction into a two-electron process insofar as the thermodynamics of the oxygen system is involved; e.g., eq 7. These relationships are exemplified by the autoxidation of $[Ru^{II}(NH_3)_5isn]^{2+}$, (isn = isonicotinamide) (Scheme 6).[151]

Scheme 6

$$Ru^{II} + O_2 \leftrightarrow Ru^{III} + O_2^- \quad k_1, k_{-1} \tag{5}$$

$$O^{2-} + H^+ \leftrightarrow HO_2 \quad K_a^{-1} \tag{6}$$

$$O_2^- + HO_2 \rightarrow O_2 + HO_2^- \quad k_2 \tag{7}$$

$$Ru^{II} + HO_2 \rightarrow Ru^{III} + HO_2^- \quad k_3 \tag{8}$$

Either eq 7, the disproportionation of superoxide, or eq 8, the oxidation of a second mole of $[Ru^{II}(NH_3)_5isn]^{2+}$ by the superoxide, would make the overall two-electron process highly exothermic. For $[Ru^{II}(NH_3)_5isn]^{2+}$ and other examples,[154-156] the second-order reaction described by eq 8, which is first order in superoxide, drives the system, rather than the disproportionation reaction (eq 7) because the concentration of superoxide is very low. Other studies[154-156] have shown that both O_2^- and HO_2 oxidize coordinately saturated metal complexes, the latter almost certainly by an outer-sphere electron-transfer path. Energy considerations, pH studies, and isotope effects indicate that the reaction of O_2^- with metal amine complexes, at high pH, involves hydrogen abstraction, either as a radical reaction or by a concerted electron and proton transfer facilitated by direct bonding to the metal ion.[154]

Scheme 7, the superoxide displacement mechanism, was proposed by Caughey[157] and has been supported by Shikama.[158] The essence of the concept is that a nucleophile (solvent, counterion, etc.) displaces the superoxide ligand by a bimolecular front-side attack at the iron(III) center.

Scheme 7

$$Mb + O_2 \leftrightarrow MbO_2 \tag{9}$$

$$MbO_2 + X^- \rightarrow \text{met-MbX} + O_2^- \tag{10}$$

Caughey[159] later suggested an alternative mechanism which involves electron-transfer Scheme 8. In the latter mechanism, potential ligands, such as solvent, counterions, etc., compete with O_2 for the available coordination site, and the rate-determining autoxidation step is an outer-sphere electron-transfer event between O_2 and iron(II) species that do not contain bound O_2.

Scheme 8

$$HbO_2 \leftrightarrow Hb + O_2 \quad K \tag{11}$$

$$Hb + L^- \leftrightarrow Hb(L^-) \quad k_1, k_{-1} \tag{12}$$

$$Hb(L^-) + O_2 \leftrightarrow \text{met-Hb}(L^-) + O_2^- \quad k_2, k_{-2} \tag{13}$$

A fourth mechanism, the unimolecular dissociation of superoxide from the dioxygen complex, is often presumed on the basis of qualitative observations, but detailed mechanistic studies have given it no support.

Any of the four pathways described above could lead to simple oxidation of the metal ion or to the accompanying oxidation of the ligand, and, of course, ligand oxidation could proceed by still different mechanisms.

3. Iron(II) Cyclidene Autoxidation, the Electron-Transfer Pathways

The kinetics of autoxidation of iron(II) cyclidenes[160-163] have been studied as functions of important stoichiometric and chemical variables, including complex concentration, dioxygen pressure, solvent, axial base, and acid–base relationships; the results have been correlated with variations in structural parameters, mainly the nature of the substituents and cavity size. With increasing cavity size, first O_2, and then solvent species, can enter and bind to iron, and this is accompanied by changes in the algebraic form of the rate law for autoxidation. Analysis strongly suggests that the molecule of O_2 that oxidizes the iron(II) is not bound, thus implicating an electron-transfer mechanism in the autoxidation process.

a. Effects of Cavity Size. The facile control over the structures of the cyclidene complexes has made it possible to observe an extreme variation in autoxidation behavior. Figure 35 depicts the dioxygen pressure dependence of the autoxidation rates of the iron cyclidene complexes as the bridging polymethylene group increases in length. At C3 (trimethylene bridge), simple first-order dependence on P_{O_2} is observed; lengthening the bridge to C4 produces saturation behavior; and increasing the bridge length still more to C5 produces a dramatic "dioxygen protection". The impact in establishing mechanism is best shown by first

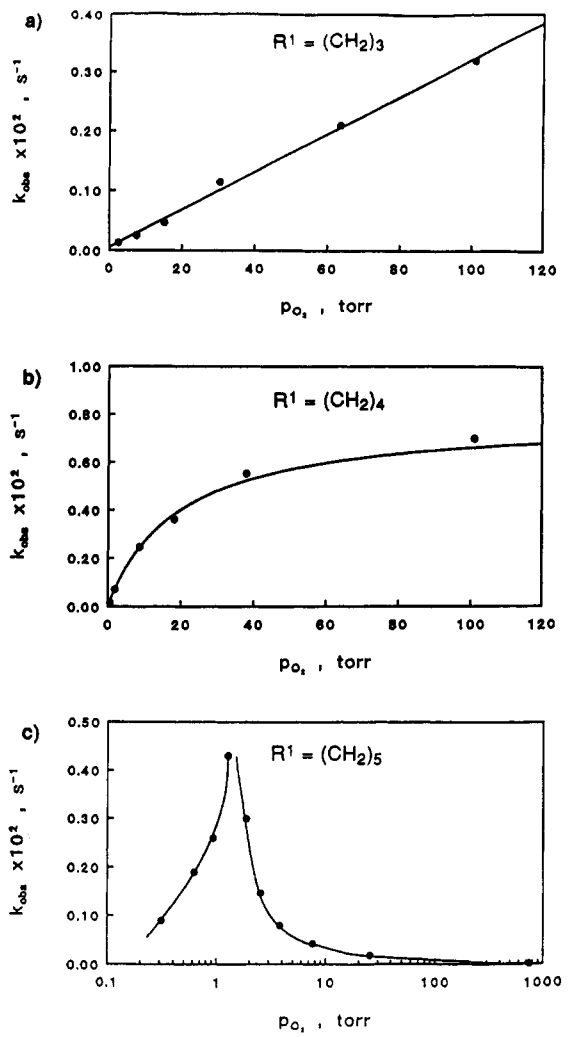

Figure 35. O_2 dependence of the rate of autoxidation of iron cyclidene complexes as the polymethylene chain increases in length. In MeOH/1 M 1-methylimidazole/0.05 M tetrabutylammonium tetrafluoroborate at 0 °C: (a) Fe(C3MeMe-[16]Cyc)Cl; (b) Fe(C4MePh[16]Cyc)Cl; (c) Fe(C5MePh[16]-Cyc)Cl.

considering the C4 case, since saturation behavior is frequently observed.

The obvious model to explain the saturation behavior of the tetramethylene bridged iron(II) cyclidene is the long-assumed superoxide dissociation mechanism (Scheme 9, eqs 14 and 15). This simply involves preequilibrium formation of the dioxygen adduct which subsequently liberates superoxide,[164] leading to the rate law in eq 16.

Scheme 9

$$Fe^{II} + O_2 \leftrightarrow Fe(O_2) \quad K_{O_2} \tag{14}$$

$$Fe(O_2) \rightarrow Fe^{III} + O_2^- \quad k \tag{15}$$

$$\text{rate} = kK_{O_2}[Fe^{II}][O_2]/\{1 + K_{O_2}[O_2]\} \tag{16}$$

It is, however, necessary to consider a second mechanism that predicts precisely the same algebraic form for the rate law. This is an electron-transfer process in competition with the dioxygen-binding equilibrium. Equations 17 and 18 (Scheme 10) present this mechanism and its rate law is given in eq 19.

Scheme 10

$$Fe^{II} + O_2 \leftrightarrow Fe(O_2) \quad K_{O_2} \tag{17}$$

$$Fe^{II} + O_2 \rightarrow Fe^{III} + O_2^- \quad k' \tag{18}$$

$$\text{rate} = k'[Fe^{II}][O_2]/\{1 + K_{O_2}[O_2]\} \tag{19}$$

Both mechanisms predict (1) first-order dependence on iron concentration, (2) saturation kinetics with zero order dependence of the rate on $[O_2]$ at high $[O_2]$, and (3) first-order dependence on $[O_2]$ at low concentrations. The choice between mechanisms (preequilibrium and superoxide dissociation vs competitive equilibrium and electron transfer) rests on the parametric dependence of the two rate laws on dioxygen affinity K_{O_2} and the effects of the facile changes that can be made in the structure of the dioxygen binding site of the cyclidene complex. Equation 16 requires the rate of autoxidation to go to zero when the dioxygen affinity (K_{O_2}) vanishes. Chemically, the complex cannot dissociate a superoxide unless it first binds O_2. In contrast, eq 19 only depends on dioxygen affinity in the denominator and, when K_{O_2} goes to zero, the rate law merely changes to simple first order (in $[O_2]$).

Despite repeated attempts to form adducts with both O_2 and CO, it has always been found that no ligand can enter the cavity of the trimethylene-bridged species, therefore the C3 case qualifies as having zero dioxygen affinity.[54] It follows that the behavior of the C3-bridged complex shown in Figure 35, simple first-order dependence on dioxygen pressure, provides a critical distinction in favor of the competitive equilibrium/electron transfer mechanism (Scheme 10) for the autoxidation of the iron cyclidene complexes. The alternative superoxide dissociation (Scheme 9) (or displacement, Scheme 7) mechanism predicts that the C3-bridged complex would not autoxidize, whereas that complex autoxidizes the most rapidly of all.[161]

The conclusion that autoxidation occurs by an electron-transfer mechanism (Scheme 10) is strongly supported by the consequences of opening the cavity further. At C3 nothing enters the cavity; at C4, O_2 enters the cavity and that process competes with electron transfer between the iron center and O_2, giving rise to O_2 saturation behavior in the autoxidation process. Opening the cavity still more by adding the fifth methylene group to the bridge leads to dioxygen protection behavior for the C5 complex that is also shown in Figure 35. This behavior manifests the competitive binding of solvent molecules in the cavity. Thus eqs 20 and 21 are added to eqs 17 and 18 to produce the overall mechanism, and the steady state (on $Fe^{II}S$) rate law is given in eq 22 (S represents a solvent molecule).

$$Fe^{II} + S \leftrightarrow Fe^{II}S \quad k_1, k_{-1} \tag{20}$$

$$Fe^{II}S + O_2 \rightarrow Fe^{III}S + O_2^- \quad k_2 \tag{21}$$

$$\text{rate} = \frac{k_1(k_2/k_{-1})[Fe^{II}][S][O_2]}{(k_2/k_{-1})K[O_2]^2 + \{(k_2/k_{-1}) + K\}[O_2] + 1} \tag{22}$$

At high O_2 pressures, the $[O_2]^2$ term in the denominator dominates, causing the rate to decrease with further

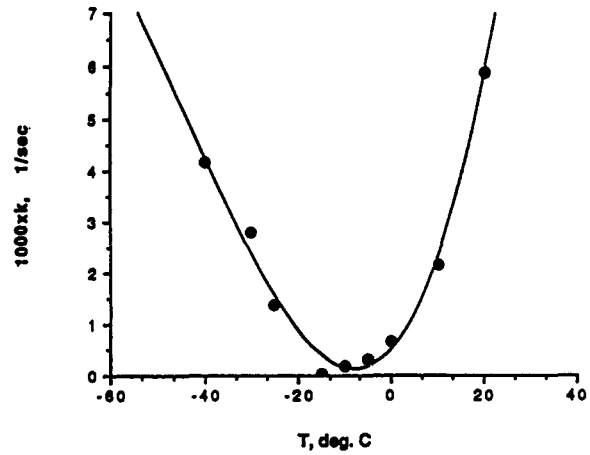

Figure 36. Temperature dependence of the rate of autoxidation of Fe(C6MePh[16]Cyc)Cl in 3:1:1 acetone/pyridine/water at 150 Torr of O_2. [T (°C), k (s^{-1}): 20, 5.92×10^{-3}; 10, 2.16×10^{-3}; 0, 6.50×10^{-4}; -5, 3.21×10^{-4}; -10, 1.79×10^{-4}; -15, 3.69×10^{-5}; -25, 1.37×10^{-3}; -30, 2.82×10^{-3}; -40, 4.18×10^{-3}.]

increases in dioxygen pressure. The observation that the autoxidation rate eventually reaches a constant value at very high pressures is explained on the basis of the competing saturation pathway (eqs 17 and 18).

Opening the cavity still more yields the C6-bridged compound, and its tendency to bind a sixth ligand is so great that the 6-coordinate derivative is a major species at low temperatures, and this produces a most revealing thermochromism.[28] Under strictly anaerobic conditions, spectral and magnetic properties appear that are characteristic of low-spin 6-coordinate iron(II) complexes with ligands having azomethine donor atoms.[28,165] The temperature dependence of the autoxidation rate of the C6 system is fascinating. As Figure 36 shows, the rate of autoxidation displays a parabolic dependence on temperature. Upon cooling from room temperature, the rate at first decreases in a normal manner, but it then increases rather dramatically so that, for example, the autoxidation rates are about the same at room temperature and at -40 °C. Since the several enthalpies of activation and/or equilibration associated with a single reaction pathway bear an additive relationship, the parabolic temperature dependence suggests the inception of a second path for autoxidation and is consistent with the overall model presented above. The two pathways involve electron transfer between O_2 and, respectively, the 5-coordinate deoxy complex and the 6-coordinate solvated complex.

b. Substituent Effects on the m-Xylylene-Bridged Complexes. [Fe(mXyBzPh[16]Cyc)]$^{2+}$ is the most notable of the iron(II) cyclidenes; it exhibits reversible dioxygen binding with remarkable autoxidation half lives of ~6 h at 20 °C in 1:1:1 acetone/pyridine/water and about 1 h in LiCl/MeOH, both in air.[162,163] However, most of the iron(II) cyclidenes are less stable in the presence of dioxygen and have substantially shorter autoxidation lifetimes. Consequently, it has been possible to select species ideally suited to investigate certain aspects of the autoxidation reactions. Rate studies in a solvent consisting of 3:1:1 by volume acetone/pyridine/water (311APW) show that the rate of autoxidation is strictly first order in the concentration of iron while its dioxygen dependence follows the saturation rate law. The parallel kinetic behavior for

Table 7. Comparison of Kinetic Parameters for Substituted Iron(II) Cyclidenes (R^1 = *m*-Xylylene, MeOH Solvent, Cl^- Axial Base)

R^2R^3	T, °C	K, $Torr^{-1}$	k, $Torr^{-1}$	$t_{1/2}$ at 1 Torr
MeMe	-25	0.084	3.0×10^{-4}	40 min
BzMe	-25	0.012	2.3×10^{-5}	8 h
MePh	-25	0.00075	3.1×10^{-6}	2.5 days
BzPh	+20	0.0030	1.7×10^{-6}	5 days

the *m*-xylylene-bridged complex and the tetramethylene-bridged species (both obey saturation kinetics) is consistent with their dioxygen affinities, which are quite similar (Table 6).

Table 7 lists the rate parameters obtained for a short series of *m*-xylylene-bridged species in which the sizes of the substituents R^2 and R^3 are increased. Depending on the solvent, increasing the bulk of these groups may retard the rate by some 10^2 to 10^4. In 311APW, when modest protection from autoxidation is provided by the bulky groups, the equilibrium constants calculated from the rate data are consistent with direct equilibrium constant measurements. In contrast, data in MeOH/LiCl shows remarkable stabilization against autoxidation by the bulky substituents, amounting to a rate reduction by a factor approaching 10^4, but the rate parameters do not agree with the simple competing equilibrium model. Instead of the simple model used earlier, it is necessary to incorporate the follow-up reaction (new eq 23, following eq 18 in Scheme 10 or eq 21 in the expansion of that scheme) involving the superoxide and a second mole of the iron complex. A simplified version of the corresponding new rate law has the same algebraic form (as observed) but differs in its parameters from the previous interpretation (eq 24). Unfortunately the new parameters are not readily

$$Fe^{II} + HO_2 \rightarrow Fe^{III} + HO_2^- \quad k_3 \qquad (23)$$

$$-d[Fe^{II}]/dt = 2k'k_3[Fe^{II}][O_2]/\{(k_3 - k_2) - k_2K_{O_2}[O_2]\} \qquad (24)$$

reduced to rate and equilibrium constants for the individual reactions. The reaction of eq 23 is, however, necessitated by the thermodynamic requirements of the one-electron mechanism, and it is gratifying to see kinetic evidence for its importance. Further confirmation of the significance of this follow-up reaction has been found in investigations of the primary products of these autoxidation processes.

c. Primary Products in the Autoxidation of [Fe(mXyMeMe[16]cyc)Cl]$^{2+}$. The first lacunar iron(II) cyclidene dioxygen carrier reported,[101] R^1 = *m*-xylylene, $R^2 = R^3 = CH_3$, was particularly useful because it undergoes autoxidation in a temperature range low enough to permit study of important reactive intermediates. Electron-spin resonance experiments have led to identification of the initial reaction products arising from the primary electron-transfer event.[162] Figure 37 shows typical ESR spectral changes during autoxidation. A signal at $g = 6$ (6.5, 5.9 sh) arises from the familar high-spin iron(III) complex, which can also be produced by chemical or electrochemical oxidation of the iron(II) cyclidene. That product is formed under all conditions and it is the only product formed at low oxygen pressures. Not present at lower oxygen pressure,

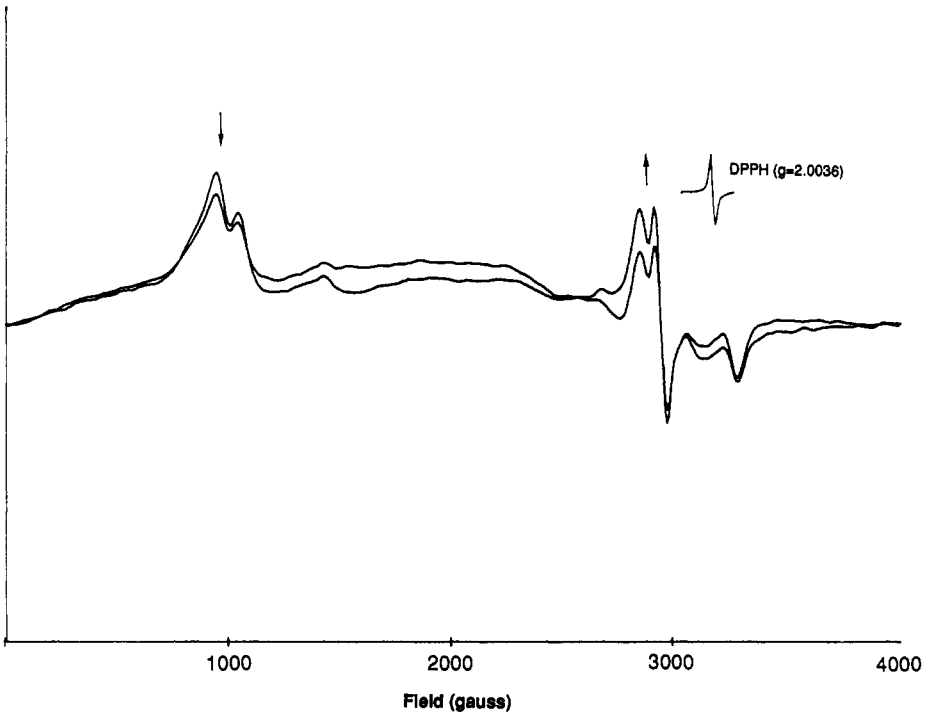

Figure 37. ESR spectra of a frozen (−196 °C) solution of Fe(mXyMeMe[16]Cyc)Cl in 3:1:1 acetone/pyridine/water during autoxidation at 760 Torr of O_2; annealed at room temperature for 1 and 2 min.

but appearing above ca. 20 Torr is a pattern of signals near $g = 2$, indicative of low-spin, 6-coordinate, orthorhombic iron(III) but with a distinctly small g anisotropy (1.93, 2.16, 2.23). Over longer autoxidation times and at higher O_2 pressures, there appears a second $g = 2$ product with a similar spread in g values (1.97, 2.10, 2.25). In addition to these resonances, a weak pattern, attributable to rhombic 6-oordinate high-spin iron(III), is also found at $g = 4.3$, especially on longer autoxidation time scales at higher O_2 pressures.

The nature of the low-spin iron(III) complexes is very important to the understanding of the mechanism of these reactions. In this intermediate, the iron almost certainly has incorporated a sixth, relatively strong ligand in its coordination sphere. Further, because such signals are never generated from the iron(III) complex in the absence of air, the new ligand is most likely to be derived from dioxygen, probably as a product of autoxidation.

The observed extremely small g anisotropy is a highly characteristic property of peroxoiron(III) complexes of the end-on, or monodentate, kind. Independently, Gasnya[166] and Symons and Petersen[167] first identified such spectra with low-spin mononuclear peroxoiron(III) complexes in studies with myoglobin and horseradish peroxidase. Subsequently, Tajima et al. prepared peroxoiron(III) complexes by the reaction of H_2O_2 with the corresponding porphyrin complex (TPP or OEP) and by the reduction of the dioxygen adduct of an iron(II) porphyrin complex and confirmed the accompanying ESR spectral features.[168-171] The occurrence of two species having the characteristic small anisotropic splitting was explained by assuming different levels of protonation of the bound peroxide.

Having concluded that the autoxidation of the iron(II) cyclidene complexes yielded peroxo complexes as primary reaction products, these species were then synthesized in solution by numerous other reactions[162] including: reduction of the dioxygen adduct, combination of hydrogen peroxide with the iron(III) complex, reaction of the iron(II) complex with superoxide, and reaction of the iron(III) complex with iodosobenzene in the presence of water. The one reaction that was not observed in aqueous media was the direct inner-sphere combination of iron(II) and superoxide, a result that may be attributable to the existence of two competing reactions of superoxide in water, as described in eqs 7 and 23, above. This observation is especially important because it supports strongly the kinetic arguments[161-163] that indicate the formation of the peroxo complex from iron(III) and previously formed peroxide.

On the basis of the arguments presented above, a detailed multistep mechanism is assembled in Scheme 11 for the *second major autoxidation mechanism* for iron compounds. The equations are numbered according to their first appearance.

Scheme 11

$$Fe^{II} + O_2 \leftrightarrow Fe(O_2) \quad K_{O_2} \tag{17}$$

$$Fe^{II} + O_2 \rightarrow Fe^{III} + O_2^- \quad k' \tag{18}$$

$$Fe^{II} + S \leftrightarrow Fe^{II}S \quad k_1, k_{-1} \tag{20}$$

$$Fe^{II}S + O_2 \rightarrow Fe^{III}S + O_2^- \quad k_2 \tag{21}$$

$$Fe^{II} + HO_2 \rightarrow Fe^{III} + HO_2^- \quad k_3 \tag{23}$$

$$Fe^{III} + HO_2^- \rightarrow Fe^{III}(HO_2^-) \tag{24}$$

4. Autoxidation of Hemoglobin (Hb) and Myoglobin (Mb)

The distinctive nature of the dioxygen dependence of the autoxidation rates for Hb and Mb has two major

consequences that are especially pertinent to this discussion: (1) it implicates these dioxygen carriers in the same autoxidation mechanism that has been assigned to the iron cyclidenes, and (2) it places Hb and Mb rather precisely in the sequence observed (as O_2 affinity increases) for the iron cyclidenes.

Neil and Hastings[172] reported in 1925 that high pressures of dioxygen protect hemoglobin from autoxidation and early studies of the autoxidation kinetics of hemoglobin[173,174] and myoglobin[175-177] found the same highly distinctive dioxygen dependences that had been observed for the C5- and C6-bridged iron(II) cyclidenes. The rates first increase with dioxygen pressure, and after passing through maxima, they decrease. Equally significantly, the rates are first order in hemoglobin or myoglobin concentration.[178] Detailed studies by Stratmann and George[176] led to the conclusion that some third iron-containing species besides the known oxy and deoxy heme proteins were involved in the reaction. The predicted species is the 6-coordinate reactant included in the mechanism of cyclidene autoxidation in eqs 20 and 21. The majority of the recent discussions of the autoxidation mechanisms of the natural dioxygen carriers have failed to give adequate attention to these results. A bimolecular displacement of superoxide by the nucleophile[157,158] was proposed to account for the simple first-order dependence of the rate of autoxidation on the concentrations of such ligands as N_3^-, SCN^-, and F^-. Caughey et al.[159] emphasized the difficulty of rationalizing the Hb and Mb autoxidation behavior with either a superoxide dissociation[179,180] or a bimolecular displacement[158] mechanism, suggesting an electron-transfer mechanism instead, and a few years later, Castro and co-workers suggested an outer-sphere electron-transfer mechanism for the autoxidation of coordinately saturated iron porphyrin complexes.[181]

For Mb, which understandably might be simpler, the maximum in the rate may be reproduced empirically by eq 25, where K is the inverse of the equilibrium constant for formation of the dioxygen adduct and k is a rate constant. The quadratic form of the denominator is consistent with the electron transfer mechanism described above for the iron(II) cyclidenes (Scheme 11).

$$k_{obs} = kK[O_2]/\{K + [O_2]\}^2 \qquad (25)$$

Of substantial importance, it follows from the electron-transfer mechanism that the dioxygen adducts of Hb, Mb, the cyclidenes, and, presumably, any other iron(II) dioxygen carriers that may be found are inherently stable. Their destruction by O_2 results from competing processes, not from the spontaneous decomposition of the adducts themselves.

B. Autoxidation of Cobalt(II) Complexes

Autoxidation has long been used to convert cobalt(II) complexes to those of cobalt(III), and the reaction is believed to proceed by way of a dinuclear μ-peroxo complex, in accord with the primary autoxidation pathway described above for iron(II) compounds. The autoxidation of cobalt(II) to cobalt(III) was a common procedure in the founding work on coordination chemistry by Alfred Werner and is, in fact, responsible for his observation of the first synthetic dioxygen complexes.[182]

Many cobalt complexes[5,7,11,183-185] react with O_2 to form peroxo-bridged products (eqs 26 and 27), but the sequence of reactions stops with the formation of the μ-peroxo dimer. The O–O bond does not cleave, a process that would result in oxidation of the cobalt ion to the tetravalent state.[108,183] Instead, the oxidation process is often completed by the loss of hydrogen peroxide from the μ-peroxo dimer (eq 28).

$$Co^{II}L + O_2 \leftrightarrow LCo^{III}(O_2^-) \qquad (26)$$

$$LCo^{III}L(O_2^-) + Co^{II}L \leftrightarrow LCo^{III}\text{–}O_2\text{–}Co^{III}L \qquad (27)$$

$$LCo^{III}\text{–}O_2\text{–}Co^{III}L + 2H_3O^+ \leftrightarrow 2LCo^{III}L(H_2O) + H_2O_2 \qquad (28)$$

The relative reversibility of peroxo dimer formation among sterically unhindered cobalt(II) complexes depends on the rate and equilibrium constants for the system. In nicely reversible cases, small equilibrium constants permit easy monomer and dimer interconversion, by concentration changes, by the presence or absence of an axial base, or by alterations in the electronic structure of the ligand.[108] For cobalt protoporphyrin in toluene/imidazole solution, the monomer/dimer dioxygen equilibrium is reversibly displaced with temperature.[186] Since the enthalpies of formation of these particular monomeric dioxygen adducts are greater than those of the corresponding μ-peroxo dimers, the monomeric complexes are more stable at lower temperatures.[187] Polar solvents favor 1:1 complex formation because of the relatively great charge separation in that species. Stronger axial bases, lower temperatures, and higher dioxygen pressures[187] also promote formation of the 1:1 dioxygen adducts among complexes of cobalt(II) with Schiff bases. In comparison to porphyrin derivatives,[188] the larger ΔH values of the cobalt Schiff base complexes favor formation of the 1:1 adducts.

The irreversible step for cobalt peroxo dimer complexes is often the loss of hydrogen peroxide, leaving the cobalt in the trivalent oxidation state. Hence autoxidation of cobalt complexes by the μ-peroxo dimer pathway often yields the cobalt(III) complex and hydrogen peroxide as the net products of autoxidation. This is illustrated by the acid-catalyzed autoxidation of *N,N'*-ethylenebis(acetylacetoniminato)cobalt(II), a reaction that has been studied extensively.[189] In the presence of excess pyridine and a catalytic amount of acid, autoxidation yields 0.5 mol of O_2, 0.5 mol of H_2O_2, and 1 mol of the cobalt(III) complex, bis(pyridine)-{*N,N'*-ethylenebis(acetylacetoniminato)}cobalt(III). Although the disproportionation of HO_2 would produce the observed yields of O_2 and H_2O_2 the system is not that simple. The proposed mechanism and the experimental rate law are given in eqs 29–32.

$$2pyLCoO_2 \leftrightarrow pyLCoO_2CoLpy + O_2 \qquad K_8 \qquad (29)$$

$$pyLCoO_2CoLpy + HOAc \leftrightarrow pyLCoO_2CoLpy\cdot HOAc \qquad K_9 \qquad (30)$$

$$pyLCoO_2CoLpy\cdot HOAc + pyH^+ \rightarrow \text{products} \qquad k_{10} \qquad (31)$$

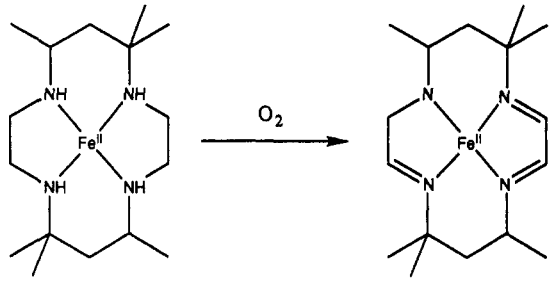

Figure 38. The autoxidation of an iron(II) complex with a macrocyclic [14]aneN$_4$ ligand.

$$\text{rate} = k_{10}K_8K_9[\text{pyLCoO}_2]^2[\text{HOAc}][\text{pyH}^+]/[\text{O}_2] \quad (32)$$

Whereas under acidic conditions, protonation of the μ-peroxo dimer may yield cobalt(III) and hydrogen peroxide, at higher pH other processes may occur. The mechanism of Scheme 7 (the nucleophilic displacement of superoxide) was proposed by Wagnerova' et al. for the reaction of the dioxygen adduct of cobalt(II) tetrasulfophthalocyanine with cyanide or hydroxide in DMSO.[190] Eaton and Reilly[191] proposed an autoxidation mechanism for the 1:1 cobalt dioxygen carriers that involves the reduction of the dioxygen adduct to hydrogen peroxide and the corresponding cobalt(III) complex. The reductant is a second mole of the cobalt(II) complex and acid may catalyze the reaction, but the rate-determining step is the dissociation of the peroxo dimer.

C. Ligand Oxidation

Ligand oxidation is the most destructive common result of autoxidation of transition metal dioxygen carriers. When the metal ion is oxidized it is usually a simple matter to reduce it back to its original state, thereby restoring the dioxygen binding capability. Ligand oxidations are often not reversible. Oxidative dehydrogenations are among the best known examples of ligand oxidations in which the actual fate of the ligand has been determined. Various macrocycles undergo autoxidative dehydrogenation, for example *trans*-[Fe(Me$_6$[14]aneN$_4$)(CH$_3$CN)$_2$]$^{2+}$ reacts with O$_2$ to produce [Fe(Me$_6$[14]1,3,8-trieneN$_4$)(CH$_3$CN)$_2$]$^{2+}$ (Figure 38).[192] A simpler example that is equally interesting is the autoxidation of the ethylenediamine to the α-diimine in Na$_2$[Fe(CN)$_4$en].[193] The autoxidative dehydrogenation mechanism for the cobalt(II) complex of Pydien, C$_5$H$_4$N(CH$_2$)NH(CH$_2$)$_2$NH(CH$_2$)$_2$NHCH$_2$C$_5$H$_4$N, has been probed by Martell and associates.[11] The ligand has two pyridine rings at the extremities of a nine-membered chain in which nitrogens occupy the 2, 5, and 8 positions. Oxidative dehydrogenation converts the amines nearest the pyridine rings into conjugated imine functions. The reaction is base catalyzed and very sensitive to the precise stereochemistry.

Autoxidation of the γ-carbon of a β-diiminate chelate ring to a carbonyl group is the second well-characterized transformation in this category of reaction. Three examples are shown in Figure 39.[191,194,195] In the case of the last example in Figure 39, replacing the hydrogen at the γ-position with acyl groups prevents autoxidation, yielding a well-behaved cobalt dioxygen carrier.[75]

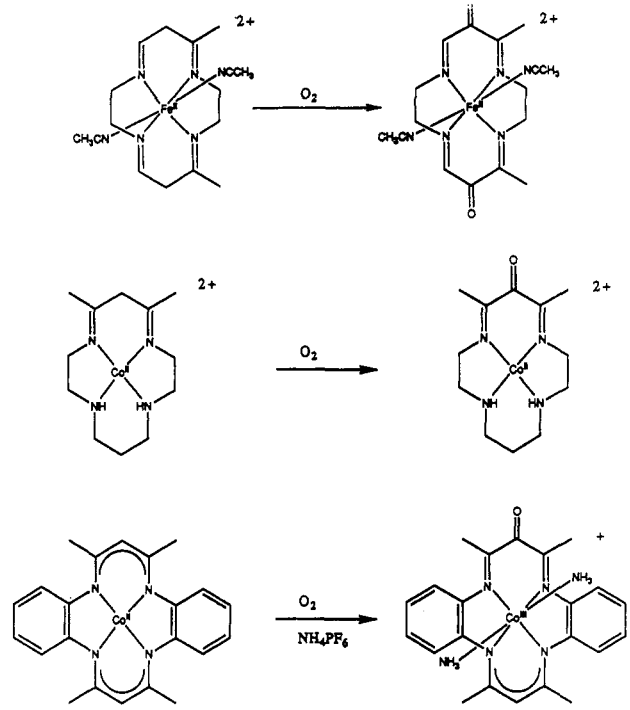

Figure 39. The autoxidation of the γ carbon to a carbonyl group in β-diiminate chelate rings of iron(II) and cobalt(II) complexes.

D. Autoxidation of the Lacunar Cobalt(II) Cyclidene Complexes

The autoxidation process for the cobalt(II) cyclidene complexes can be observed in the decay of the ESR signal due to the oxygen adduct (for example, $g_I = 2.016$, $g_{II} = 2.091$)[13] and may conveniently be followed by UV–visible spectroscopy as either a decay of the cobalt(II) bands (λ_{max} = 320 and 376 nm) or of the dioxygen adduct bands (λ_{max} = 350 nm), depending on the partial pressure of dioxygen and the dioxygen affinity of the particular complex.[26,196] The detailed kinetic behavior depends on structure, and the discussion presented here applies to those species having polymethylene chains ranging from C5 through C12. Cobalt cyclidenes having very small cavities appear to react by a different mechanism that has not been studied extensively. The autoxidation, in acetonitrile in the presence of a base such as 1-methylimidazole, follows first-order kinetics when the concentration of the cobalt complex serves as the reaction variable. The dioxygen dependence of the rate displays saturation kinetics which is consistent with either a preequilibrium dioxygen binding mechanism similar to Scheme 9 or a competitive equilibrium dioxygen binding mechanism like Scheme 10. Because observations require an ionizable proton, the preequilibrium model is favored, with the subsequent reactions being ascribed mainly to the dioxygen adduct, formally a derivative of cobalt(III).

Examination of the effects of 1-methylimidazole concentration and of the basicities of a variety of added bases on the rate of autoxidation indicates that the reaction involves deprotonation of the cyclidene ligand in a step that precedes the irreversible autoxidation reaction. Deuterium substitution of the cyclidene at the R^3 position and the addition of either H$_2$O or D$_2$O to the reaction mixture showed that, under mildly basic conditions, the rate of deprotonation is rate limiting,

with a kinetic isotope effect of about six, approaching the predicted value.[197] These and additional studies have proven that the autoxidation of the cobalt(II) cyclidene complexes involves deprotonation of the R^3 methyl group when that moiety is present. Further, the relatively great acidity of the $R^3 = CH_3$ substituent had already been established in earlier studies. The analogous neutral doubly deprotonated cobalt(II) complex has been isolated and its structure has been established by X-ray diffraction studies (Figure 12).[33]

Additional support for the preequilibrium deprotonation, or conjugate mechanism, is found in the behavior of the cobalt cyclidene complexes having $R^2 = H$, which undergo more rapid autoxidation than their analogues with R^2 = Me. Substitution of a phenyl group at the R3 position removes the suspected acidic function and this does indeed greatly inhibit the autoxidation process of the cobalt(II) cyclidene complexes. For [(C6MeMe-[16]Cyc)Im]$^{2+}$ and [(C6MePh[16]Cyc)Im]$^{2+}$ the rate constants in acetonitrile/1.5 M MeIm, at 30 °C and 760 Torr of O_2 are 4.0×10^{-4} and 2.0×10^{-5} s^{-1}, respectively, a 20-fold retardation. All of these observations are consistent with the autoxidation pathway involving initial deprotonation of the R^3 methyl group, and the mechanism is presented in Scheme 12.

Scheme 12

$$[Co^{II}(Cyc)MeIm]^{2+} + O_2 \overset{K_{O_2}}{\leftrightarrow} [Co^{II}(Cyc)MeIm(O_2)]^{2+} \quad (33)$$

$$[Co^{II}(Cyc)MeIm(O_2)]^{2+} + B \overset{KB}{\leftrightarrow} [Co^{II}(Cyc\text{-}H)MeIm(O_2)]^{+} + BH^{+} \quad (34)$$

$$[Co^{II}(Cyc\text{-}H)MeIm(O2)]+ \overset{k}{\rightarrow} \text{products} \quad (35)$$

In view of the variation of dioxygen affinity with cavity width and other structural variables, it is of interest to see their effect on autoxidation rates.[197] Turning first to polymethylene bridge length and related cavity width—the cobalt(II) cyclidene complexes with shorter bridges (n = 3, 4) give no evidence of O_2 binding under the conditions where the autoxidation reactions have been studied and their autoxidation rates are notably retarded; interestingly their autoxidation rates are about the same as that of the R^3 = Ph derivative. For the next longer group of bridges, the striking observation is the insensitivity of the autoxidation rate to changes in cavity size, particularly within the group having penta-, hexa-, hepta-, and octamethylene bridges. This contrasts with a variation by about a factor of 70 in dioxygen affinity and is best understood on the basis of the assumption that the autoxidation reaction occurs subsequent to dioxygen binding, since the dioxygen affinities are fairly large for all of these compounds. In contrast, the rate of autoxidation increases dramatically on increasing n from 9 through 12. This greatly enhanced propensity toward autoxidation is probably a consequence of the lid-on/lid-off transformation occurring on lengthening the bridging group, though the mechanism of this effect remains unclear.

Electrochemical studies provide evidence that the cyclidene ligand may be oxidized during the autoxidation process.[70] The ESR spectra of electrolyzed solutions of the shorter bridged cyclidenes (n = 3, 4, 5) showed the presence of an organic radical. The electron density at the metal center may be important in determining the ultimate consequence of the autoxidation reaction. A simple electrochemical argument predicts that the more negative the M(III,II) couple, the easier the autoxidation, but the more positive the M(III,II) redox couple, the greater the probability that the ligand will subsequently be oxidized. It follows that the metal with the most positive M(III,II) redox potential is most likely to promote ligand oxidation in the course of autoxidation. This explains why manganese cyclidene complexes autoxidize more rapidly than do those of cobalt, although the ligand is more often oxidized in the cobalt complexes.

Acknowledgments. We thank the U.S. National Science Foundation, Air Products and Chemicals, Inc., and NATO for the support of our investigations on dioxygen carriers. We also deeply appreciate the assistance of Mr. Delong Zhang with tables and figures and Ms. Sue Mohr for preparation of the manuscript. Thanks also to Drs. C. Day and G. P. Pez who kindly provided the coordinates for an unpublished structure.

VI. References

(1) Busch, D. H.; Olszanski, D. J.; Stevens, J. C.; Schammel, W. P.; Kojima, M.; Herron, N.; Zimmer, L. L.; Holter, K. A.; Mocak, J. *J. Am. Chem. Soc.* **1981**, *103*, 1472.
(2) Schammel, W. P.; Mertes, K. S. B.; Christoph, G. G.; Busch, D. H. *J. Am. Chem. Soc.* **1979**, *101*, 1622.
(3) Traylor, T. G.; Traylor, P. S. *Ann. Rev. Biophys. Bioeng.* **1982**, *11*, 105.
(4) Collman, J. P.; Halbert, T. R.; Suslick, K. S. In *Metal Ion Activation of Dioxygen*; Spiro, T. G., Ed.; Wiley & Sons: New York, 1980.
(5) Niederhoffer, E. C.; Timmons, J. H.; Martell, A. E. *Chem. Rev.* **1984**, *84*, 137.
(6) Smith, T. D.; Pilbrow, J. R. *Coord. Chem. Rev.* **1981**, *39*, 295.
(7) Jones, R. D.; Summerville, D. A.; Basolo, F. *Chem. Rev.* **1979**, *79*, 139.
(8) McLendon, G.; Martell, A. E. *Coord. Chem. Rev.* **1976**, *19*, 1.
(9) Vaska, L. *Acc. Chem. Res.* **1976**, *9*, 175.
(10) Basolo, F.; Hoffman, B. M.; Ibers, J. *Acc. Chem. Res.* **1975**, *8*, 384.
(11) Martell, A. E. In *Oxygen Complexes & Oxygen Activation By Transition Metals*; Martell, A. E., Sawyer, D. T., Eds.; Plenum Press: New York, 1988.
(12) Warburton, P. R.; Busch, D. H. Dynamics of IronII and CobaltII Dioxygen Carriers. In *Perspectives on Bioinorganic Chemistry*; Hay, R. W., Dilworth, J. R., Nolan, K. B., Eds.; JAI Press Ltd.: London, 1993; Vol. 2, pp 1–79.
(13) Busch, D. H. In *Oxygen Complexes and Oxygen Activation by Transition Metals*; Martell, A. E., Sawyer, D. T., Eds.; Plenum Publishing Corporation: New York, 1988.
(14) Busch, D. H. *La Transfusione del Sangue* **1988**, *33*, 57.
(15) Busch, D. H.; Stephenson, N. A. *J. Inclusion Phenom. Mol. Recognit. Chem.* **1989**, *7*, 137.
(16) Busch, D. H.; Stephenson, N. A. *Inclusion Compounds Volume 5: Inorganic and Physical Aspects of Inclusion*; Atwood, J., Davies, E., MacNicol, D., Eds.; Oxford University Press: Oxford, 1991; pp 276–310.
(17) *Nomenclature of Inorganic Chemistry, Recommendations, 1990, from the Commission on the Nomenclature of Inorganic Chemistry, International Union of Pure and Applied Chemistry*; Leigh, G. J., Ed.; Blackwell Scientific Publications: Oxford, 1990.
(18) Alcock, N. W.; Lin, W. Kan; Jircitano, A.; Mokren, J. D.; Corfield, P. W. R.; Johnson, G.; Novotnak, G.; Cairns, C.; Busch, D. H. *Inorg. Chem.* **1987**, *26*, 440.
(19) Alcock, N. W.; Lin, W. K.; Cairns, C.; Pike, G. A.; Busch, D. H. *J. Am. Chem. Soc.* **1989**, *111*, 6630.
(20) Busch, D. H.; Zimmer, L. L.; Grzybowski, J. J.; Olszanski, D. J.; Jackels, S. C.; Callahan, R. C.; Christoph, G. G. *Proc. Natl. Acad. Sci. U.S.A.* **1981**, *78*, 5919.
(21) Jackson, P. J.; Cairns, C.; Lin, W. K.; Alcock, N. W.; Busch, D. H. *Inorg. Chem.* **1986**, *25*, 4015.
(22) Thomas, R.; Fendrick, C. M.; Lin, W. K.; Glogowski, M. W.; Chavan, M. Y.; Alcock, N. W.; Busch, D. H. *Inorg. Chem.* **1988**, *27*, 2534.
(23) Stevens, J. C.; Jackson, P. J.; Schammel, W. P.; Christoph, G. G.; Busch, D. H. *J. Am. Chem. Soc.* **1980**, *102*, 3283.

(24) Busch, D. W.; Jackson, P. J.; Kojima, M.; Chmielewski, P.; Matsumoto, N.; Stevens, J. C.; Wu, W.; Nosco, D.; Herron, N.; Ye, N.; Warburton, P. R.; Masarwa, M.; Stephenson, N. A.; Christopy, G.; Alcock, N. W. *Inorg. Chem.*, in press.
(25) Alcock, N. W.; Padolik, P. A.; Pike, G. A.; Kojima, M.; Cairns, C. J.; Busch, D. H. *Inorg. Chem.* **1990**, *29*, 2599–2607.
(26) Chia, P. S. K.; Masarwa, M.; Warburton, P. R.; Wu, W.; Kojima, M.; Nosco, D.; Alcock, N. W.; Busch, D. H. *Inorg. Chem.* **1993**, *32*, 2736.
(27) Chen, J.; Ye, N.; Alcock, N. W.; Busch, D. H. *Inorg. Chem.* **1993**, *32*, 904–910.
(28) Herron, N. L.; Zimmer, L.; Grzybowski, J. J.; Olszanski, D. J.; Jackels, S. C.; Callahan, R. W. *J. Am. Chem. Soc.* **1983**, *105*, 6585.
(29) Korybut-Daskiewicz, B.; Kojima, M.; Cameron, J. H.; Herron, N.; Chavan, M. Y.; Jircitano, A. J.; Coltrain, B. K.; Neer, G. L.; Alcock, N. W.; Busch, D. H. *Inorg. Chem.* **1984**, *23*, 903.
(30) Padolik, P. A.; Jircitano, A. J.; Alcock, N. W.; Busch, D. H. *Inorg. Chem.* **1991**, *30*, 2713–2724.
(31) Novotnat, G.; Alcock, N. W.; Busch, D. H. Unpublished results.
(32) Alcock, N. W.; Cairns, C.; Jircitano, A. J.; Nosco, D. L.; Busch, D. H. *Acta Crystallogr.* **1987**, *C43*, 2069.
(33) Goldsby, K. A.; Jircitano, A. J.; Nosco, D. L.; Stevens, J. C.; Busch, D. H. *Inorg. Chem.* **1990**, *29*, 2523.
(34) Norman, J. A. T.; Pez, G.; Roberts, D. A. In *Oxygen Complexes and Oxygen Activation by Transition Metals*; Martell, A. E., Sawyer, D. T., Eds.; Plenum Publishing Corporation: New York, 1988; p 107.
(35) Alcock, N. W.; Clase, H.; Errington, J. W.; Stephenson, N. A.; Wu, W.; Busch, D. H. *J. Chem. Soc., Chem. Commun.* **1993**, *4*, 422–424.
(36) Hoshino, N.; Jircitano, A.; Busch, D. H. *Inorg. Chem.* **1988**, *27*, 2292.
(37) Busch, D. H.; Christoph, G. G.; Zimmer, L. L.; Jackels, S. C.; Grzybowski, J. J.; Callahan, R. C.; Kojima, M.; Holter, K. A.; Mocak, J.; Herron, N.; Chavan, M.; Schammel, W. P. *J. Am. Chem. Soc.* **1981**, *103*, 5107.
(38) Takeuchi, K. J.; Busch, D. H.; Alcock, N. W. *J. Am. Chem. Soc.* **1983**, *105*, 4261.
(39) Meade, T. J.; Kwik, W.-L.; Herron, N.; Alcock, N. W.; Busch, D. H. *J. Am. Chem. Soc.* **1986**, *108*, 1954.
(40) Meade, T. J.; Alcock, N. W.; Busch, D. H. *Inorg. Chem.* **1990**, *29*, 3766–3776.
(41) Cameron, J. H.; Kojima, M.; Korybut-Daszkiewicz, B.; Coltrain, B. K.; Meade, T. J.; Alcock, N. W.; Busch, D. H. *Inorg. Chem.* **1987**, *26*, 427.
(42) Davis, W. M.; Dzugan, S. J.; Glogowski, M. W.; Delgado, R.; Busch, D. H. *Inorg. Chem.* **1991**, *30*, 2724–2731.
(43) Goldsby, K. A.; Jircitano, A. J.; Minahan, D. M.; Ramprasad, D.; Busch, D. H. *Inorg. Chem.* **1987**, *26*, 2651.
(44) Ramprasad, D.; Lin, W.-K.; Goldsby, K. A.; Busch, D. H. *J. Am. Chem. Soc.* **1988**, *110*, 1480.
(45) Abushamleh, A. S.; Chmielewski, P. J.; Warburton, P. R.; Morales, L. N.; Stephenson, N. A.; Busch, D. H. *J. Coord. Chem.* **1991**, *23*, 91–111.
(46) Lance, K. A.; Lin, W.-K.; Busch, D. H.; Alcock, N. W. *Acta Crystallogr.* **1991**, *C47*, 1401–1403.
(47) Retey, J. *Helv. Chim. Acta* **1971**, *54*, 2747.
(48) Baker, A. T.; Martin, R. L.; Taylor, D. *J. Chem. Soc., Dalton Trans.* **1979**, 1503.
(49) Kamenar, B.; Kaitner, B.; Katovic, V.; Busch, D. H. *Inorg. Chem.* **1979**, *18*, 815.
(50) Tweedy, H. E.; Alcock, N. W.; Matsumoto, N.; Padolik, P. A.; Stephenson, N. A.; Busch, D. H. *Inorg. Chem.* **1990**, *29*, 616.
(51) Martell, A. E. *J. Mol. Catal.* **1988**, *44*, 1.
(52) Menif, R.; Reibenspies, J.; Martell, A. E. *Inorg. Chem.* **1991**, *30*, 3446.
(53) Lin, W.-K.; Alcock, N. W.; Busch, D. H. *J. Am. Chem. Soc.* **1991**, *113*, 7603–7608.
(54) Herron, N.; Chavan, M. Y.; Busch, D. H. *J. Chem. Soc., Dalton Trans.* **1984**, 1491.
(55) Masarwa, M.; Sauer-Masarwa, A.; Ye, N.; Busch, D. H. *J. Coord. Chem.* **1993**, *28*, 355.
(56) Lance, K. A. Ph.D. Dissertation, The Ohio State University, 1988.
(57) Yatsimirskii, A. B.; Kolchinskiii, A. G. *Dokl. Akad. Nauk SSSR* **1979**, *246*, 895.
(58) Busch, D. H. *Chem. Rev.* **1993**, *93*, 847–860.
(59) Jager, E. *Z. Anorg. Allg. Chem.* **1966**, *346*, 76.
(60) Jager, E. *Z. Chem.* **1968**, *8*, 392.
(61) Corfield, P. W. R.; Mokren, J. D.; Hipp, C. J.; Busch, D. H. *J. Am. Chem. Soc.* **1973**, *95*, 4465.
(62) Schammel, W. P.; Zimmer, L. L.; Busch, D. H. *Inorg. Chem.* **1980**, *19*, 3159.
(63) Busch, D. H. *Pure Appl. Chem.* **1980**, *52*, 2477.
(64) Cairns, C.; Lin, W.-K.; Jircitano, A. J.; Busch, D. H. Unpublished work.
(65) Delgado, R.; Glogowski, M. W.; Busch, D. H. *J. Am. Chem. Soc.* **1987**, *109*, 6855.
(66) Lance, K. A.; Goldsby, K. A.; Busch, D. H. *Inorg. Chem.* **1990**, *29*, 4537–4544.
(67) Sakata, K.; Ueno, A. *Synth. React. Inorg. Met.-Org. Chem.* **1991**, *21*, 729.
(68) Busch, D. H. *Acc. Chem. Res.* **1978**, *11*, 392.
(69) Carter, M. J.; Rillema, D. P.; Basolo, F. *J. Am. Chem. Soc.* **1974**, *96*, 392.
(70) Chavan, M. Y.; Meade, T. J.; Busch, D. H.; Kuwana, T. *Inorg. Chem.* **1986**, *25*, 314.
(71) Herron, N.; Busch, D. H. *Inorg. Chem.* **1983**, *22*, 3470.
(72) Busch, D. H.; Jackels, S. C.; Callahan, R. C.; Grzybowski, J. J.; Zimmer, L. L.; Kojima, M.; Olszanski, D. J.; Schammel, W. P.; Stevens, J. C.; Holter, K. A.; Mocak, J. *Inorg. Chem.* **1981**, *20*, 2834.
(73) Herron, N.; Schammel, W. P.; Jackels, S. C.; Grzybowski, J. J.; Zimmer, L. L.; Busch, D. H. *Inorg. Chem.* **1983**, *22*, 1433.
(74) Hoshino, N.; Goldsby, K. A.; Busch, D. H. *Inorg. Chem.* **1986**, *25*, 3000.
(75) Dzugan, S. J.; Busch, D. H. *Inorg. Chem.* **1990**, *29*, 2528.
(76) Reference 68 and references therein.
(77) Diemente, D.; Hoffman, B. M.; Basolo, F. *J. Chem. Soc., Chem. Commun.* **1970**, 467.
(78) Tovrog, B. S.; Kitko, D. J.; Drago, R. S. *J. Am. Chem. Soc.* **1976**, *98*, 5144.
(79) Drago, R. S.; Corden, B. B. *Acc. Chem. Res.* **1980**, *13*, 353.
(80) Smith, T. D.; Pilbrow, J. R. *Coord. Chem. Rev.* **1981**, *39*, 295.
(81) Ransohoff, S.; Adams, M. T.; Dzugan, S. J.; Busch, D. H. *Inorg. Chem.* **1990**, *29*, 2945–2947.
(82) Chavan, M. Y. Ph.D. Dissertation, The Ohio State University, 1983.
(83) Masarwa, M.; Sauer-Masarwa, A.; Ye, N.; Busch, D. H. *J. Coord. Chem.* **1993**, *28*, 355.
(84) Goldsby, K. A.; Meade, T. J.; Kojima, M.; Busch, D. H. *Inorg. Chem.* **1985**, *24*, 2588.
(85) Meade, T. J.; Fendrick, C. M.; Padolik, P. A.; Cottrell, C. E.; Busch, D. H. *Inorg. Chem.* **1987**, *26*, 4252.
(86) Nakamoto, K. *Coord. Chem. Rev.* **1990**, *100*, 363.
(87) Nakamoto, K.; Nonaka, Y.; Ishiguro, T.; Urban, M. W.; Szuki, M.; Kozuka, M.; Nishida, Y.; Kida, S. *J. Am. Chem. Soc.* **1982**, *104*, 3386.
(88) Bajor, K.; Kincaid, J. R.; Nakamoto, K. *J. Am. Chem. Soc.* **1984**, *106*, 7741.
(89) Busch, D. H.; Cairns, C. In *Progress Macrocycle Chemistry*; Izatt, R. M., Christensen, J. J., Eds.; Wiley-Interscience: New York, 1987; pp 1–55.
(90) Ye, N.; Busch, D. H. *Inorg. Chem.* **1991**, *30*, 1819.
(91) Takeuchi, K. J. Ph.D. Dissertation, The Ohio State University, 1981.
(92) Norman, J. A. T.; Ramprasad, D.; Busch, D. H. U.S. Patent 4,735,634, April 5, 1988.
(93) Ramprasad, D.; Busch, D. H. U.S. Patent 4,680,037, July 14, 1987.
(94) Stevens, J. C.; Busch, D. H. *J. Am. Chem. Soc.* **1980**, *102*, 3285.
(95) Phillips, S. E. V.; Schoenborn, B. P. *Nature* **1981**, *292*, 81.
(96) Gerothanassis, I. P.; Momenteau, M.; Loock, B. *J. Am. Chem. Soc.* **1989**, *111*, 7006.
(97) Coltrain, B. K.; Herron, N.; Busch, D. H. In *The Activation of Dioxygen and Homogeneous Catalytic Oxidation*; Barton, D. H. R., Martell, A. E., Sawyer, D. T., Eds.; Plenum Press: New York, 1993; pp 381–394.
(98) Coltrain, B. K.; Ph.D. Dissertation, The Ohio State University, 1984.
(99) Goldsby, K. A.; Beato, B. D.; Busch, D. H. *Inorg. Chem.* **1986**, *25*, 2342.
(100) Herron, N.; Busch, D. H. *J. Am. Chem. Soc.* **1981**, *103*, 1236.
(101) Herron, N.; Cameron, J. H.; Neer, G. L.; Busch, D. H. *J. Am. Chem. Soc.* **1983**, *105*, 298.
(102) Carter, M. J.; Rillema, D. P.; Basolo, F. *J. Am. Chem. Soc.* **1974**, *96*, 392.
(103) Lance, K. A.; Busch, D. H. *Chem. Eng. News* **1987**, *65*, No. 16, 68.
(104) Bakac, A.; Brynildson, M. E.; Espenson, J. H. *Inorg. Chem.* **1986**, *25*, 4108.
(105) Baldwin, J. G.; Huff, J. *J. Am. Chem. Soc.* **1973**, *95*, 5757.
(106) Jaffe, E. R.; Neuman, G. *Nature* **1964**, *202*, 607.
(107) Bodansky, O. *Pharm. Rev.* **1951**, *3*, 144.
(108) Taube, H. *Prog. Inorg. Chem.* **1986**, *34*, 607.
(109) Sawyer, D. T.; Valentine, J. S. *Acc. Chem. Res.* **1981**, *14*, 393–400.
(110) Bard, A. J. In *Oxygen and Oxy-Radicals in Chemistry and Biology*; Rodgers, M. A. J., Powers, E. L., Eds.; Academic Press: New York, 1981; pp 15–43.
(111) Hammond, G. S.; Wu, C.-H. *Adv. Chem. Ser.* **1968**, *77*, 186.
(112) George, P. *J. Chem. Soc.* **1954**, 4349.
(113) Joyner, T. B.; Wilmarth, W. K. *J. Am. Chem. Soc.* **1961**, *83*, 516.
(114) Paeng, I. R.; Nakamoto, K. *J. Am. Chem. Soc.* **1990**, *112*, 3289.
(115) Cotton, F. A.; Wilkinson, G. *Adv. Inorg. Chem., 5th Ed.*; John Wiley: New York, 1988.
(116) Chin, D. H.; LaMar, G. N.; Balch, A. L. *J. Am. Chem. Soc.* **1980**, *102*, 5947.
(117) Groves, J. T.; Haushalter, R. C.; Nakamura, M.; Nemo, T. E.; Evans, B. J. *J. Am. Chem. Soc.* **1981**, *103*, 2884.
(118) Mandon, D.; Weiss, R.; Franke, M.; Bill, E.; Trautwein, A. X. *Angew. Chem.* **1989**, *28*, 1709.
(119) Wolowiec, S.; Kochi, J. K. *J. Chem. Soc., Chem. Commun.* **1990**, 1782.
(120) Oertling, W. A.; Kean, R. T.; Wever, R.; Babcock, G. T. *Inorg. Chem.* **1990**, *29*, 2633–2645.

(121) Bill, E.; Ding, Z. A.; Bominaar, E. L.; Trautwein, A. X.; Winkler, H.; Mandon, D.; Weiss, R.; Gold, A.; Jayaraj, K.; Hatfield, W. E.; Kirk, M. L. *Eur. J. Biochem.* **1990**, *188*, 665–672.
(122) Murata, K.; Panicucci, R.; Gopinath, E.; Bruice, T. C. *J. Am. Chem. Soc.* **1990**, *112*, 6072–6083.
(123) Shedbalker, V. P.; Modi, S.; Mitra, S. *J. Chem. Soc., Chem. Commun.* **1988**, 1238.
(124) Chang, C. K.; Kuo, M.-S. *J. Am. Chem. Soc.* **1979**, *101*, 3413.
(125) Collins, T. J.; Kosta, K. L.; Munck, E.; Uffelman, E. S. *J. Am. Chem. Soc.* **1990**, *112*, 5637–5639.
(126) Proniewicz, L. M.; Bajdor, K.; Nakamoto, K. *J. Phys. Chem.* **1986**, *90*, 1760.
(127) Collins, T. J.; Slebodnick, C.; Uffelman, E. S. *Inorg. Chem.* **1990**, *29*, 3433.
(128) Krumpolc, M.; Roçek, J. *J. Am. Chem. Soc.* **1979**, *101*, 3206.
(129) Buchler, J. W.; Lay, K. L.; Castle, L.; Ullrick, V. *Inorg. Chem.* **1982**, *21*, 842.
(130) Creager, S. E.; Murray, R. W. *Inorg. Chem.* **1985**, *24*, 3824.
(131) Chinn, P. M. Ph.D. Dissertation, The Ohio State University, 1991.
(132) Nill, K. H.; Wasgestian, F.; Pfeil, A. *Inorg. Chem.* **1979**, *18*, 564.
(133) Budge, J. R.; Gatehouse, B. M. K.; Nesbit, M. C.; West, B. O. *J. Chem. Soc., Chem. Commun.* **1981**, 370.
(134) Liston, D. J.; West, B. O. *Inorg. Chem.* **1985**, *24*, 1568.
(135) Alben, J. O.; Fuchsman, W. H.; Beaudreau, C. A.; Caughey, W. S. *Biochemistry* **1968**, *7*, 624.
(136) Wallace, W. J.; Houtchens, R. A.; Maxwell, J. C.; Caughey, W. S. *J. Biol. Chem.* **1982**, *257 9*, 4966.
(137) Cohen, I. A.; Caughey, W. S. *Biochemistry* **1968**, *7*, 636.
(138) Castro, C. E. In *The Porphyrins*; Dolphin, D., Ed.; Academic Press: New York, 1978; Vol. V, p 1.
(139) Collman, J. P. *Acc. Chem. Res.* **1977**, *10*, 26.
(140) Almog, J.; Baldwin, J. E.; Huff, J. *J. Am. Chem. Soc.* **1975**, *97*, 227.
(141) Battersby, A. R.; Buckley, D. G.; Hartley, S. G.; Turnbull, M. D. *J. Chem. Soc., Chem. Commun.* **1976**, 879.
(142) Balch, A. L.; Chan, Y. W.; Cheng, R. J.; La Mar, G. N.; Latos-Grazynski, L.; Renner, M. W. *J. Am. Chem. Soc.* **1984**, *106*, 7779.
(143) Chin, D. H.; Del, G. J.; La Mar, G. N.; Balch, A. L. *J. Am. Chem. Soc.* **1977**, *99*, 5486.
(144) Chin, D. H.; La Mar, G. N.; Balch, A. L. *J. Am. Chem. Soc.* **1980**, *102*, 4344.
(145) Kowalewski, P.; Merlin, J. C.; Bremard, C.; Moreau, S. *J. Mol. Struct.* **1988**, *175*, 55.
(146) Mizutani, Y.; Hashimoto, S.; Tatsuno, Y.; Kitawana, T. *J. Am. Chem. Soc.* **1990**, *112*, 6809.
(147) Chin, D. H.; Balch, A. L.; La Mar, G. N. *J. Am. Chem. Soc.* **1980**, *102*, 1446.
(148) Groves, J. T.; Quinn, R.; McMurry, T. J.; Nakamura, M.; Lang, G.; Boso, B. *J. Am. Chem. Soc.* **1985**, *107*, 354.
(149) Czernuszewicz, R. S.; Macor, K. A.; Raman, J. *Spectroscopy* **1988**, *19*, 553.
(150) Peterson, M. W.; Rivers, D. S.; Richmond, R. M. *J. Am. Chem. Soc.* **1985**, *107*, 2907.
(151) Stanbury, D. M.; Haas, O.; Taube, H. *Inorg. Chem.* **1980**, *19*, 518.
(152) Ilan, Y. A.; Czapski, G.; Meisel, D. *Biochim. Biophys. Acta* **1976**, *430*, 209.
(153) Sawada, Y.; Lyanugi, T.; Yamazaki, I. *Biochemistry* **1975**, *14*, 3761.
(154) Bakac, A.; Espenson, J. H.; Creaser, I. I.; Sargeson, A. M. *J. Am. Chem. Soc.* **1983**, *105*, 7625.
(155) Bernhard, P.; Sargeson, A. M.; Anson, F. C. *Inorg. Chem.* **1988**, *27*, 2754.
(156) Bernhard, P.; Anson, F. C. *Inorg. Chem.* **1988**, *27*, 4574.
(157) Wallace, W. J.; Maxwell, J. C.; Caughey, W. S. *Biochem. Biophys. Res. Commun.* **1974**, *57*, 4 1104.
(158) Shikama, K. *Coord. Chem. Rev.* **1988**, *83*, 73–91.
(159) Wallace, W. J.; Houtchens, R. A.; Maxwell, J. C.; Caughey, W. S. *J. Biol. Chem.* **1982**, *257* 9, 4966.
(160) Herron, N.; Dickerson, L.; Busch, D. H. *J. Chem. Soc., Chem. Commun.* **1983**, *884*.
(161) Dickerson, L. D.; Sauer-Masarwa, A.; Herron, N.; Fendrick, C. M.; Busch, D. H. *J. Am. Chem. Soc.* **1993**, *115*, 3623.
(162) Sauer-Masarwa, A.; Herron, N.; Fendrick, C. M.; Busch, D. H. *Inorg. Chem.* **1993**, *32*, 1086.
(163) Sauer-Masarwa, A.; Dickerson, L. D.; Herron, N.; Busch, D. H. *Coord. Chem. Rev.* **1993**, *128. 117 Bailar Memorial Volume*).
(164) This rate law applies equally well to a bimolecular process in which the superoxide is displaced from the preformed dioxygen adduct by a solvent nucleophile.
(165) Lever, A. B. P. *Inorganic Electronic Spectroscopy*, 2nd ed.; Elsevier: Amsterdam, 1984.
(166) Gasyna, Z. *FEBS Lett.* **1979**, *106*, 213.
(167) Symons, M. C. R.; Petersen, R. L. *Biochim. Biophys. Acta* **1978**, *535*, 241.
(168) Tajima, K.; Yoshino, M.; Mikami, K.; Edo, T.; Ishizu, K.; Ohya-Nishiguchi, H. *Inorg. Chim. Acta* **1990**, *172*, 83.
(169) Tajima, K.; Shigematsu, M.; Jinno, J.; Ishizu, K.; Ohya-Nishiguchi, H. *J. Chem. Soc., Chem. Commun.* **1990**, 144.
(170) Tajima, K.; Jinno, J.; Ishizu, K.; Sakurai, H.; Ohya-Nishiguchi, H. *Inorg. Chem.* **1989**, *28*, 709.
(171) Tajima, K.; Shigematsu, M.; Jinno, J.; Ishizu, K.; Ohya-Nishiguchi, H. *Stud. Surf. Sci. Catal.* **1991**, *66*, 305.
(172) Neil, J. M.; Hastings, A. B. *J. Biol. Chem.* **1925**, *25*, 479.
(173) Brooks, J. *Proc. R. Soc., B* **1931**, *109*, 35.
(174) Brooks, J. *Proc. R. Soc., B* **1935**, *118*, 560.
(175) George, P.; Stratmann, C. *Biochem. J.* **1952**, *51*, 103.
(176) George, P.; Stratmann, C. *Biochem. J.* **1952**, *51*, 418.
(177) George, P.; Stratmann, C. *Biochem. J.* **1954**, *57*, 568.
(178) The first-order dependence on heme protein distinguishes this mechanism from the well-known dioxygen protection from free prophyrins which cannot apply to the heme proteins Hb and Mb since each prosthetic group is sequestered within its globular protein sheath. See discussion of peroxo bridged mechanism for the other case of protection from oxidation by the binding of O_2.
(179) Misra, H. P.; Fridovich, I. *J. Biol. Chem.* **1972**, *247*, 6960.
(180) Carrell, R. W.; Winterbourn, C. C.; Rachmilowitz, E. *Br. J. Haematol.* **1975**, *30*, 259.
(181) Chu, M. L. M.; Castro, C. E.; Hathaway, G. M. *Biochemistry* **1978**, *17*, 481.
(182) Werner, A.; Mylius, A. *Z. Anorg. Chem.* **1898**, *16*, 24.
(183) Fallab, S.; Mitchell, P. R. In *Advances in Inorganic & Bioinorganic Mechanisms*; Sykes, A. G., Ed.; Academic Press: London, 1984; Vol. 3.
(184) Martell, A. E. *Acc. Chem. Res.* **1982**, *15*, 155.
(185) Haim, A.; Wilmarth, W. K. *J. Am. Chem. Soc.* **1961**, *83*, 509.
(186) Stynes, D. V.; Stynes, H. C.; Ibers, J. A.; James, B. R. *J. Am. Chem. Soc.* **1973**, *95*, 1142.
(187) Nakamoto, K.; Nonaka, Y.; Ishugura, T.; Urban, M. W.; Suzuki, M.; Kozuka, M.; Nishida, Y.; Kida, S. *J. Am. Chem. Soc.* **1982**, *104*, 3386.
(188) Wicker, C. M., Jr.; Morgan, R. D.; Rillema, D. P. *Inorg. Chim. Acta* –1983, *78*, 181.
(189) Eaton, D. R.; O'Reilly, A. *Inorg. Chem.* **1987**, *26*, 4185.
(190) Wagnerova', D. M.; Lang, K.; Damerau, W. *Inorg. Chim. Acta* **1989**, *162*, 1.
(191) Riley, D. P.; Busch, D. H. *Inorg. Chem.* **1983**, *22*, 4141.
(192) Dabrowiak, J. C.; Busch, D. H. *Inorg. Chem.* **1975**, *14*, 1881.
(193) Goedken, V. L. *J. Chem. Soc., Chem. Commun.* **1972**, 207.
(194) Durham, B.; Anderson, T. J.; Switzer, J. A.; Endicott, J. F.; Glick, M. D. *Inorg. Chem.* **1977**, *16*, 271.
(195) Weiss, M. C.; Goedken, V. L. *J. Am. Chem. Soc.* **1976**, *98*, 3389.
(196) Masarwa, M.; Warburton, P. R.; Evans, W. E.; Busch, D. H. *Inorg. Chem.* **1993**, *32*, 3826.
(197) Westheimer, F. H. *Chem. Rev.* **1961**, *61*, 265.